University of Cambridge

Synthesis and Coordination Chemistry of Main Group Pyridyl Ligands

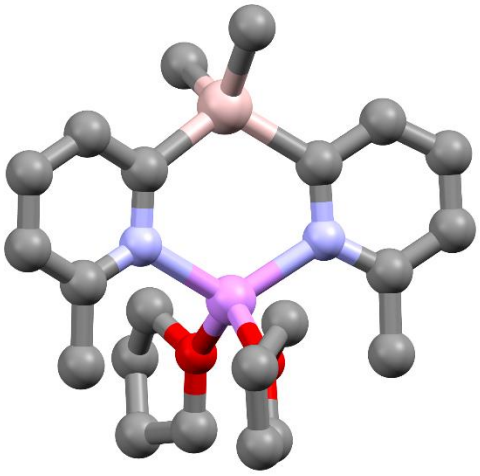

Marina Rincón Nocito

Gonville and Caius College

September 2021

Acknowledgments

First and foremost I would like to thank Prof. Dominic Wright for giving me this project, which I have thoroughly enjoyed, and for being the most supportive supervisor I could have ever asked for, even before I joined the group. Thank you for giving me the opportunity to join your group.

I would also like to thank Jess for teaching me everything about how to make pyridyl ligands, and for being so supportive throughout the whole project, and to Jonny for helping me with any problem I had during the course of this project.

I thank Rosa, Nadia, Steven, Raj, Cassius, and the whole Wright group for making everything much more enjoyable, for the coffee breaks, for the laughs and for the perfect atmosphere in the lab. Thank you for making my stay in Cambridge memorable.

Last but not least, I would like to thank my parents for all the support and encouragement, and for giving me the opportunity to come here.

Table of contents

Abbreviations

COSY	Correlated spectroscopy
DCM	dichloromethane
DEPT	Distortionless Enhancement by Polarization Transfer
d	Doublet
Et	Ethyl
HMBC	Heteronuclear Multiple Bond Correlation
HOESY	Heteronuclear Overhauser Effect Spectroscopy
HSQC	Heteronuclear Single Quantum Coherence
Me	Methyl
2-Me-8-qy	2-Methyl-8-quinolyl
3-Me-2-py	3-Methyl-2-pyridyl
5-Me-2-py	5-Methyl-2-pyridyl
6-Me-2-py	6-Methyl-3-pyridyl
^{n}Bu	Normal-Butyl
^{n}BuLi	N butyl lithium
NMR	Nuclear Magnetic Resonance
OMe	Methoxy
py	Pyridyl
2-py	2-pyridyl
4-py	4-pyridyl
s	singlet
^{s}Bu	Sec-Butyl
t	Triplet
^{t}Bu	Tert-butyl
^{t}BuLi	Tert-Butyl lithium
THF	Tetrahydrofuran

List of compounds

	Compound
1	[MeAl(2-py)$_3$Li]
1 · THF	[MeAl(2-py)$_3$Li · THF]
[1]$_2$	[MeAl(2-py)$_3$Li]$_2$
2	[{Cu(2-py)}$_3$]$_\infty$
3	[{MeAl(2-py)$_3$}$_2$Fe]
4	[{MeAl(2-py)$_3$}$_2$Mn]
5	[{MeAl(2-py)$_3$}$_2$Ca]
6	[{MeAl(2-py)$_3$}$_2$Mo(CO)$_3$Li(THF)$_3$]
7	[{MeAl(2-py)$_3$ZnCl]
8	[{MeAl(2-py)$_3$Li}{MeAl(2-py)$_2$O}Sm]$_2$
9	[{MeAl(2-py)$_3$}$_2$Al]$^+$[{MeAl(2-py)$_3$}Li]$_2$Cl$^-$
10	[EtAl(2-py)$_3$Li · THF]
11	[^{n}BuAl(2-py)$_3$Li · THF]
12	[^{s}BuAl(2-py)$_3$Li · THF]
13	[^{t}BuAl(2-py)3Li · THF]
14	[MeAl(3-Me-2-py)$_3$Li(μ-Br)Li(THF)$_3$]
15	[MeAl(5-Me-2-py)$_3$Li · THF]
16	[MeAl(6-Me-2-py)$_3$Li · THF]
17	[EtAl(6-Me-2-py)$_3$Li]
17 · THF	[EtAl(6-Me-2-py)$_3$Li · THF]
18	[{^{n}BuAl(2-py)$_3$}$_2$Ca](toluene)
19	[{^{n}BuAl(2-py)$_3$}$_2$Mn](toluene)
20	[{^{n}BuAl(2-py)$_3$}$_2$Fe]
21	[{^{s}BuAl(2-py)$_3$}$_2$Ca](toluene)
22	[{^{s}BuAl(2-py)$_3$}$_2$Mn](toluene)
23	[{MeAl(5-Me-2-py)$_3$}$_2$Ca]
24	[{EtAl(6-Me-2-py)$_3$}$_2$Ca]
25	[{EtAl(6-Me-2-py)$_3$}Mn(μ-Cl)Li{(6-Me-2-py)$_3$AlEt}]
26	[{EtAl(2-py)$_3$}{EtAl(2-py)$_2$O}Sm]$_2$
27	[{EtAl(2-py)$_3$Sm]

28	[{EtAl(6-Me-2-py)$_3$}$_2$Sm]
29	[EtAl(6-Br-2-py)$_3$Li]
30	[EtAl(6-CF$_3$-2-py)$_3$Li]
31	[{EtAl(6-Me-2-py)$_3$}$_2$Eu]
32	[{EtAl(6-Me-2-py)$_3$}$_2$Yb]
33	[EtAl(6-Me-2-py)$_3$Yb(THF)$_2$]
34	[{EtAl(6-Br-2-py)$_3$}$_2$Eu]
35	[{EtAl(6-Br-2-py)$_3$}$_2$Yb]
36	[EtAl(OH)(6-CF$_3$-2-py)$_2$]$^-$
37	[{EtAl(6-Br-2-py)$_2$(OH)}Li]$_2$
38	[{EtAl(2-py)$_2$(OMe)}Li]$_2$
39	[{EtAl(6-Br-2-py)$_2$(OMe)}Li]$_2$
40	[Me$_2$Al(6-Me-2-py)$_2$Li·2THF]
41	[Et$_2$Al(6-Me-2-py)$_2$Li·2THF]
42	[Ph$_2$Al(6-Me-2-py)$_2$Li·2THF]
43	[^{t}Bu$_2$Al(6-Me-2-py)$_2$Li·2THF]
44	[Me$_2$Al(5-Me-2-py)$_2$Li·2THF]
45	[Me$_2$Al(3-Me-2-py)$_2$Li·2THF]
46	[Me$_2$Al(6-Me-2-py)$_2$Na·2THF]
47	[Me$_2$Al(6-Me-2-py)$_2$K·2THF]
48	[Bi(4-py)$_3$]

Abstract

The bis(2-pyridyl) ligands [$Me_2Al(6\text{-}Me\text{-}2\text{-}py)_2Li{\cdot}2THF$] (**40**) and [$Me_2Al(5\text{-}Me\text{-}2\text{-}py)_2Li{\cdot}2THF$] (**44**) were synthesized by reacting 2-bromo-6-methylpyridine and 2-bromo-5-methylpyridine, respectively, with $^{n}BuLi$ at –78 °C (1:1 equiv), followed by reaction with Me_2AlCl (2:1 equiv). Reaction with 2-bromo-3-methylpyridine was attempted (**45**), but the crystalline material [$BrLi(6\text{-}Me\text{-}py)_3$] was obtained. Further experiments were tried, with different R-bridgehead groups (R = Et (**41**), Ph (**42**), ^{t}Bu (**43**)) trying to be introduced. Although some of the reactions were believed to be successful, the isolation of the products was extremely difficult, given the oily nature of most of the obtained compounds, presumably by the presence of hydrolysed material. Substitution of the Li^+ cation in **40** by Na^+ (**46**) and K^+ (**47**) by the reaction of **40** with $NaO^{t}Bu$ or $KO^{t}Bu$ (1:1 equiv), respectively, was also attempted, although neither of the reactions showed successful results.

Transmetallation reactions between **40** and various metals (Fe, Ca, Mn, Nb, Eu, Yb or Sm) did not yield any crystal structures. However, the reaction between the in situ ligand **41** and $FeCl_2$ appeared to be successful. Unfortunately, no characterization analysis could be performed on it.

The synthesis of the already reported [$Bi(4\text{-}py)_3$] ligand (**48**) by reaction of 4-bromopyridine with $^{n}BuLi$ (1:1 equiv), followed by reaction with $BiCl_3$ (3:1 equiv) is described. Further reactions with $Ni(BF_4)_2$, $NiBr_2$, $Co(BF_4)_2$ and $CoBr_2$ are also mentioned, although the layering of the **48** solution and the different metal solutions did not yield any crystalline material that could be observed.

The NMR-scale reaction of **48** with [$Bi(6\text{-}Me\text{-}2\text{-}py)_3$] (1:2 equiv) in d_6-benzene and d_8-THF was also attempted, although no change in the ^{1}H NMR spectra could be observed, indicating that both reactions were unsuccessful.

1. Introduction

Over the last two decades a multitude of tripodal tris(2-pyridyl) complexes (see Figure 1) have been investigated and have been the subject of research interest.[1] The complexes of tris(2-pyridyl) ligands with various metals, together with those of related tris-pyrazolyl borates[2] and methanes,[3] have been the subject of interest due to their various applications in coordination and organometallic chemistry, as well as in homogeneous catalysis. The main difference between tris(2-pyridyl) and tris(pyrazolyl) ligands is that the former is a better σ-donor and π-acceptor, which leads to a difference in the coordination and physical properties of the metal complexes.[1] Metal-coordination properties of tris(2-pyridyl) ligands can be shaped, not only by substitution of the pyridyl ring units (changing their steric and electronic character) but also by changing the bridgehead atom. This can have a large effect on both the geometrical and electronic characteristics and is a useful way of tuning ligand behaviour, for example, in catalysis. Numerous examples have been reported[1] in which the bridgehead atoms are non-metallic p-block elements in the second and third periods such as CX (X = H,[4,5] OH,[6] OR,[7] NH_2[8]), N,[9] P,[10] as well as P=O.[11] However, more recently the introduction of p-block metals and semimetals (e.g. As)[12] as bridgeheads has also been a focus of study.[13–19] These tris(2-pyridyl) ligands usually have larger bite angles than the analogues containing the lighter elements, mostly because of the larger Y–C bond lengths.[20] Moreover, the introduction of metals in the structure has other advantages, including the possibility of having neutral and anionic ligands of this type as well as the potential of both variable oxidation states and redox chemistry at the bridgehead, and electronic interactions between the bridgehead atom and the metal coordinated to the pyridyl-N atom.[20] The coordination of a metal-based tris(2-pyridyl) ligand to another metal ion also provides a simple route to the synthesis of heterometallic compounds.[19]

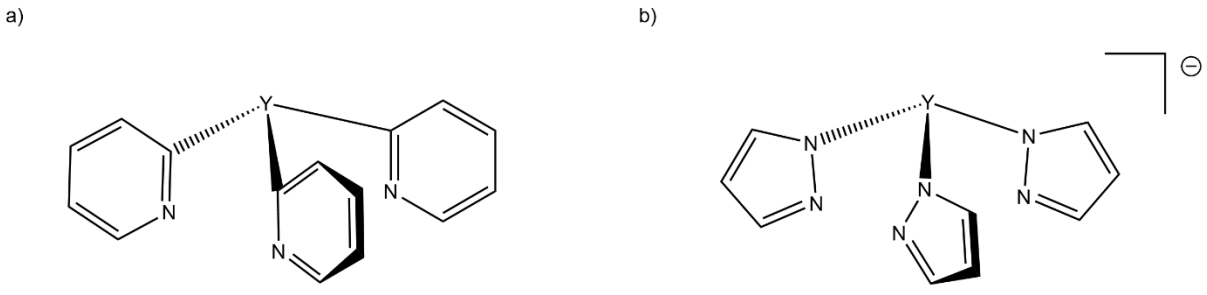

Figure 1. General structures of a) tris(2-pyridyl) and b) tris(pyrazolyl) ligands (Y = main group element)

This project involved the investigation of anionic ligands containing aluminium(III) as the bridgehead atom in 2-pyridyl ligand arrangements so the introduction to this report will focus specifically on this type of arrangement and the coordination chemistry with a range of metal ions.

1.1. Aluminium(III) as a Bridgehead Atom

Introducing aluminium as a bridgehead affects the coordination of tris(2-pyridyl) ligands in an important way, since the resulting aluminates of type $[RAl(2\text{-py}')_3]^-$ (where py' is a substituted or unsubstituted pyridyl group and R is an organic substituent) possess a negative charge (unlike the vast majority of other tris(2-pyridyl) ligands), which leads to a greater affinity for metal ions than the neutral variants containing elements in Groups 14 and 15.[20]

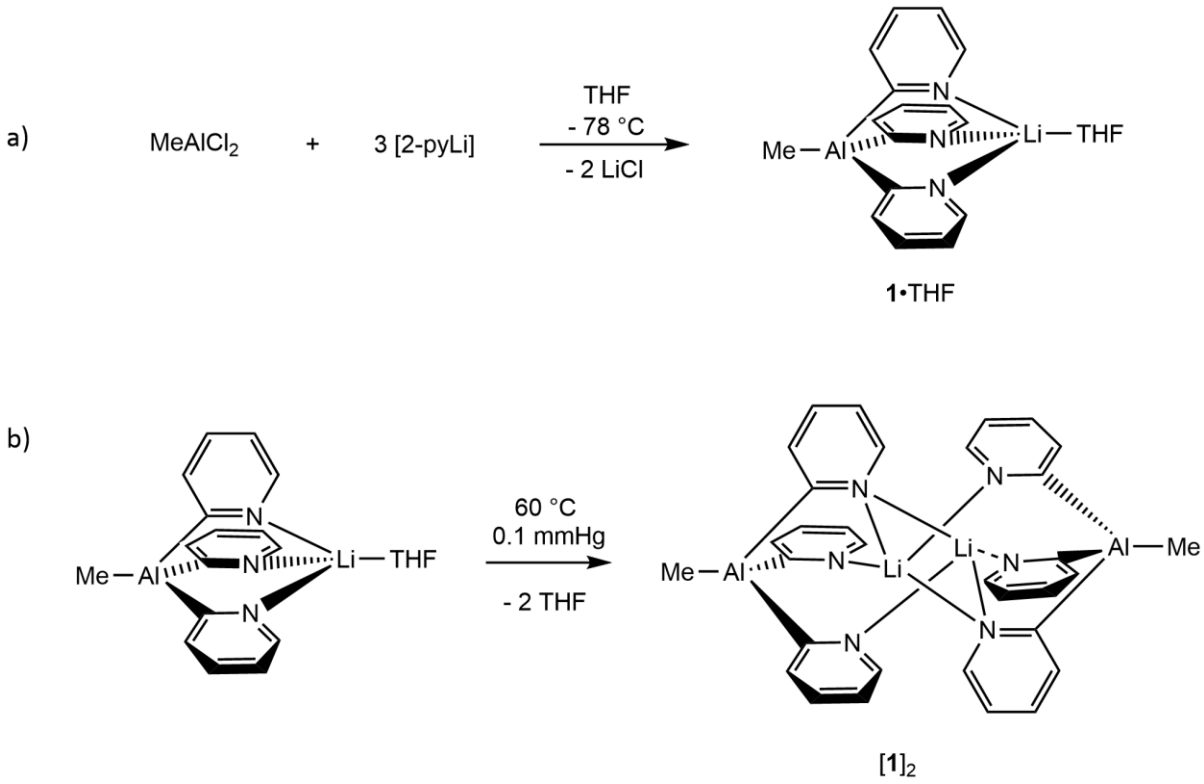

Scheme 1. The synthesis of a) compound **1**·THF and b) the dimer $[\mathbf{1}]_2$

The first reported complex with aluminium as a bridgehead was $[MeAl(2\text{-py})_3Li \cdot THF]$ (**1**·THF), obtained by the reaction of $MeAlCl_2$ with three equivalents of 2-lithio-pyridine in THF (Scheme 1a). The complex was found to be in equilibrium in THF solution with the unsolvated dimer $[MeAl(2\text{-py})_3Li]_2$ ($[\mathbf{1}]_2$).[17] In fact, $[\mathbf{1}]_2$ can be obtained by drying **1**·THF under vacuum while heating (Scheme 1b). In early studies it was found that **1**·THF can act as a stable 2-pyridyl-transfer reagent, as shown by its reaction with CuCl (1:1 equivalents). The result is the organometallic compound $[\{Cu(2\text{-py})\}_3]_\infty$ (**2**) (see Scheme

2), which, interestingly, cannot be synthesized by direct reaction of CuCl with 2-lithiopyridine.[17] However, reactions with $FeCl_2$ or Cp_2Mn (1:1 and 1:2 equivalents respectively) showcased a different characteristic. In these cases the $[MeAl(2\text{-}py)_3]^-$ anion is transferred directly onto the Fe(II) and Mn(II) centres building the heterobimetallic 'sandwich-type' compounds $[\{MeAl(2\text{-}py)_3\}_2Fe]$ (**3**) and $[\{MeAl(2\text{-}py)_3\}_2Mn]$ (**4**) (see Scheme 2).[19] The different results obtained for the Cu(I), and Fe(II) and Mn(II) reactions with the $[MeAl(2\text{-}py)_3]^-$ anion are believed to be due to the preference for linear metal coordination in $[\{Cu(2\text{-}py)\}_3]_\infty$, while both the Fe(II) (of **3**) and Mn(II) (of **4**) ions show an octahedral coordination to the two $[MeAl(2\text{-}py)_3]^-$ ligands. Compounds **3** and **4** illustrated the first cases of a metal-based tris(2-pyridyl) arrangement acting as a ligand. Furthermore, compound **3** was also shown to be a highly selective catalyst for the epoxidation of styrene in the presence of dry air,[19] illustrating the potential of heterometallic compounds of this type in catalysis for the first time. Later on, reactions with a more extensive variety of metals were investigated, obtaining a range of new complexes that contain the $[MeAl(2\text{-}py)_3]^-$ ligand; $[\{MeAl(2\text{-}py)_3\}_2Ca]$ (**5**), $[\{MeAl(2\text{-}py)_3\}Mo(CO)_3Li(THF)_3]$ (**6**) and $[\{MeAl(2\text{-}py)_3\}ZnCl]$ (**7**) (see Scheme 2).[18] The reaction of $[MeAl(2\text{-}py)_3Li\cdot THF]$ with CaI_2 (1:2 equivalents) yields a similar sandwich complex (**5**) to those formed in the cases of **3** and **4** in which the metal centre is tris-coordinated by two aluminates, while reacting $[MeAl(2\text{-}py)_3Li\cdot THF]$ with $[(C_7H_8)Mo(CO)_3]$ at room temperature gave the trimetallic complex $[\{MeAl(2\text{-}py)_3\}Mo(CO)_3Li(THF)_3]$ (**6**). However, reaction of **1**$\cdot$THF with $ZnCl_2$, using 1:1 or 1:2 equivalents, results in the bimetallic Al^{III}/Zn

complex **7**, having a half-sandwich arrangement in which only one aluminate ligand coordinates.

a) 3 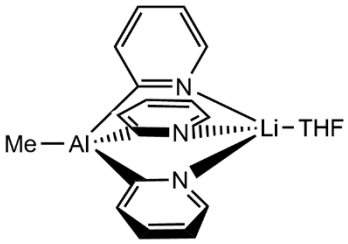

CuCl

- LiCl

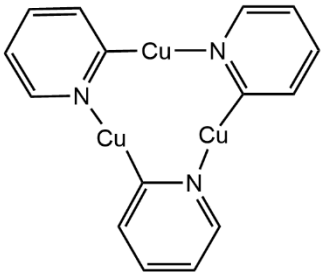

2

b) 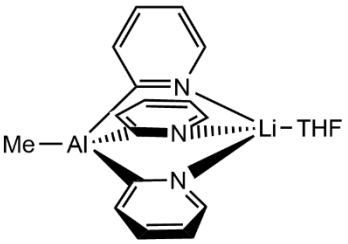

MX_2

M = Fe, X = Cl (1:1)
M = Mn, X = Cp (2:1)
M = Ca, X = I (2:1)

- LiCl

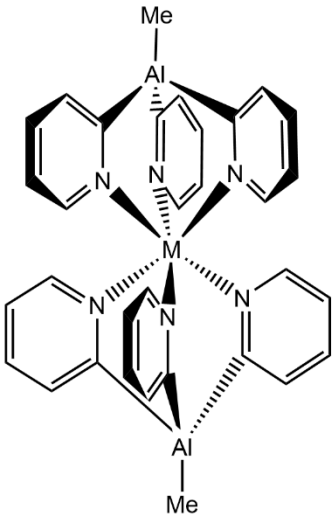

M = Fe (**3**)
M = Mn (**4**)
M = Ca (**5**)

c) 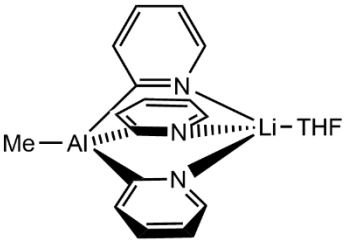

$[(C_7H_8)Mo(CO)_3]$

- C_7H_8

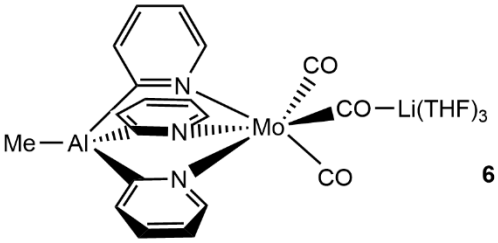

6

d) 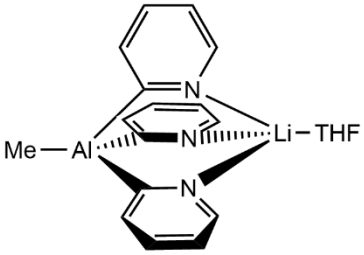

$ZnCl_2$

- LiCl

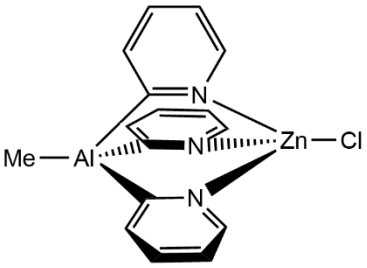

7

Scheme 2. Synthesis of the metal complexes **2** (a), **3-5** (b), **6** (c) and **7** (d)

Moreover, when attempting to synthesize the Sm^{II} sandwich complex using 2:1 stoichiometric ratio of [**1**·THF]:SmI_2, the unexpected product [{**1**}{MeAl(2-py)$_2$O}Sm]$_2$ (**8**) was formed, in which one of the 2-pyridyl ligands of the putative sandwich compound is substituted by an O-atom (see Figure 2. In the process of this formation, the Sm^{II} is oxidised to Sm^{III}, and a new heteroleptic dianion ([MeAl(2-py)$_2$O]$^{2-}$ is formed.[20] The formation of this anion appears to be the result of aerial oxidation with O_2 and this result is relevant to the activity of the Fe(II) complex **3** in the expoxidation of styrene to styrene oxide (as a model intermediate in this reaction).

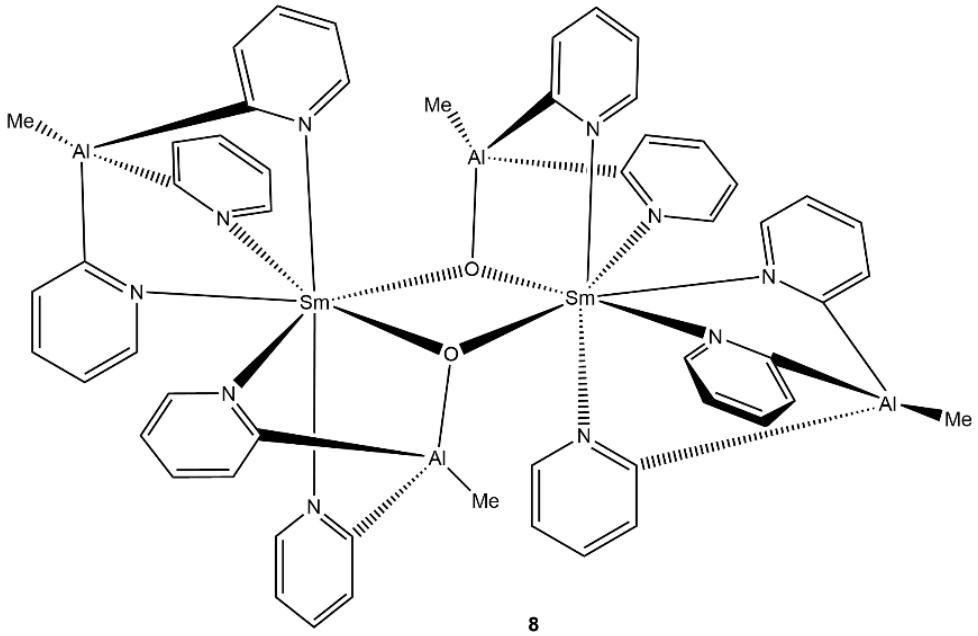

Figure 2. Structure of compound **8**

These precious studies show that mono- or bis-coordination of [RAl(2-py')$_3$]$^-$ anions to divalent metal ions (M^{II}) is preferred, generating complexes of the type [{RAl(2-py')$_3$}$_2$MX] or [{RAl(2-py')$_3$}$_2$M]. A further interesting study has revealed what happens when a trivalent metal ion is used in a study of the coordination of [MeAl(2-py)$_3$]$^-$ anions with the trivalent Al^{III} cation.[16] This is achieved by the reaction of **1**·THF with $AlCl_3$ (4:1 equivalents), which forms the complex [{MeAl(2-py)$_3$}$_2$Al]$^+$[{MeAl(2-py)$_3$}Li]$_2$Cl$^-$ (**9**), containing both a sandwich-type cation ([{MeAl(2-py)$_3$}$_2$Al]$^+$) and anion ([{MeAl(2-py)$_3$}Li]$_2$(μ-Cl)$^-$) (see Figure 3). Interestingly, this arrangement is not observed for other neutral

analogues. The $[\{MeAl(2\text{-}py)_3\}_2Al]^+$ cation contains a linear arrangement of three Al^{III} atoms, and the coordination of the Cl^- anion within the $[\{MeAl(2\text{-}py)_3\}Li]_2(\mu\text{-}Cl)^-$ anion is also linear. The main interest in the structure of **9** is in the way in which the neutral $[\{MeAl(2\text{-}py)_3\}Li]$ unit and the $[MeAl(2\text{-}py)_3]^-$ ligand coordinate both the cation (Al^{III}) and the anion (Cl^-) of $AlCl_3$. Compound **9** was the first containing an anion with a Li(μ-Cl)Li fragment to be reported, as well as the first tris(2-pyridyl) ligand to be coordinate to a group 13-trivalent salt.

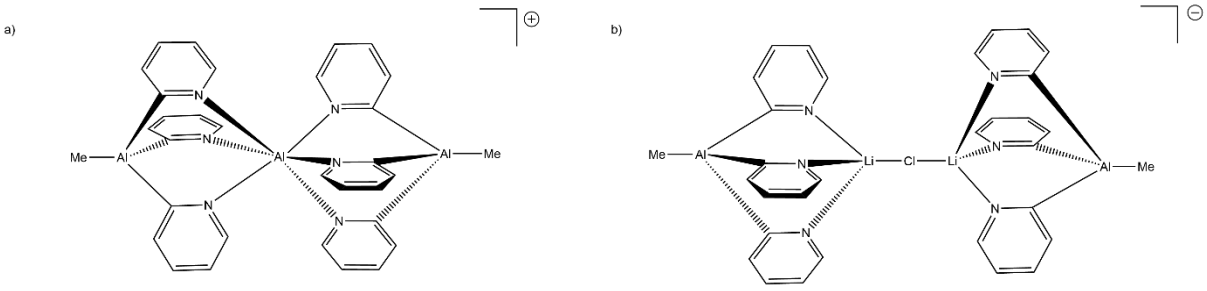

Figure 3. Structure of the a) cation and b) anion of compound **9**

In further research, a series of different tris(2-pyridyl) aluminates was synthesized following the simple, one-pot, stoichiometric procedure which had already been used to obtain [^{n}BuIn(2-py)$_3$Li · THF].[18] In these cases, the AlX_3 halide is reacted with different organolithium compounds (R'Li) (1:1 equiv.), followed by reaction with 2-lithium-pyridine (1:3 equiv.) (see Scheme 3).

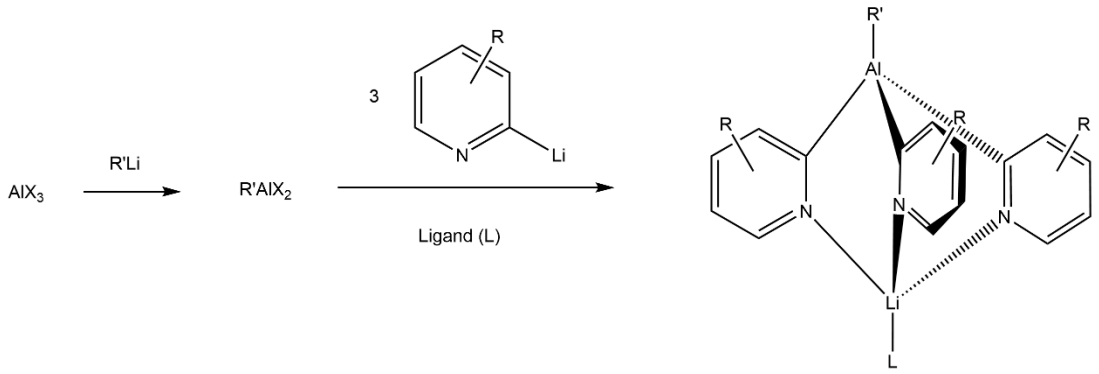

Scheme 3. General procedure for the synthesis of tris(pyridyl) aluminate ligands

This gave aluminates with different R-groups at the bridgehead position (Et, ^{n}Bu, ^{s}Bu and ^{t}Bu); which were [EtAl(2-py)$_3$Li·THF] (**10**), [^{n}BuAl(2-py)$_3$Li·THF] (**11**), [^{s}BuAl(2-py)$_3$Li·THF] (**12**) and [^{t}BuAl(2-py)$_3$Li·THF] (**13**) (see Figure 4).

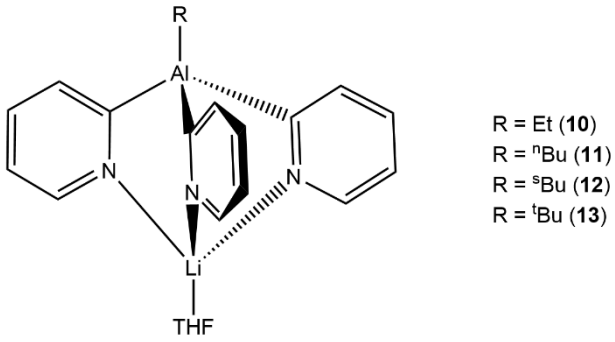

Figure 4. General structure of compounds **10** - **13**

The influence of different substituents in the pyridyl rings was also investigated. For this, 2-bromo-3-methylpyridine, 2-bromo-5-methylpyridine and 2-bromo-6-methylpyridine were reacted with ^{n}BuLi for 3 hours at –78 °C, followed by reaction with commercially available $MeAlCl_2$. The new complexes: [MeAl(3-Me-2-py)$_3$Li(μ-Br)Li(THF)$_3$] (**14**), [MeAl(5-Me-2-py)$_3$Li·THF] (**15**), and [MeAl(6-Me-2-py)$_3$Li·THF] (**16**) were obtained (see Figure 5). ^{1}H NMR analysis for all these compounds shows no major differences between the shifts of the Me-Al groups of the 3-methyl-, 5-methyl- and 6-methyl-pyridyl derivatives compared to the unsubstituted [MeAl(2-py)$_3$Li·THF],[17] which leads to the conclusion that substitution at the 2-pyridyl rings has no or little electronic effect on the bridgehead-aluminium atom.

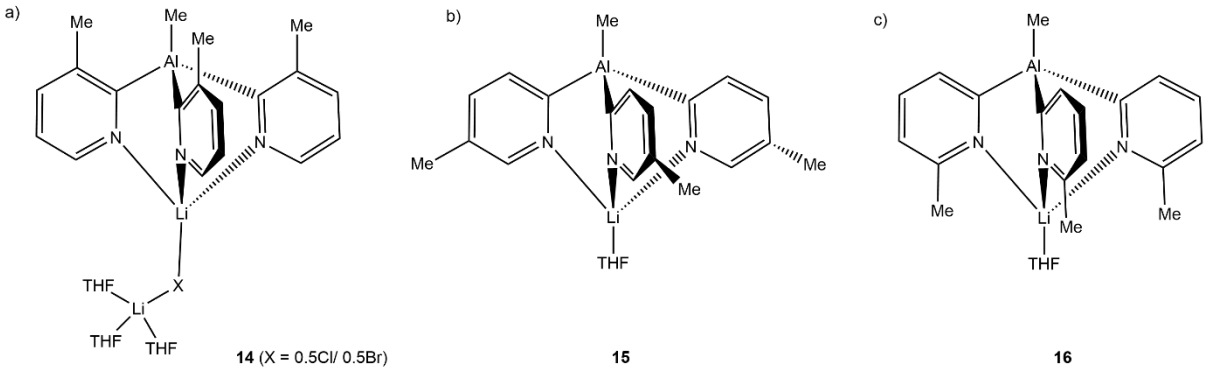

Figure 5. Structures of a) compound **14**, which presents an unparallelled Li coordination, b) compound **15** and c) compound

A variable-temperature and concentration ^{1}H NMR analysis of complex **16**, showed that both the solvated and non-solvated complexes are in dynamic equilibrium and suggested that the THF solvation is highly labile. This behaviour is similar to that of the previously mentioned complex [MeAl(2-py)$_3$Li · THF] (**1**) which loses THF easily to form the unsolvated dimer [MeAl(2-py)$_3$Li]$_2$ [**1**]$_2$.[17] The lability of the THF ligand of **16** is due to the steric congestion at the coordination site of the lithium of aluminate anion due to the adjacent 6-Me groups. Placing **16** under vacuum results in the formation of unsolvated [MeAl(2-py)$_3$Li]. Remarkably, the complex is a monomer in the solid state being the Li in a tetrahedral, four coordinate environment, with dimerization again being prevented by the steric effect of the 6-Me groups. Interestingly, the ethyl analogue **17**·THF shows a bent Li$^+$-THF coordination different to previous species (e.g. **16**), for which the usual coordination is linear (See Figure 6).

The X-ray structures of the [RAl(2-py)$_3$Li·THF] complexes (R = Et (**10**); ^{n}Bu (**11**); ^{s}Bu (**12**); ^{t}Bu (**13**)) are all similar. In each case, the [RAl(2-py)$_3$]$^-$ anion is coordinated to a Li$^+$ cation, which is solvated by a THF molecule. Interestingly, complex **14** displays an unparalleled lithium coordination in which the Li$^+$ cation is coordinated to the N-pyridyl atoms but is not solvated by a THF molecule, but instead coordinates a bridging Li-bridging halide ion [with site occupancy Cl/Br (50:50) from the X-ray data]. Overall, comparison of the ligand bite angles of complexes **10**, **13** and **16** show that substitution with bulky groups at the Al bridgehead and substitution at the 6-position of the 2-pyridyl ring units have a great effect on the ligand bite angle as a result of steric effects.

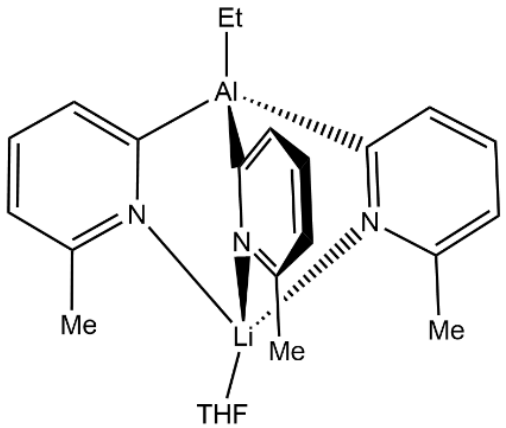

17·THF

Figure 6. Unlike other complexes, the Li-THF bond in compound **17**·THF is bent instead of linear

Investigation of the coordination chemistry of this range of derivatives (with different substituents at the Al bridgehead and within the 2-pyridyl ring units) was conducted mainly with Ca^{II}, Mn^{II} and Fe^{II}.[21] The reactions of CaX_2, MnX_2 and FeX_2 (X = Cl/I) with the aluminates [RAl(2-py')$_3$Li·THF] (R = ^{n}Bu, 2-py' = 2-pyridyl; R = ^{s}Bu, 2-py' = 2-pyridyl; R = Me, 2-py' = 5-Me-2-pyridyl, 6-Me-2-pyridyl; R = Et, 2-py' = 6-Me-2-pyridyl (**17**·THF) (see Figure 6)), gave the heterometallic sandwich compounds [{^{n}BuAl(2-py)$_3$}$_2$M] [M = Ca (**18**); M = Mn(**19**); M = Fe (**20**)], [{^{s}BuAl(2-py)$_3$}$_2$M] [M = Ca(**21**); M = Mn(**22**)], [{MeAl(5-Me-2-py)$_3$}$_2$Ca] (**23**), and [{EtAl(6-Me-2-py)$_3$}$_2$Ca] (**24**) (see Figure 7). Complexes **18**-**24** exhibit similar arrangements [{RAl(2-py')$_3$}$_2$M] with the metal cations in a six-coordinate, octahedral environment; the same as that seen previously for [{MeAl(2-py)$_3$}$_2$M] (M = Fe^{II} (**3**), Mn^{II} (**4**)[19], Ca^{II} (**5**)[18]). Bond angles and lengths for compounds **18**-**22** are similar, regardless of the differences in the ionic radii of the metal centres coordinated and the R-bridgehead group present. Metric parameters for the calcium compound **23**, and compounds **18**, **21** and **5**[18] are almost identical.[21] The presence of the 5-Me substituent in **23** has little effect of the coordination environment compared to the unsubstituted analogues. However, methyl groups at the 6-position of the pyridine rings have a massive effect on the formation of the sandwich compound **24**. Proof of this is shown in the Ca-N bond lengths of compound **24**, which are noticeably increased compared to the related Ca sandwich compounds **18**, **21** and **23**, and **5**[18] (there is also a large increase in the ligand bite angle in this case also). The steric

confrontation of the 6-methyl groups of the $[EtAl(6\text{-}Me\text{-}2\text{-}py)_3]^-$ ligands across the sandwich complex is the main reason for this.

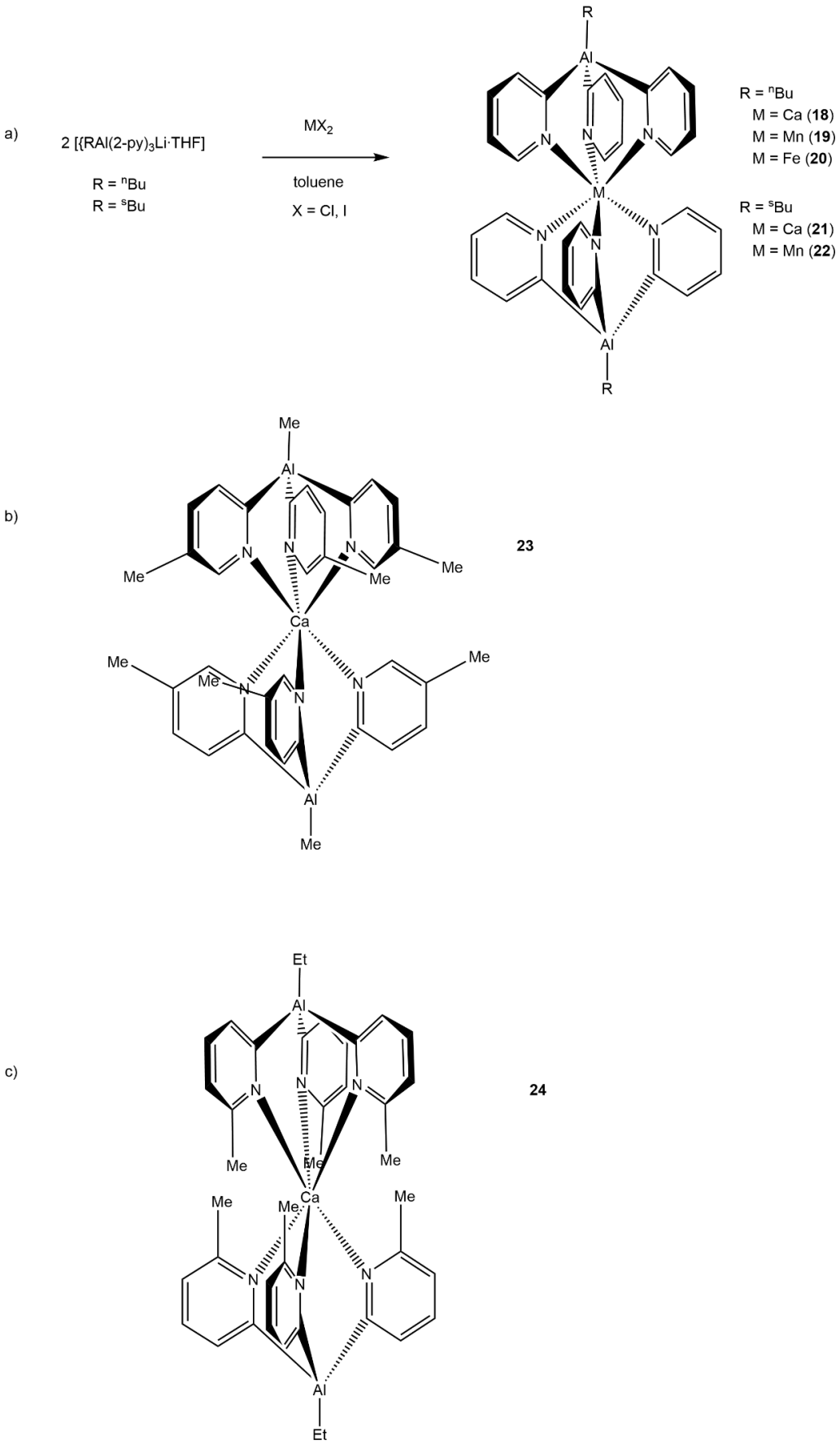

Figure 7. Structures of the sandwich compounds **18** – **22** (a), compound **23** (b) and compound **24** (c)

Considering this effect, the formation of the co-complex [{EtAl(6-Me-2-py)$_3$}Mn(μ-Cl)Li{(6-Me-2-py)$_3$AlEt}] (**25**) (see Figure 8) in the 2 : 1 reaction of [EtAl(6-Me-2-py)$_3$Li · THF] with $MnCl_2$ is probably the result of the smaller ionic radius for the Mn^{II} cation compared to Ca^{II}, as the Mn^{II} sandwich complex would lead to the 6-Me groups being unfavourably close in the sandwich complex.[21] Instead, in **25** only one of the [{EtAl(6-Me-2-py)$_3$}]$^-$ anions coordinates to Mn^{II} while the other [EtAl(6-Me-2-py)$_3$Li] forms a bridge to the Mn-Cl fragment (placing the 6-Me groups as far apart as possible). The formation of co-complex **25** can be seen as closely related to that of the half-sandwich complex [{MeAl(2-py)$_3$}ZnCl] (**7**),[18] again due to the small ionic radii of the Zn^{II} cation.[21]

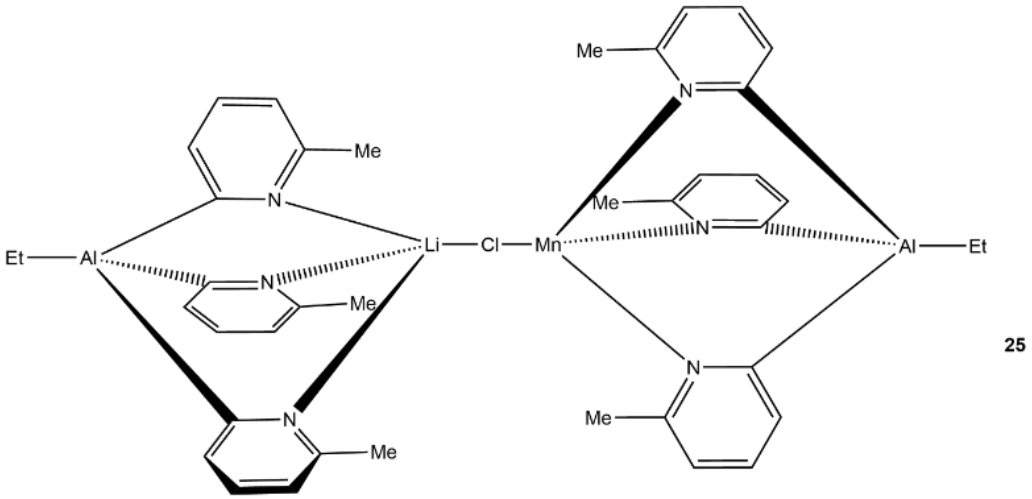

25

Figure 8. Structure of the manganese co-complex **25**

In a related reaction to that described previously for [MeAl(2-py)$_3$Li · THF] (**1** · THF),[20] the coordination of Sm^{II} was investigated with [EtAl(2-py)$_3$Li · THF] (**10**).[22] **10** was reacted with SmI_2 (2 to 1 equivalents) in THF at room temperature, giving the Al^{III}/Sm^{III} compound[{EtAl(2-py)$_3$}{EtAl(2-py)$_2$O}Sm]$_2$ (**26**) after prolonged storage (see Scheme 4). The presence of the O-atom in one of the ligands is believed to occur by O_2 oxidation rather than by H_2O hydrolysis. In fact, **26** can be synthesized from the reaction of the [{EtAl(2-py)$_3$}$_2$Sm] **27** in situ with dry excess of O_2 gas. To prove the existence of this sandwich intermediate, the reaction was repeated using the more sterically hindered analogue [EtAl(6-Me-2-py)$_3$Li · THF] (**17** · THF). The reaction was again done using a 2:1 stoichiometry of the aluminate with SmI_2 at room temperature, which led to the formation of the desired sandwich compound [{EtAl(6-Me-2-py)$_3$}$_2$Sm] (**28**) (see Scheme 4). It is worth noting, that the reaction of **28** with O_2 does not lead to the oxo-compound like **27**, presumably because of the steric shielding the 6-methyl groups around the Sm^{II} cation, which would prevent the oxidation of the metal centre.

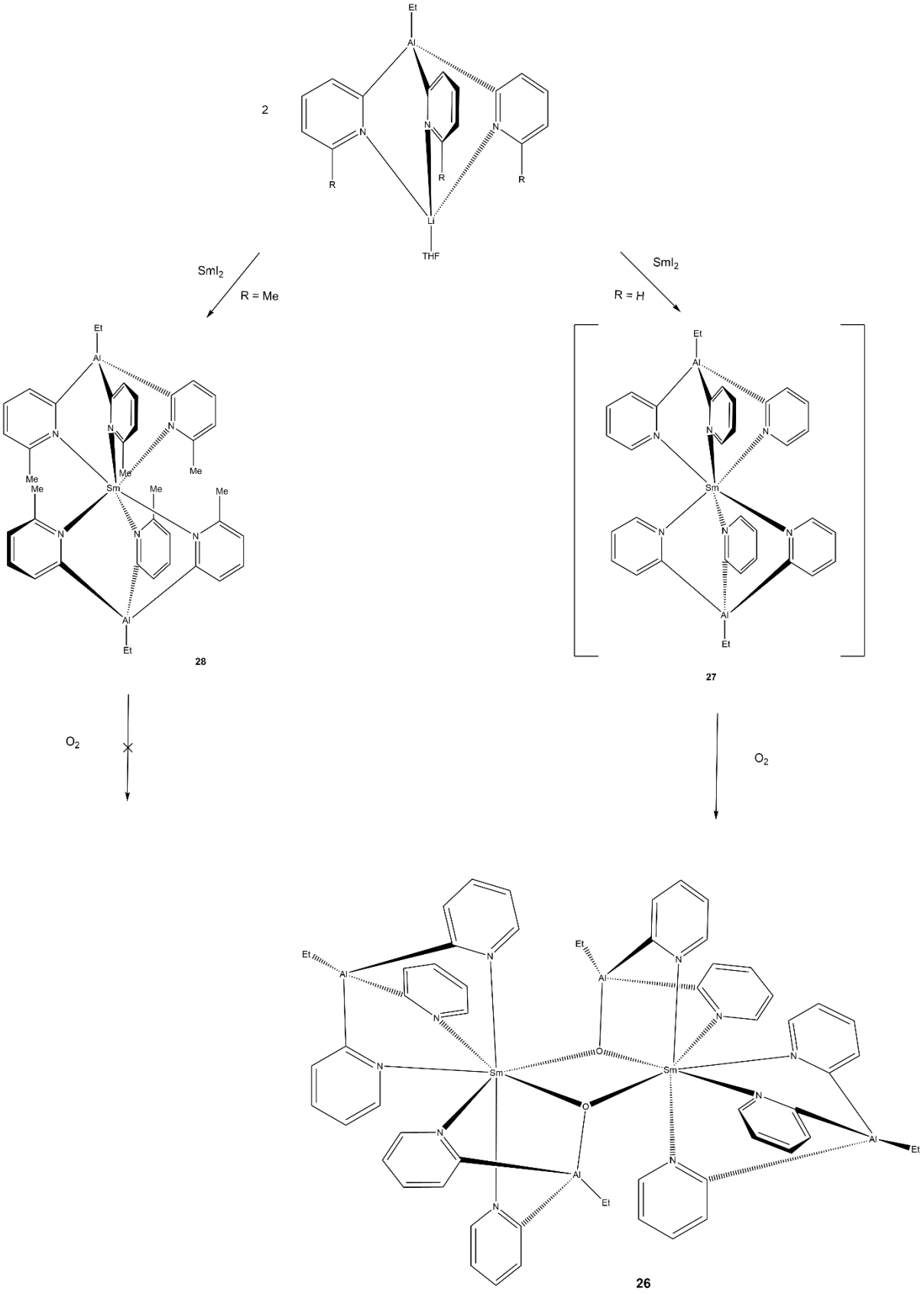

Scheme 4. Procedure for making the oxo-complex **26** through the intermediate **27**, and the 6-methyl analogue **28**

The stabilisation effect of the 6-Me groups in the aluminate due to steric shielding of the coordinated metal opened led to the investigation of the related ligands [EtAl(6-Br-2-py)$_3$Li] (**29**) and [EtAl(6-CF_3-2-py)$_3$Li] (**30**) (see Figure 9), which also allowed the effect of electron-withdrawing substituents on the coordination behaviour to be explored.[23] Compounds **29** and **30** were synthesized following the procedure already mentioned for the majority of the compounds, that is, reacting the corresponding lithio-pyridines with $EtAlCl_2$ at –78 °C. It is worth mentioning that the lithiation of 2,6-dibromo-2-pyridine to form **29** is more successful if the pyridine is added to ^{n}BuLi in this reaction, instead of the other way around (as it is done in all of the other syntheses). The influence of the new pyridyl-substituents can be appreciated in the solid state structures of both complexes, as neither of them show THF coordination of Li^+. As seen in compound **17**, the Li^+ cations in **29** and **30** also show a trigonal pyramidal geometry. The reactions of both complexes with $FeCl_2$ fail to coordination the metal, providing evidence of both the steric effect of the substituents at the 6-positions of the pyridyl rings and of the electron-withdrawing effect of Br and CF_3 (which leads to weaker σ-donor character than Me).

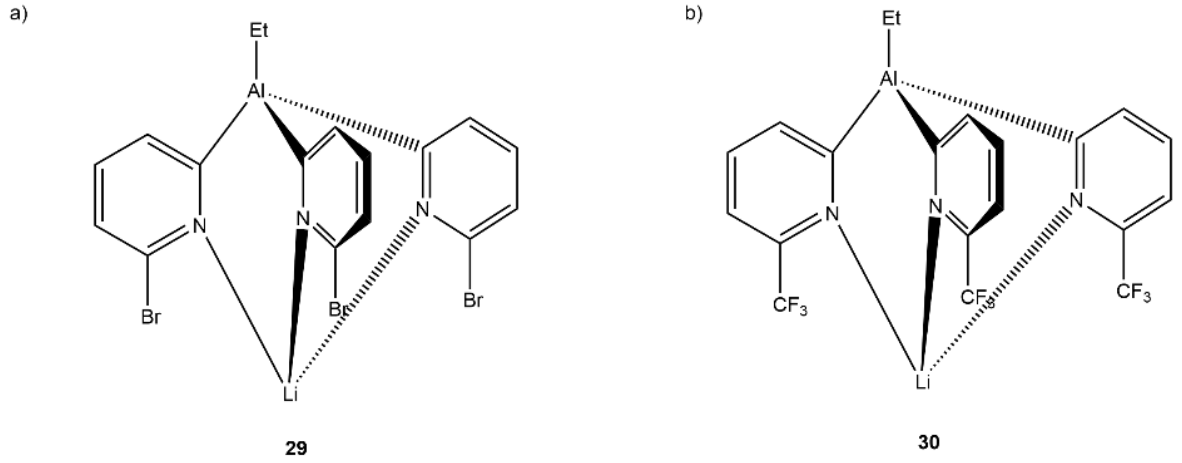

Figure 9. Structure of the 6-bromo (a) and the 6-CF_3 (b) substituted tris(2-pyridyl) aluminates

The formation of further lanthanide complexes have been investigated using **17**, which has been shown to stabilize unusual lanthanide oxidation states,[22] as well as **29**. Eu and Yb were chosen because of their stable nature in the +2 oxidation state, caused by their half-filled f^7 and filled f^{14} electronic configurations, respectively.[24] The reaction of **17** with EuI_2 and YbI_2 (2 to 1 equivalents) in THF at room temperature gave [EtAl(6-Me-2-py)$_3$]$_2$Eu{LiI·THF$_x$} (**31**(LiI)) and [EtAl(6-Me-2-py)$_3$]$_2$Yb{LiI·THF$_x$} (**32**(LiI)) respectively (see Scheme 5a). Both sandwich compounds [{EtAl(6-Me-2-py)$_3$}$_2$Ln] (Ln = Eu (**31**), Yb (**32**)) co-crystallise with THF-solvated LiI. For the Eu complex, a [(THF)$_2$Li(μ-I)]$_2$ unit is found within

the crystal lattice, while for the Yb analogue two $(THF)_3LiI$ units are observed. The lanthanide ions in the complexes are six-coordinated, with a distorted-octahedral geometry in a sandwich arrangement. In order to get the sandwich complexes without the inclusion of solvated LiI units, the reaction solvent was changed to acetonitrile, which led to the desired products **31** and **32**. Tracking of the Yb reaction by ^1H NMR spectroscopy shows that the half-sandwich compound $[EtAl(6\text{-}Me\text{-}2\text{-}py)_3Yb(THF)_2]$ (**33**) is an intermediate in the reaction that leads to the sandwich compound **32**. Additional research on the system showed that **33** can also be obtained by reacting **17** with YbI_2 in a 1:1 ratio in THF. As seen for the sandwich compound **32**, the Yb centre in **33** exhibits a distorted octahedral geometry, which in this case is coordinated to two THF molecules and an iodine atom. To explore the coordination behaviour of the previously mentioned compounds **29** and **30**, they were reacted with EuI_2 and YbI_2 in acetonitrile at room temperature. While the reactions with **29** yielded the sandwich compounds $[\{EtAl(6\text{-}Br\text{-}2\text{-}py)_3\}_2Eu]$ (**34**) and $[\{EtAl(6\text{-}Br\text{-}2\text{-}py)_3\}_2Yb]$ (**35**) (see Scheme 5b), the reactions with the CF_3 analogue **30** were not successful. This is due to the steric

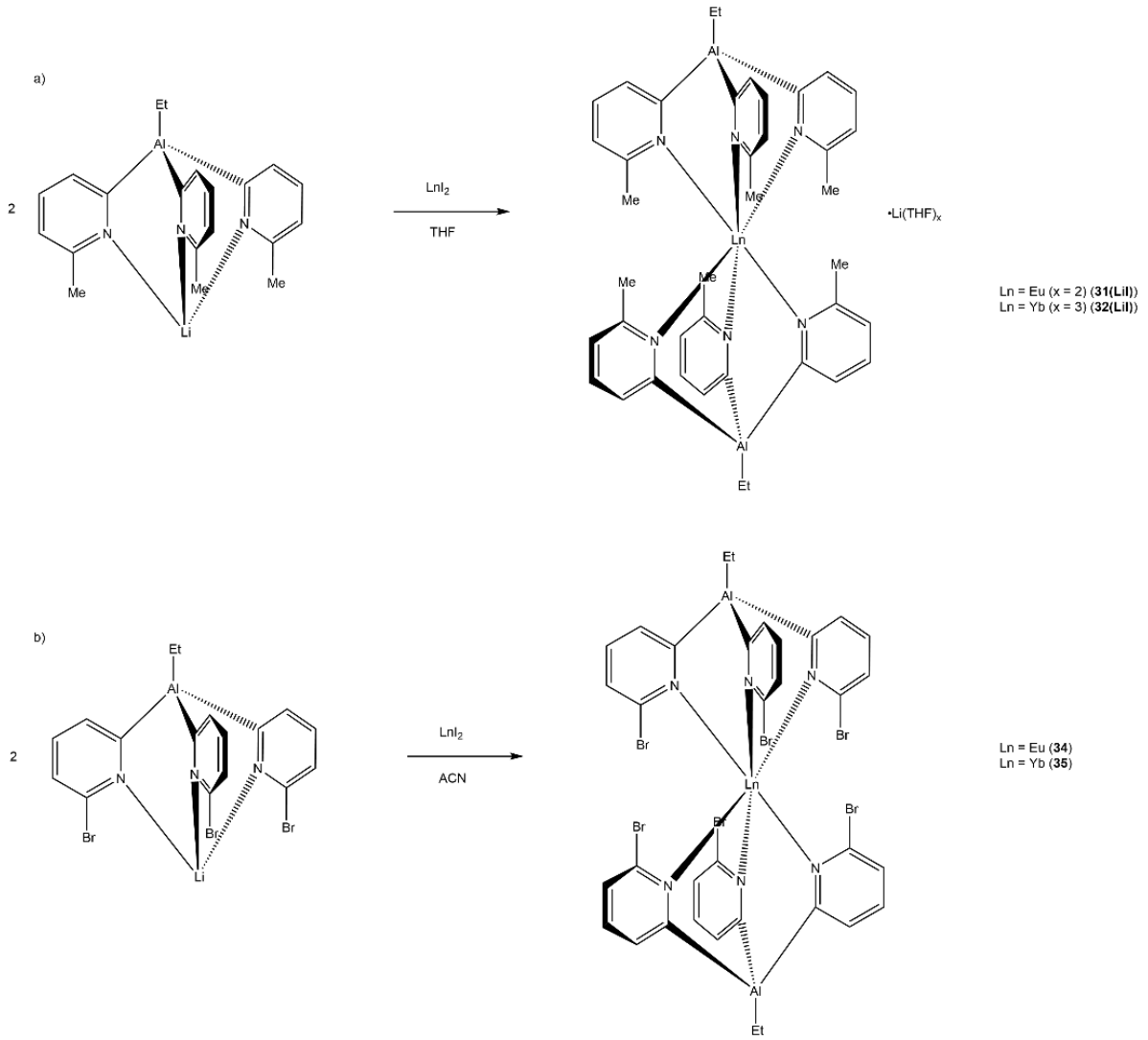

Scheme 5. Structure of the a) solvated complexes **31(LiI)** and **32(LiI)**, and the b) unsolvated 6-bromo analogues **34** and **35**

hindrance presented by the CF_3-pyridyl groups, together with the electron-withdrawing nature of these groups. Evidence of the lower coordination ability towards metals when changing the CH_3 groups to Br is seen by the Eu–N bond lengths found for **34**. Even though the geometry of the Eu^{II} ion is similar to those found for complexes **31**, and the van der Waals radii of Br is smaller than the one of the CH_3 groups, the Eu-N lengths are greater in **34** than in **31** analogue, presumably because of the electron-withdrawing effect of the Br-atoms that consequently lower the donor ability of the aluminate.

Post-functionalisation of the aluminates can also be used to obtain heteroleptic complexes, which can be used for various applications. First attempt on this was performed reacting complex [EtAl(6-CF_3-2-py)$_3$Li] (**30**) with 1-2 equivalents of water, which led to the formation of the [EtAl(6-CF_3-2-py)$_2$(OH)]$^-$ (**36**) anion (see Figure 11a), and was closely followed by the same reaction but using [EtAl(6-Br-2-py)$_3$Li] (**29**) as the aluminate precursor.[23] The latter gave a similar Al–OH bonded dimer [{EtAl(6-Br-2-py)$_2$(OH)}Li]$_2$ (**37**) (see Figure 11b). The stabilisation of an OH group in **37** is due to the location of the OH in a cleft within the structure of the dimers. To confirm that tris(2-pyridyl) aluminates can be used as general precursors for these type of heteroleptic compounds, reactions with alcohols were also performed. The reaction of MeOH with [EtAl(2-py)$_3$]Li·THF (**10**) and [EtAl(6-Br-2-py)$_3$Li] (**29**) gave [{EtAl(2-py)$_2$(OMe)}Li]$_2$ (**38**) and [{EtAl(6-Br-2-py)$_2$(OMe)}Li]$_2$ (**39**), respectively (see Figure 11c).

Having tris(pyridyl) aluminates as building blocks for making heteroleptic compounds presents a huge advantage, as the tuning of the steric and donor characteristics of the aluminate ligand is simple. Moreover, the introduction of chiral amines or alcohols is also facile.[23] The non-chiral [EtAl(6-Me-2-py)$_3$Li] (**17**) aluminate can be used as a reagent for the determination of enantiomeric excess of chiral alcohols by ^{1}H and ^{7}Li NMR spectroscopy.[25] The formation of the heteroleptic dimers in reactions of the aluminate with chiral alcohols allows the discrimination between racemic and enantiomerically pure alcohols. Due to the thermal stability and the possibility of storing it under N_2 indefinitely, aluminate **17** is considered to be a good fit for laboratory use.[25]

a)

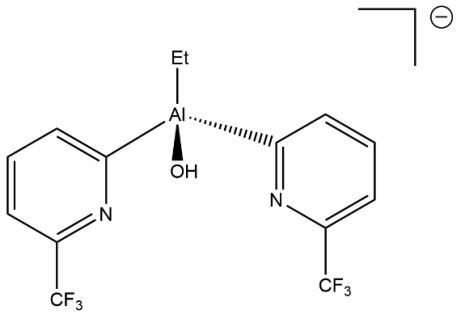

36

b)

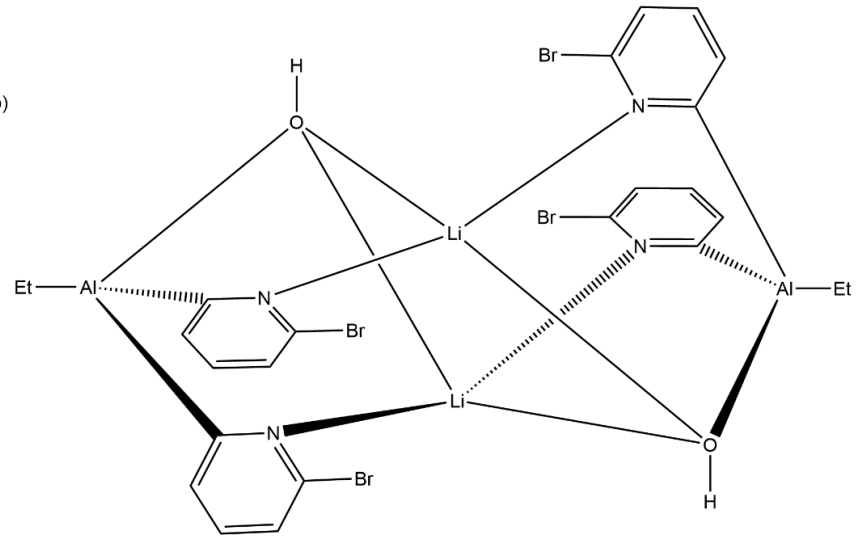

37

c)

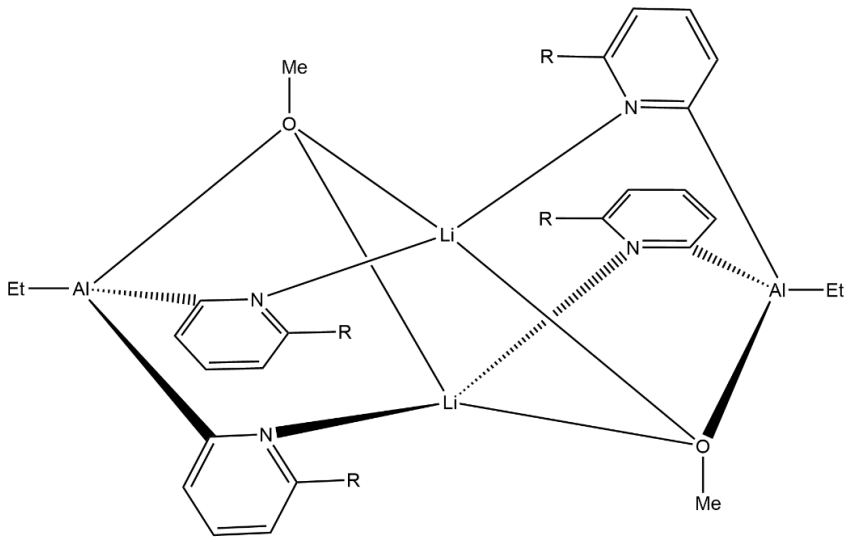

R = H (**38**)
R = Me (**39**)

Figure 10. Structures of compounds **36** (a), **37** (b) and **38** – **39** (c)

Additional experiments regarding the introduction of aldehydes and carboxylic acids into the [EtAl(6-Me-2-py)$_3$]$^-$ unit were also carried out. Interestingly, the reaction of **17** with benzaldehyde results in the desymmetrization of the methyl groups in the 6-position of the pyridyl rings, which indicates that compound **17** could have further future potential in chiral discrimination of chiral aldehydes.[26] It is also possible to engineer chirality into the aluminates themselves.[27] The stepwise reaction of the **17** with two different alcohols produces 'chiral-at-aluminium' aluminates, where the Al bridgehead is bonded to an Et group, a 6-methyl-2-pyridyl ligand, and to two different alkoxide groups (OR_1) and (OR_2).

Aims of the Project

It can be seen from the previous discussion that there has already been significant development of the coordination chemistry of tris(2-pyridyl) aluminates and of their reactivity and post-functionalisation. The primary focus of this report is on the synthesis and investigation of bis(2-pyridyl) aluminate complexes, which have so far not been explored in the literature (see Figure 11). As such, this is a new area of chemistry in this field. The presence of only two 2-pyridyl groups will clearly lead to bidentate arrangements and this modification should have a large effect on the metal coordination environment and their potential use in catalysis.

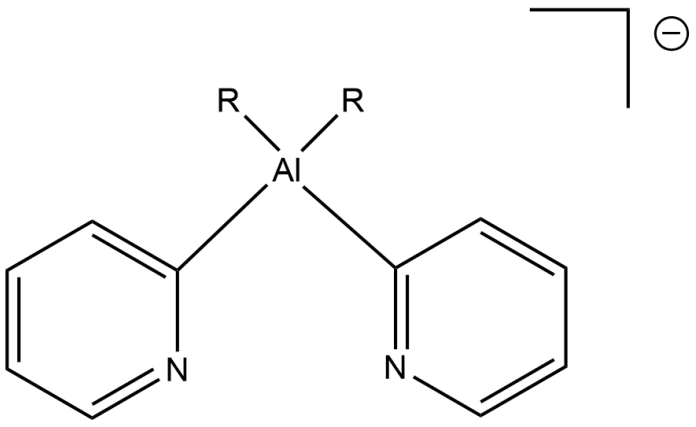

Figure 11. General structure of bis(2-pyridyl) aluminates

2. Results and Discussion

2.1. Aluminates

Reacting 2-bromo-6-methylpyridine with ^{n}BuLi (1:1 equivalents), followed by reaction with the commercially available precursor Me_2AlCl (2:1 equivalents) at –78 °C in THF gave an orange solution. The solvent of the reaction was removed in vacuo until some precipitate was observed, which was then gently heated until it redissolved and the solution was stored at –14 °C for almost a month. As the appearance of crystals was not observed, it was decided to change the solvent to toluene. This produces a precipitate, which can be filtered through Celite. The precipitate is the side product of the reaction, LiCl, which is soluble in THF but not soluble in toluene. Once filtered, the solvent was removed in vacuo until precipitate was observed and resolvation was attempted by gently heating the solution. However, heating did not result in dissolution of the product, which required the addition of a minimal amount of THF get the compound back into solution. Storage of this solution at –14 °C for a week gave colourless crystals which were identified by X-Ray crystallography as [$Me_2Al(6\text{-Me-2-py})_2Li \cdot 2THF$] (**40**). It is worth mentioning that the isolation of the crystals was extremely difficult due to the presence of an orange oil, which resulted in poor elemental analysis. Nevertheless, the ligand was also identified by NMR spectroscopy.

Solid structure of the compound (see Figure 12) shows the aluminium bridgehead atom in a slightly distorted tetrahedral structure (range 106.98(11)-113.70(8)°), which is coordinated to two methyl groups and two methyl-substituted pyridyl ligands. These pyridyl ligands also coordinate a Li^+ cation by the N-atoms. Expectedly, this Li^+ cation coordinates two THF molecules to reach the four coordination number, which is more stable than three. Meanwhile, the tris(2-pyridyl) analogue (**16**) just coordinates one THF molecule (See Figure 13).[28] Obviously, the change in the molecule from a tris(pyridyl) to a bis(pyridyl) compound has some effect on the structure of the new ligand. Firstly, the C_{Me}–Al distances for the new bis(pyridyl) compound are slightly longer [1.996(2) -2.000(2) Å] than that found for the tris(pyridyl) single C_{Me}–Al distance [1.981(2) Å]. This expansion is probably due to the increase in the steric hindrance created by the presence of two methyl groups instead of one, as observed for the [$MeAl(6\text{-Me-2-py})_3Li \cdot THF$] (**16**) ligand. Moreover, the C_{py}–Al distance is also longer for **40** [2.028(2)-2.030(2) Å] in comparison with compound **16** [2.003(2)-2.025(2) Å], which is probably due to the same reason, that is, the additional Al-Me group. The N–Li distances [2.052(3)-2.068(3) Å] are shorter than those seen for **16** [2.095(4)-2.195(4) Å], as well as the Li-O distances [1.971(3)-1.978(3) Å], in opposition to 1.997(4) Å for **16**. This suggests that the removal of a pyridyl ligand in **40**, with the subsequent Me group attached to the 6-position, reduces the steric hindrance around the Li^+ cation, in comparison to **16**, for which the coordination of the THF to the cation is more complicated

given the three py-Me groups. Thus, it can be concluded that the slightly less bulky THF groups help reduce the N-Li and Li-O distances, bringing the different moieties slightly closer.

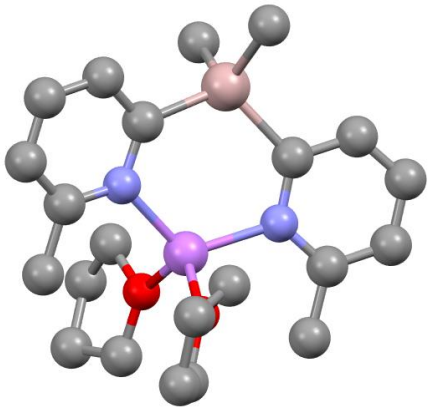

Figure 12. Solid-state structure of **40**. H-atoms omitted for clarity. Selected bond lengths (Å) and angles (°): C_{Me}–Al range 1.996(2)-2.000(2), C_{py}–Al range 2.028(2)-2.030(2), N–Li range 2.052(3)-2.068(3), Li–O range 1.971(3)-1.978(3), C_{py}–Al–C_{py} 113.70(8), C_{Me}–Al–C_{Me} 112.91(12), N–Li–N 118.36(15), O–Li–O 115.86(15). Colour code: C (grey), Al (pink), N (blue), Li (magenta), O (red).

The N–Li–N angle for **40** is 118.36(15)°, a significant increase to the range found for **16** [97.1(2)-114.4(2)°], for which, as noted above, the N-Li distances are greater.

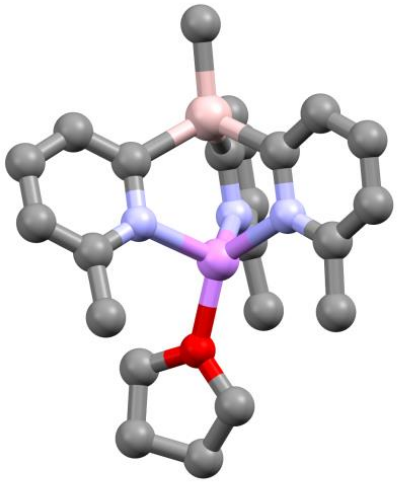

Figure 13. Solid state structure of **16**. H-atoms omitted for clarity. Selected bond lengths (Å) and angles (°): C_{Me}–Al 1.981(2), C_{py}–Al range 2.003(2)-2.025(2), N–Li range 2.095(4)-2.195(4), Li–O 1.997(4), C_{py}–Al–C_{py} range 104.19(9)-106.60(8), C_{Me}–Al–C_{py} range 112.2(1)-114.7(1), N–Li–N range 97.1(2)-114.4(2). Colour code: C (grey), Al (pink), N (blue), Li (magenta), O (red).

Further characterisation could be obtained by NMR spectroscopy. The ^{1}H NMR spectrum of ligand **40** shows 5 main signals at δ 7.95, 7.14, 6.60, 2.22 and 0.03 ppm (see Figure 14). Additional signals at δ 3.41, 1.25 and 0.30 ppm correspond to the two THF and silicon grease signals, respectively. The

doublet at δ 7.95 ppm corresponds to the C(3)–H pyridyl protons, while the one at δ 6.60 ppm corresponds to the C(5)–H protons. Meanwhile, the signal for the C(4)–H pyridyl protons is located at δ 7.14 ppm in the form of a triplet. Each of these signals integrate to 2 H. Moving to the aliphatic area two singlets are observed; the 6 H singlet at δ 2.22 ppm is due to the two methyl groups in the pyridyl rings, while the one at δ 0.03 ppm corresponds to the methyl-bridgehead groups, which also has a 6 H intensity.

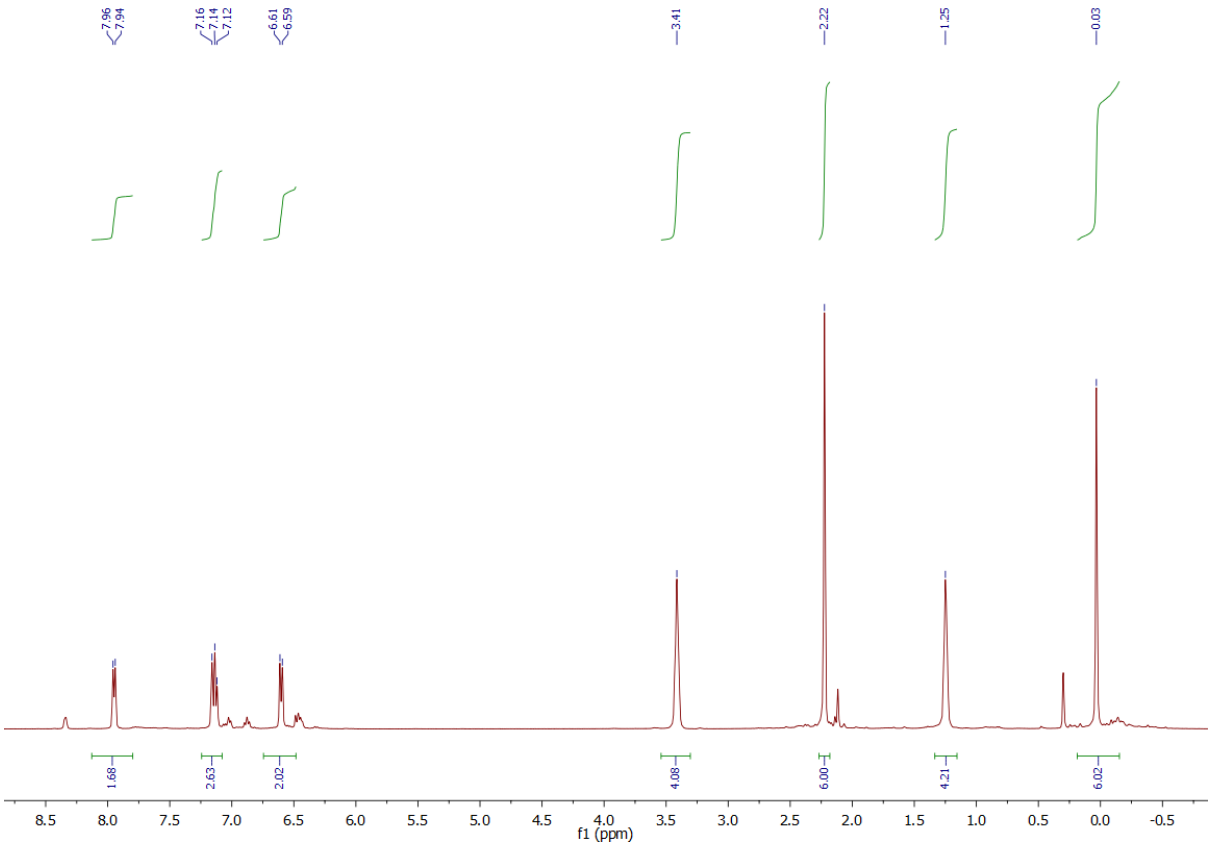

Figure 14. ^{1}H NMR spectrum of **40** (d_6-benzene)

Interestingly, in the ^{1}H NMR spectrum of **40** in d_6-benzene it can be observed that the THF signals only integrate to 4 protons each, which means that only one THF molecule is present in the molecule. However, the solid state structure of the compound shows two molecules coordinating to the Li^{+} cation. Using d_8-THF as the NMR solvent does not result in this observation, as some of the THF coordinating molecules are deuterated (see Figure 15).

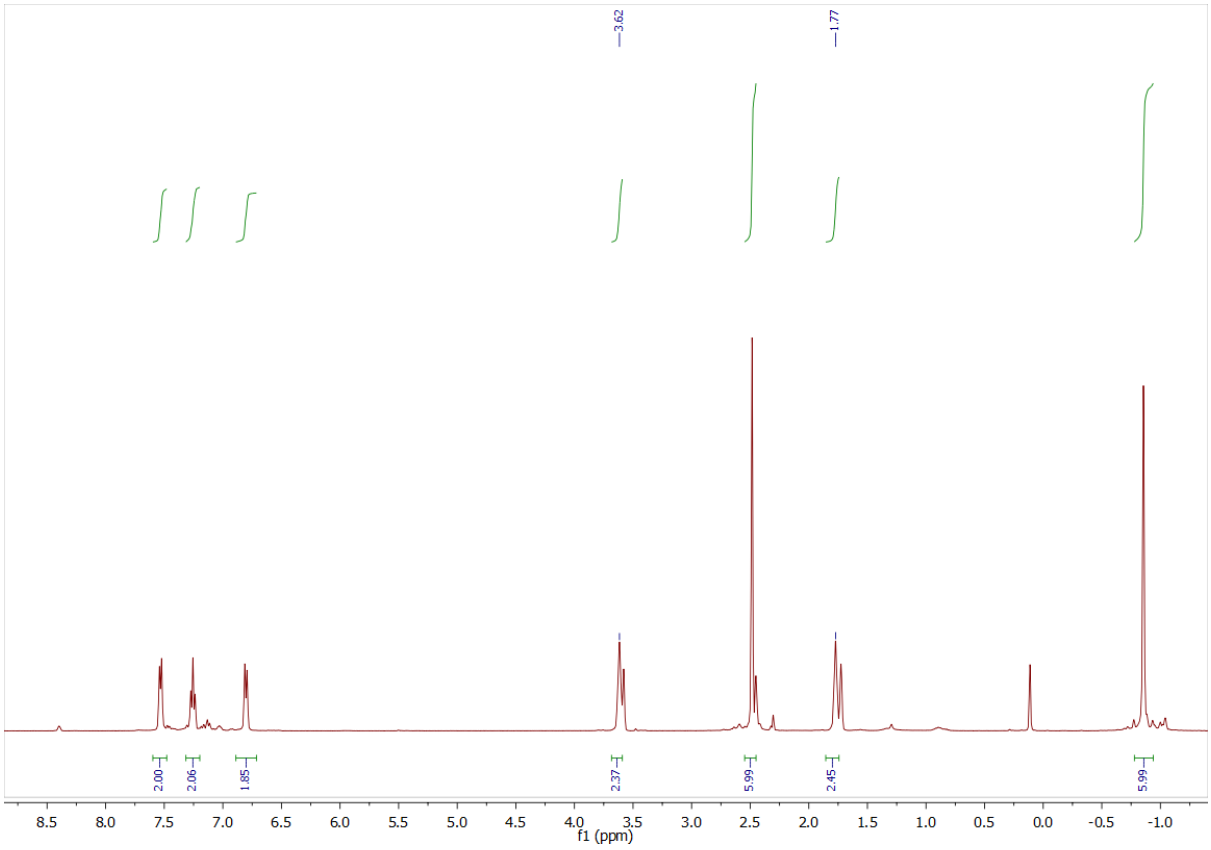

Figure 15. ^{1}H NMR spectrum of **40** (d_8-THF)

^{13}C NMR spectroscopy of the compound shows multiple signals (see Figure 16). With help of the ^{13}C DEPT spectrum and the ^{1}H-^{13}C HSQC and ^{1}H-^{13}C HMBC 2D NMR spectra it is possible to assign the signals that correspond to **40** (see Figures 17-19). Singlets at δ 133.4, 130.9, 119.7 and 24.6ppm show correlations with ^{1}H NMR peaks in the HSQC spectrum, which helps with the assignment. The δ 133.43 ppm peak can be assigned to the C(4) pyridyl carbon, whereas the δ 130.86 and 119.74 ppm peaks correlate with the C(3)–H and C(5)–H pyridyl protons, respectively. Moving into the upfield, the δ 24.61 ppm signal corresponds to the C(6)–Me carbons. Correlations in the HMBC spectrum allow the assignment of the signal of the C(6) carbons, which is located at δ 154.92 ppm. Peaks at δ 68.70 and 25.39 ppm correspond to the THF carbons. The C(2)–pyridyl carbon peak cannot be seen, presumably because of their proximity with the aluminium bridgehead atom resulting in very broad peaks. In fact, the Al-Me carbon peak is observed as a very broad signal at δ -9 ppm.

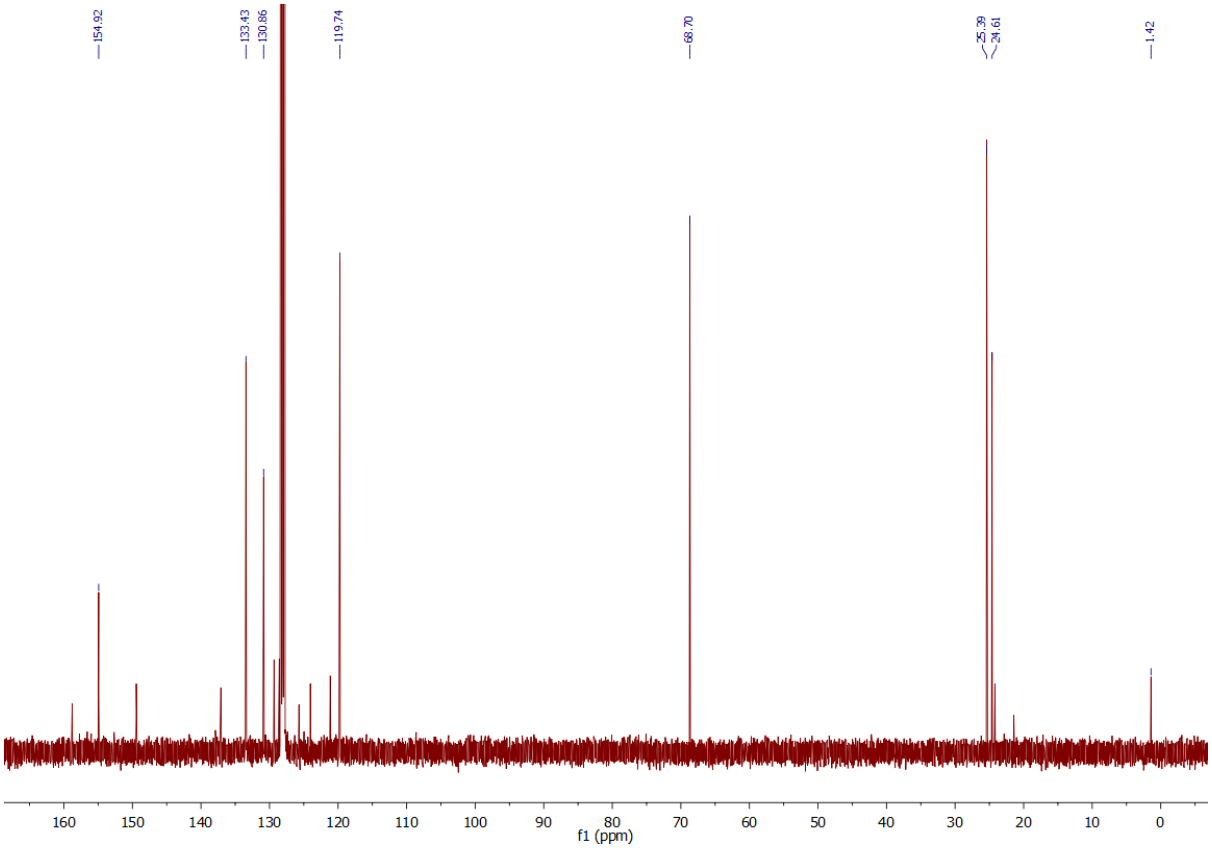

Figure 16. ^{13}C NMR spectrum of **40** (d_6-benzene)

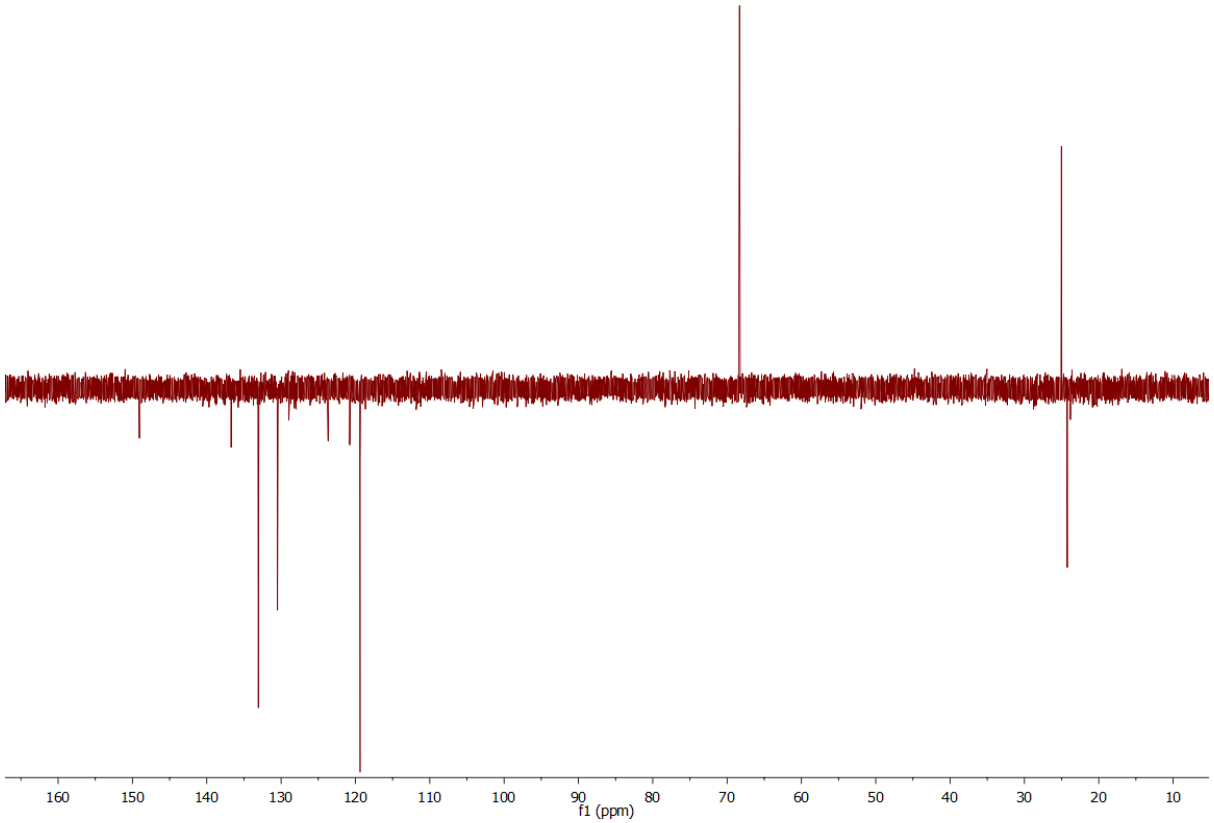

Figure 17. ^{13}C DEPT NMR spectrum of **40** (d_6-benzene)

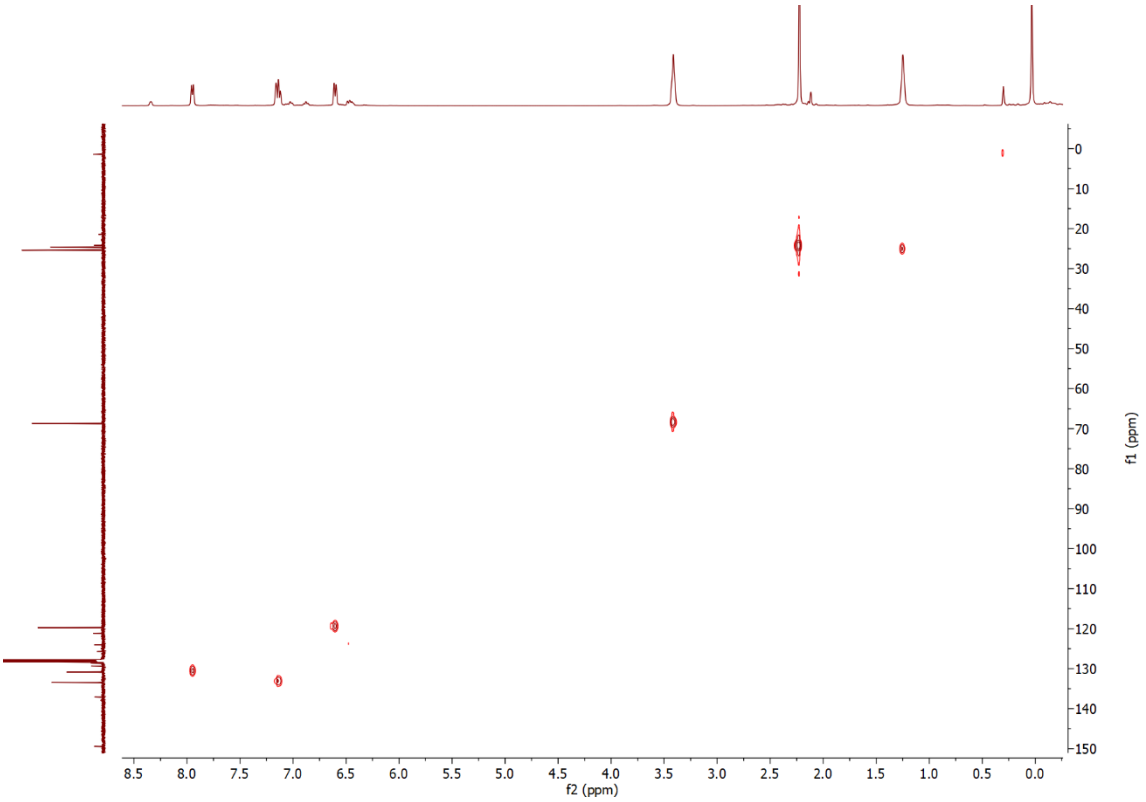

Figure 18. ^{1}H-^{13}C HSQC NMR spectrum of **40** (Colour code: red [CH, CH_3], blue [CH_2]) (d_6-benzene)

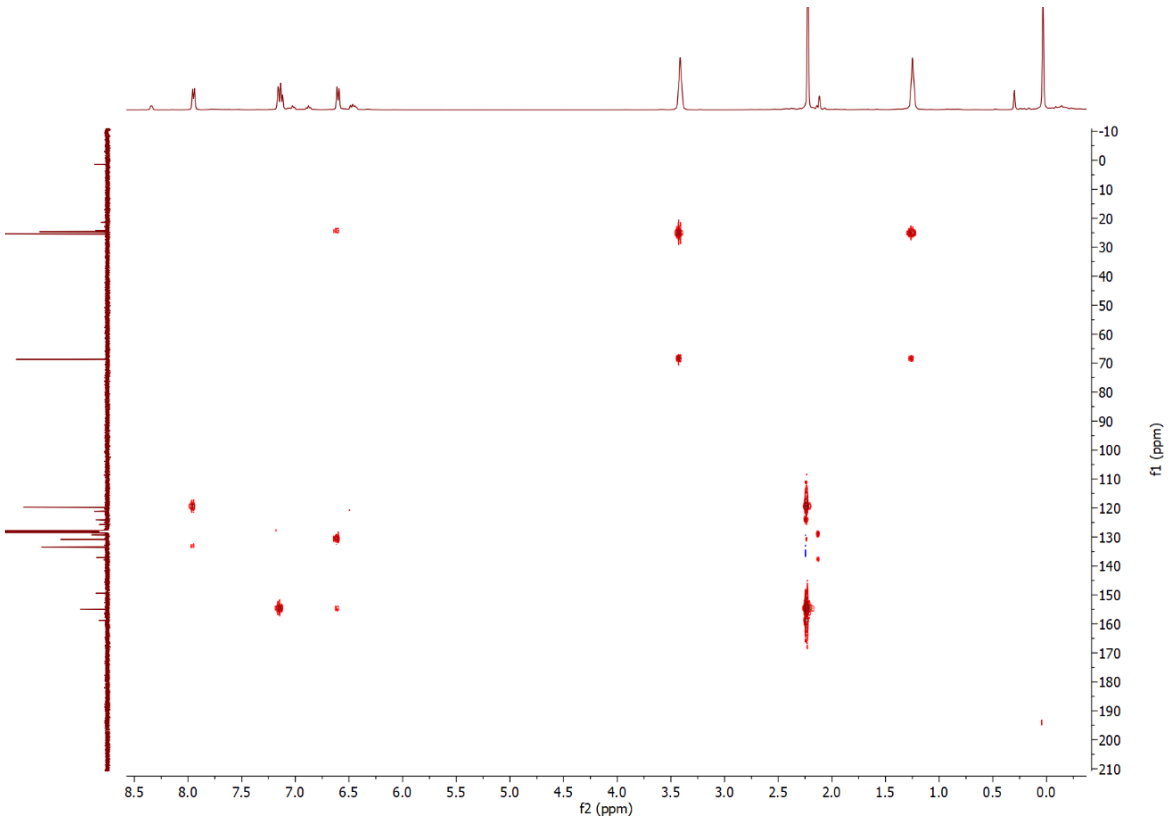

Figure 19. ^{1}H-^{13}C HMBC NMR spectrum of **40** (d_6-benzene)

^{7}Li and ^{27}Al NMR spectroscopy were also performed. In the ^{7}Li NMR spectrum (see Figure 20) a single peak at δ 1.21 ppm can be observed, which concludes that only one species with a coordinated lithium is present. The ^{27}Al NMR spectrum (see Figure 21) confirms that a 4-coordinated aluminium is present, as the sharp peak is located at δ 142.0 ppm.

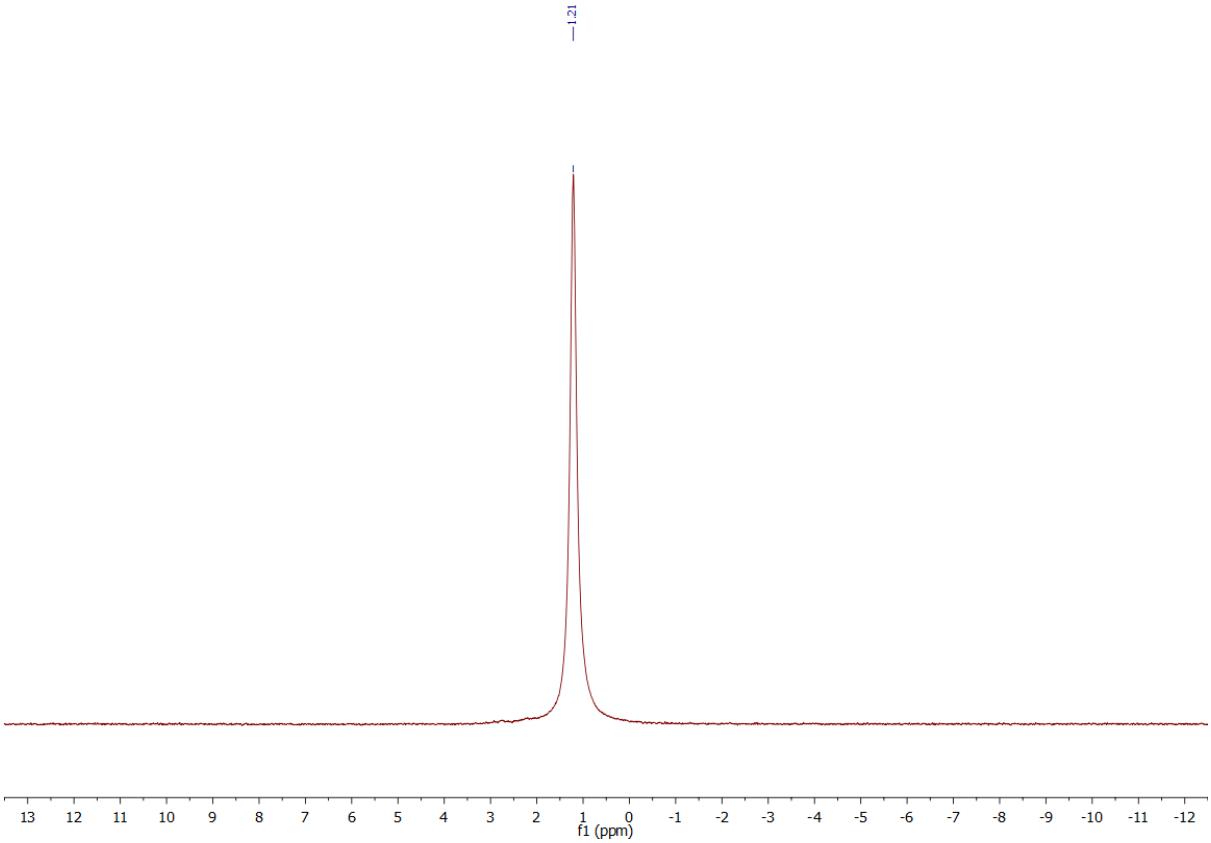

Figure 20. ^{7}Li NMR spectrum of **40** (d_8-THF)

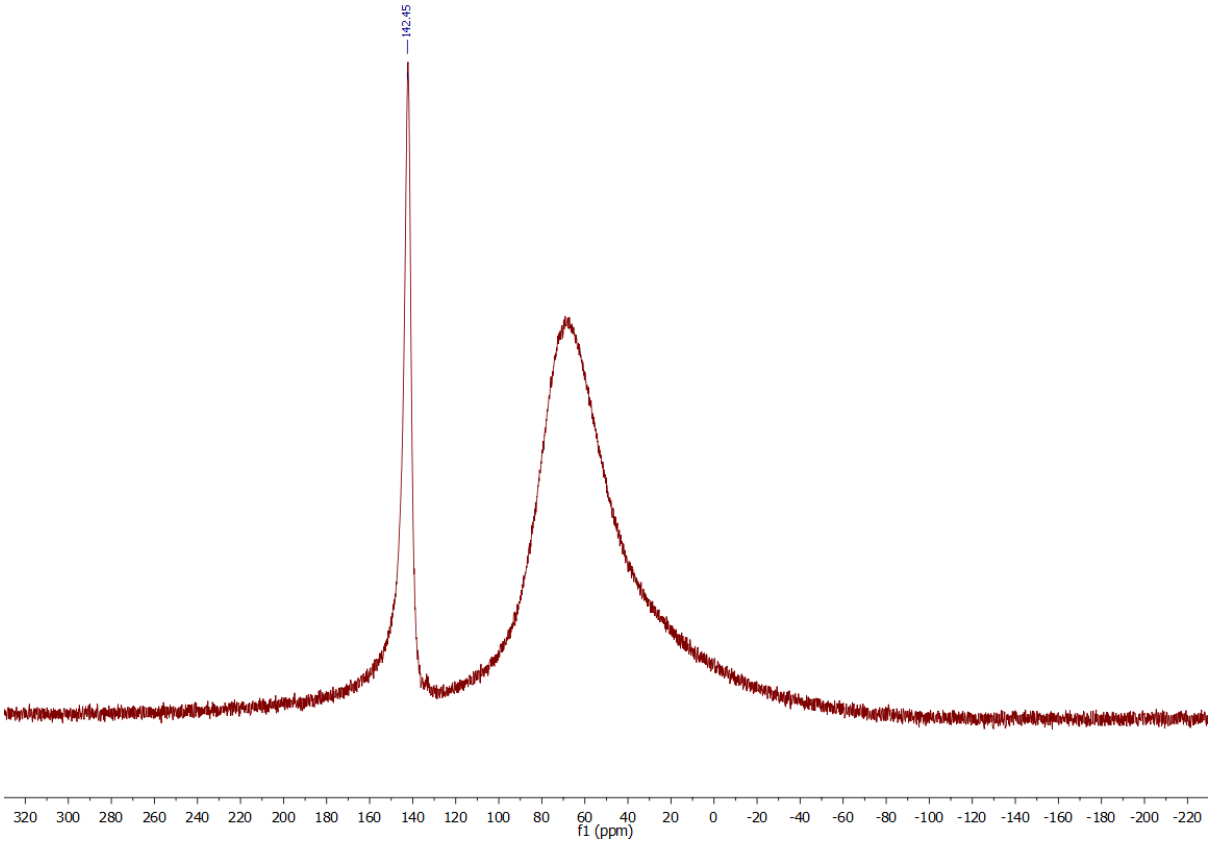

Figure 21. ^{27}Al NMR spectrum of **40** (d_8-THF) (Instrument signal at δ 70 ppm)

Some similar compounds with quinolyl ligands such as the [$Me_2Al(2\text{-}Me\text{-}8\text{-}qy)_2Li\cdot THF$] show that one of the Al–Me bridgehead groups interacts with the Li^+ cation.[29] Thus, it could be expected that a similar behaviour was encountered for compound **40**. For this reason, a ^1H-^7Li HOESY NMR experiment was done (see Figure 22).

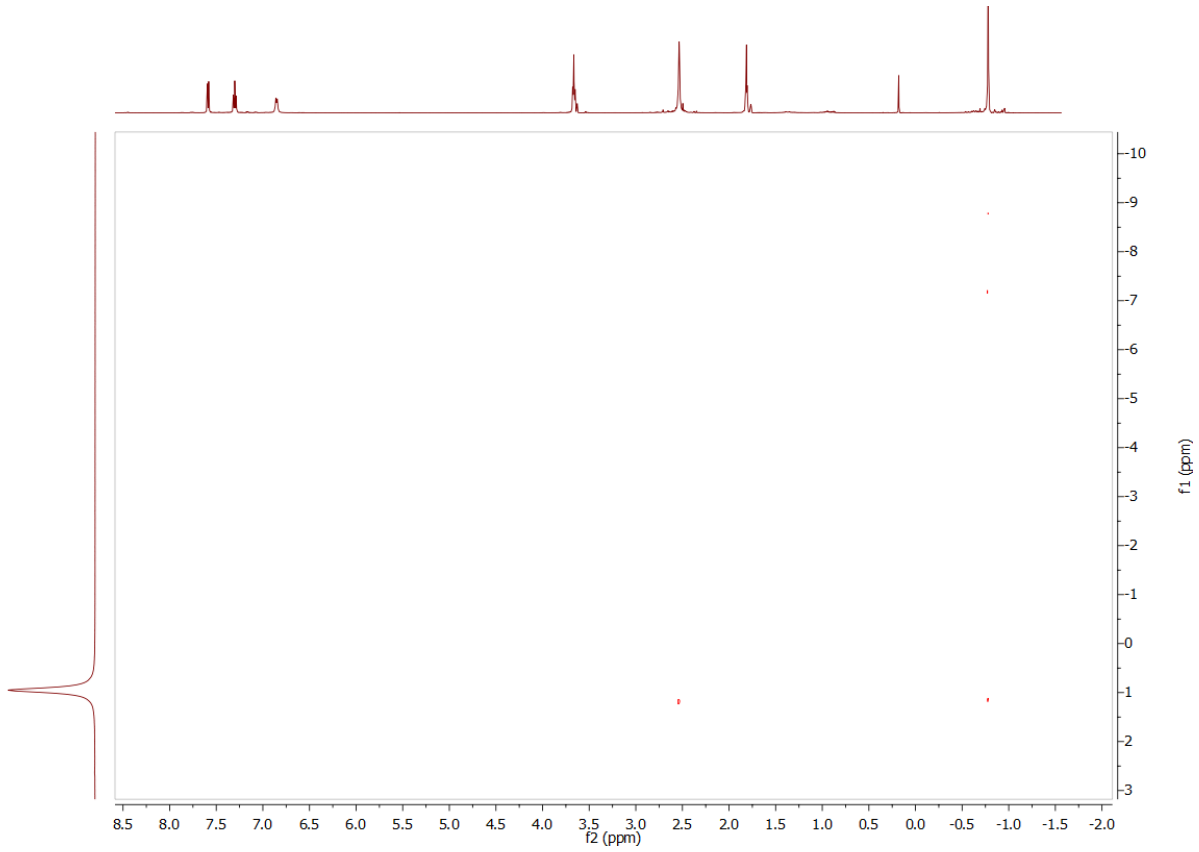

Figure 22. ^{1}H-^{7}Li HOESY NMR spectrum of **40** (d_8-THF)

As expected, a correlation between the ^{7}Li peak and the C(6)–CH_3 methyl groups is clearly seen, given the proximity of the methyl protons and the Li^+ cation (2.728 Å). Another cross peak is observed for the Li signal and the Al–Me singlet, however, it is not clear of whether it is caused by the actual proximity of the Al-CH_3 protons and the Li+ cation (4.285 Å) or the high intensity of the Al-Me signal, as some other signals are observed for this 1H peak. Although the results of the ^{1}H-^{7}Li HOESY NMR spectrum are not conclusive, it could be suggested that an interaction between the Al-Me protons and the Li^+ cation could be possible, as that found for the $[Me_2Al(2\text{-}Me\text{-}8\text{-}qy)_2Li{\cdot}THF]$[29] complex. This could be caused by the loss of a THF molecule, as observed in the ^{1}H NMR, and the consequent interaction of one of the Al-Me peaks with the Li^+ cation.

Reproducing the structure found for **40** with different R-bridgehead groups was attempted. Firstly, replacement of the methyl groups by ethyl groups was attempted to form $[Et_2Al(6\text{-}Me\text{-}2\text{-}py)_2Li{\cdot}2THF]$ (**41**). For that, 2-bromo-6-methylpyridine was reacted with ^{n}BuLi (1:1 equivalents) at –78 °C in THF, followed by reaction with the commercially available reagent Et_2AlCl (2:1 equivalents) also at –78 °C. After warming up the reaction overnight, the solvent from the orange solution obtained was removed *in vacuo*. The resulting orange oil was dissolved in toluene and filtered through Celite to remove LiCl.

Although recrystallization of the compound from toluene and THF was attempted, storage of the solution at –30 °C did not yield any crystals. However, NMR spectroscopy analysis from the crude product indicates that the expected product could have been formed.

The ^{1}H NMR spectrum of the crude light brown oil obtained after removing the solvent shows a multitude of peaks (see Figure 23). However, some of them fit in with the expected peaks for the compound, in terms of integration and multiplicity.

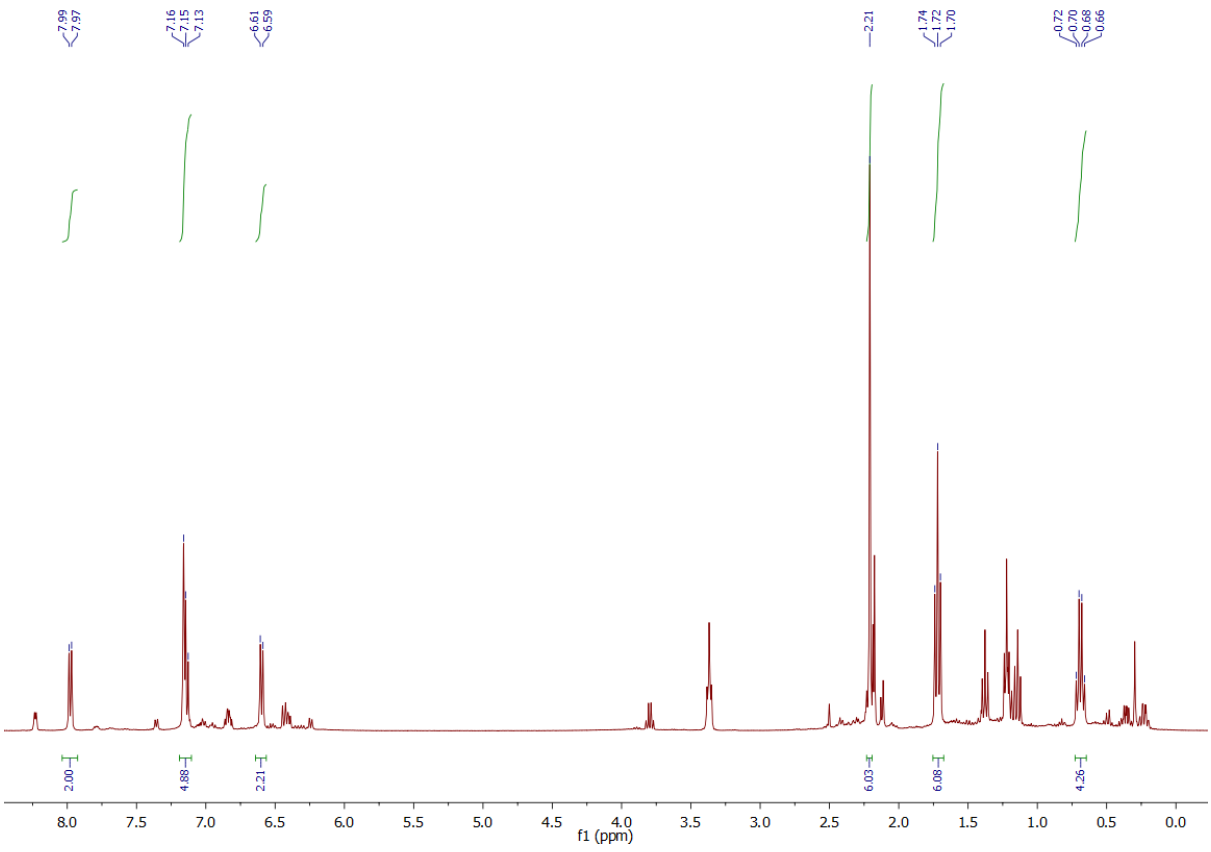

Figure 23. ^{1}H NMR spectrum of crude reaction mixture in attempt to make **41** (d_6-benzene)

In the aromatic region there are two doublets at *δ* 7.98 and 7.53 ppm, integrating for 2 protons each. These can be assigned to the C(3)–H and C(5)–H protons, respectively. The triplet found at *δ* 7.14 ppm in the middle of the two doublets, which also has an intensity of 2 H, can be assigned to the C(4)–H pyridyl protons. Moving to the upfield, a singlet at *δ* 2.21 ppm is observed, which corresponds to the methyl groups in the pyridyl rings. A direct consequence of the switch of the Al–R group is that now a triplet and quartet, which would correspond to the Al–CH_2–CH_3 and the Al–CH_2 protons respectively, are observed instead of the Me-singlet encountered for the previous compound **40**. The triplet is

located at δ 1.72 ppm and the quartet is at δ 0.69 ppm. Their integrals of 6 H and 4 H for the triplet and quartet match the expected results for the ethyl-bridgehead group. Given the existence of multiple signals in both the aromatic and aliphatic regions, a ^{1}H-^{1}H COSY NMR spectrum of the product was required to help assign the peaks (see Figure 24).

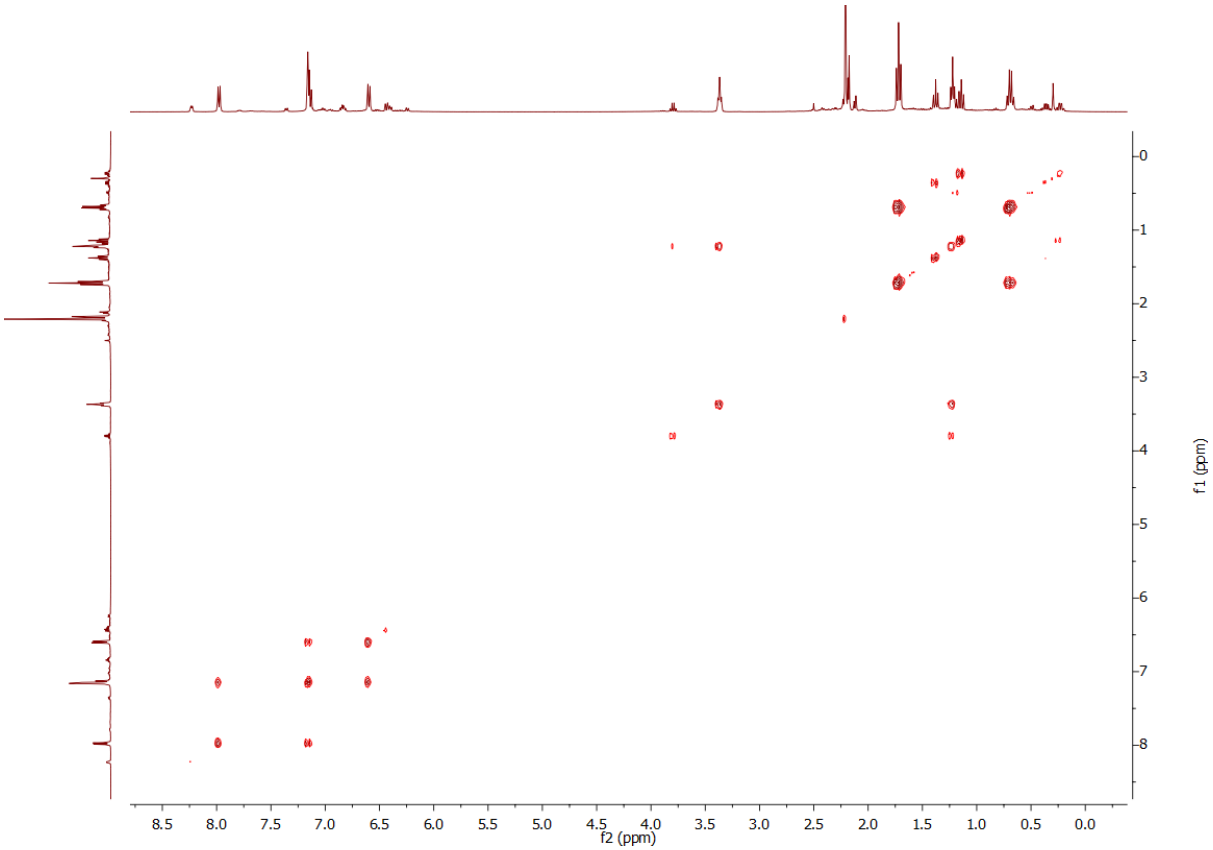

Figure 24. ^{1}H-^{1}H COSY NMR spectrum of crude reaction mixture in attempt to make **41** (d_6-benzene)

As expected, the ^{13}C NMR spectrum of the crude product shows a multitude of peaks (see Figure 25). However, with the help of ^{13}C DEPT, ^{1}H-^{13}C HMBC and ^{1}H-^{13}C HSQC NMR spectra, the different peaks could be assigned to the respective carbons in the compound.

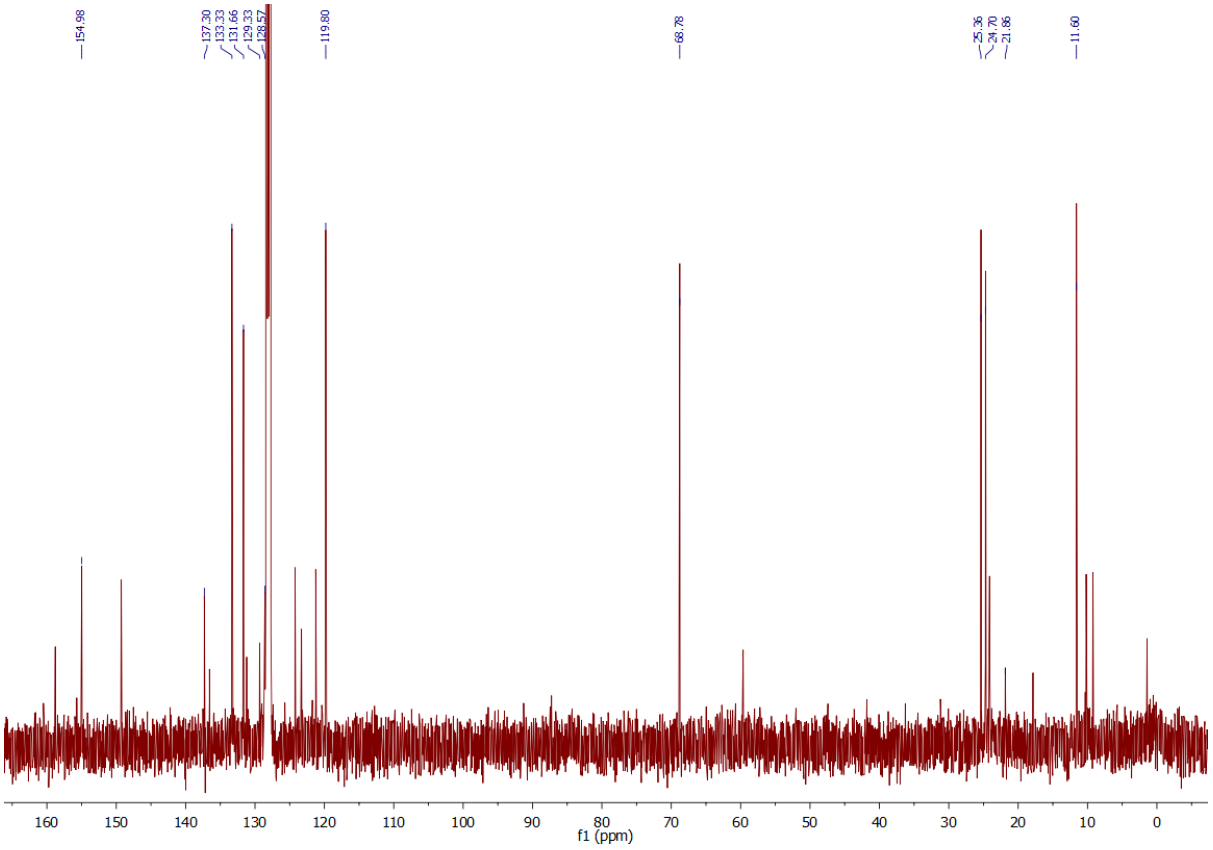

Figure 25. ^{13}C NMR spectrum of crude reaction mixture in attempt to make **41** (d_6-benzene)

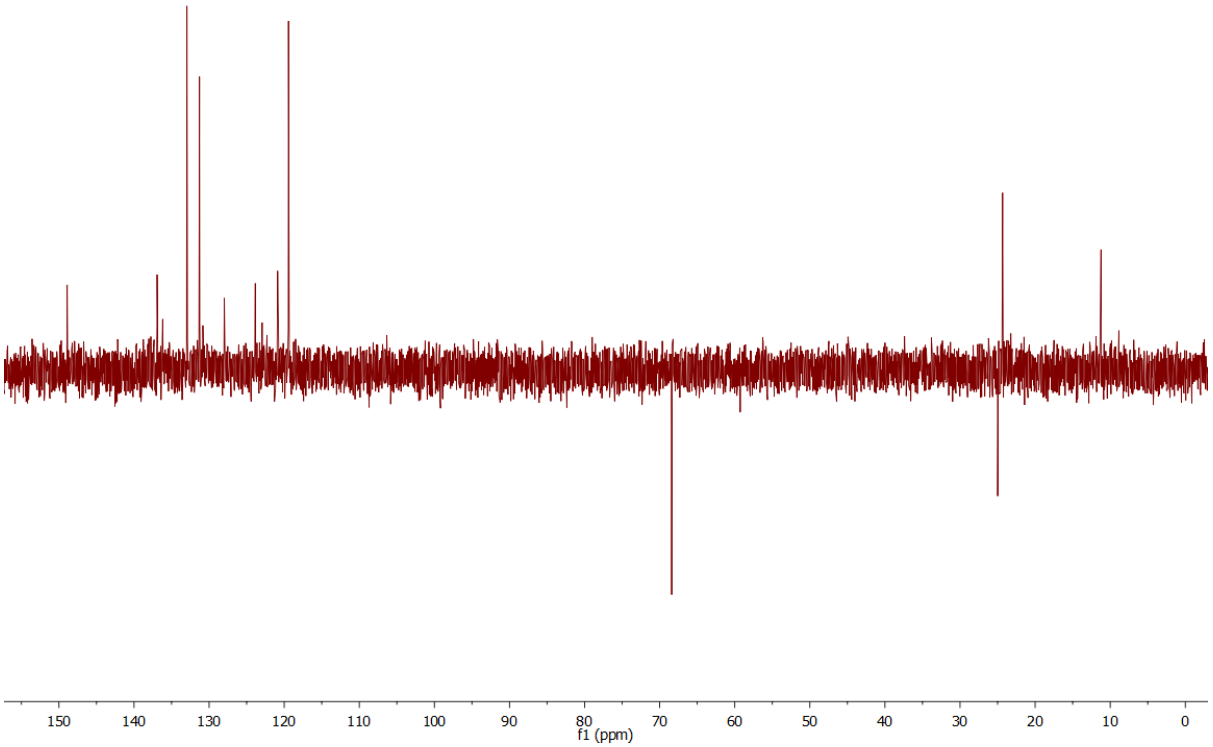

Figure 26. ^{13}C DEPT NMR spectrum of crude reaction mixture in attempt to make **41** (d_6-benzene)

Cross peaks in the ^{1}H-^{13}C HSQC NMR spectrum allow the assignment of the peaks at δ 133.3, 131.2, 119.8 and 11.6ppm to the C(4), C(3), C(5) and Al–CH_2–CH_3 carbons, respectively (see Figure 27). Not only are these peaks assigned, but also those corresponding to the different solvents such as THF or toluene. THF carbon peaks are located at δ 68.77 and 25.36 ppm, whilst the toluene peaks are at δ 137.30, 129.33, 128.56 and 21.85 ppm.

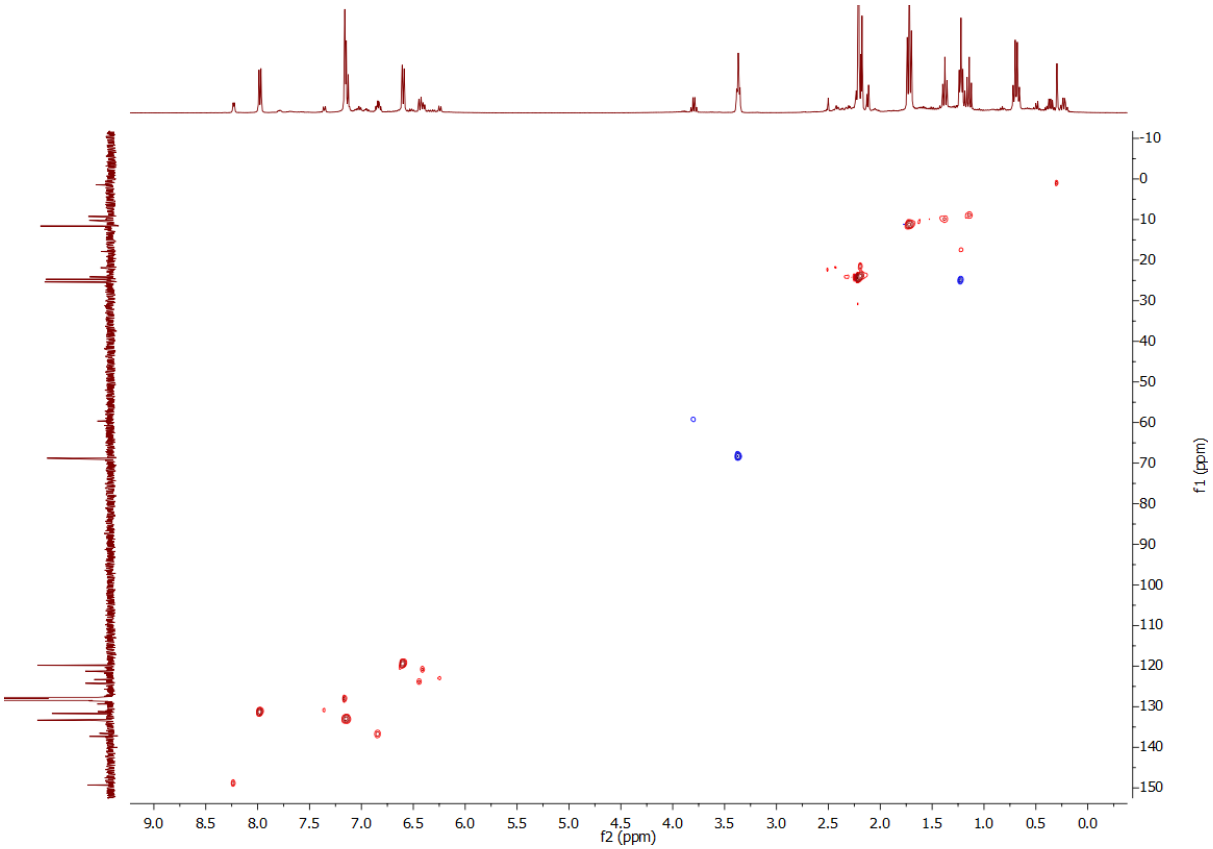

Figure 27. ^{1}H-^{13}C HSQC NMR spectrum of crude reaction mixture in attempt to make **41** (Colour code: red [CH, CH_3], blue [CH_2]) (d_6-benzene)

The last peak of the compound was able to be assigned by looking at the ^{1}H-^{13}C HMBC NMR spectrum (see Figure 28). The correlation between the δ 6.60 ppm doublet with the δ 154.97 ppm singlet in the ^{13}C NMR spectrum, although weak, leads to the conclusion that the latter is the signal for the C(6) pyridyl carbons. It should be noted that the C(2)–pyridyl carbons and the Al–CH_2 are not observed, presumably due to their proximity to the aluminium-bridgehead atom.

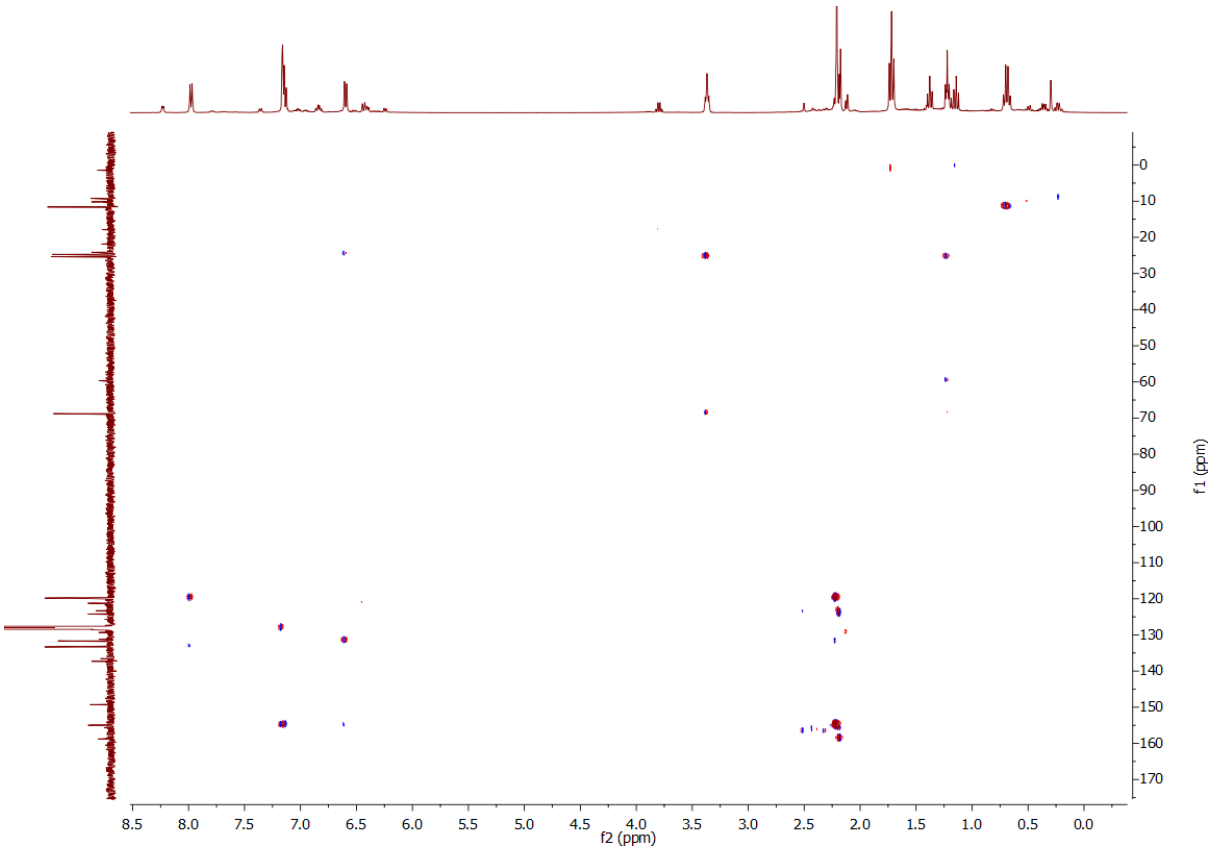

Figure 28. ^{1}H-^{13}C HMBC NMR spectrum of crude reaction mixture in attempt to make **41** (d_6-benzene)

As for the previous methyl analogue, ^{7}Li and ^{27}Al NMR spectroscopy were run in order to further characterize the crude reaction mixture. On the one hand, in the ^{7}Li NMR spectrum two singlets at δ 1.29 and 0.98 ppm are observed (see Figure 29). The existence of two singlets is not unexpected, since it has been seen in previous spectra where there is more than one species present. The singlet at δ 1.29 ppm is, however, the predominant one. On the other hand, the ^{27}Al NMR spectrum shows a single peak at δ 142.8 ppm, indicating a four-coordinated Al (see Figure 30). In this case, the aluminium peaks from different molecules could be overlapping.

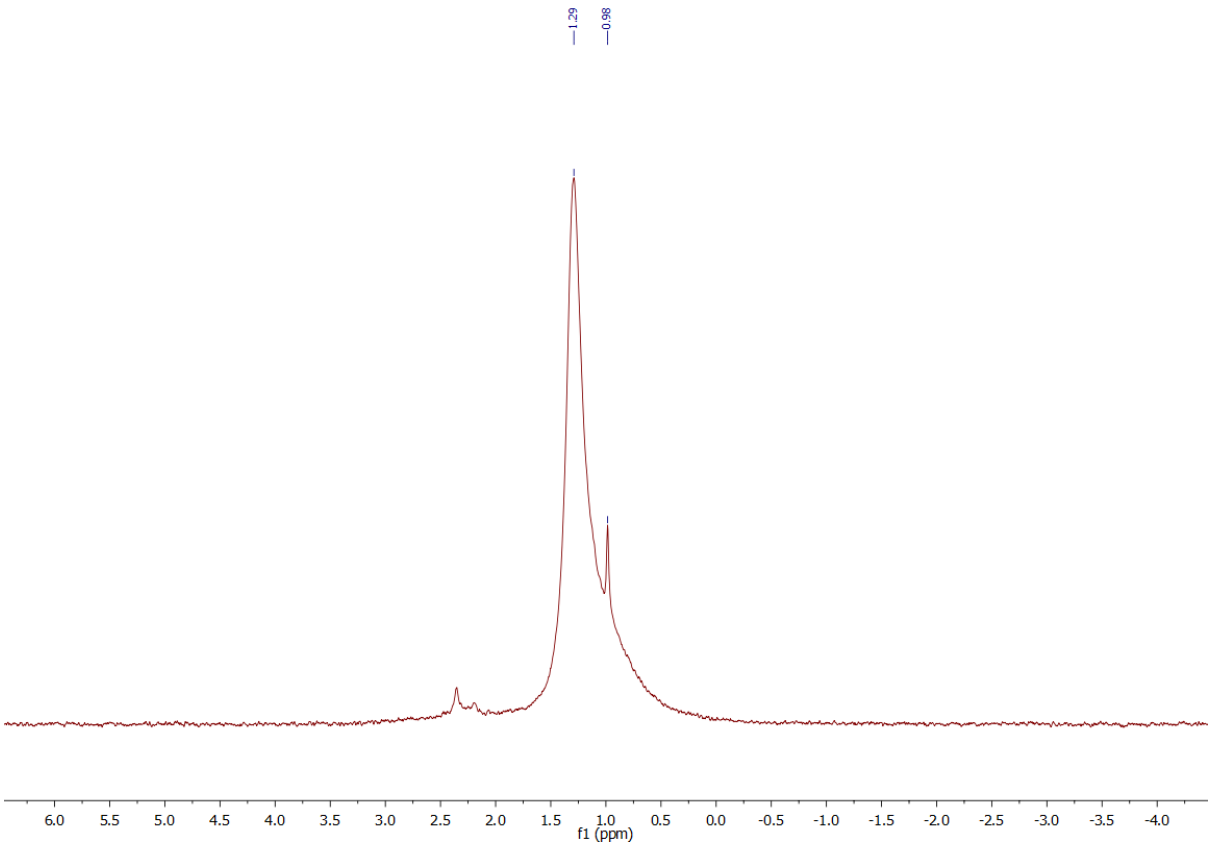

Figure 29. ^{7}Li NMR spectrum of crude reaction mixture in attempt to make **41** (d_8-THF)

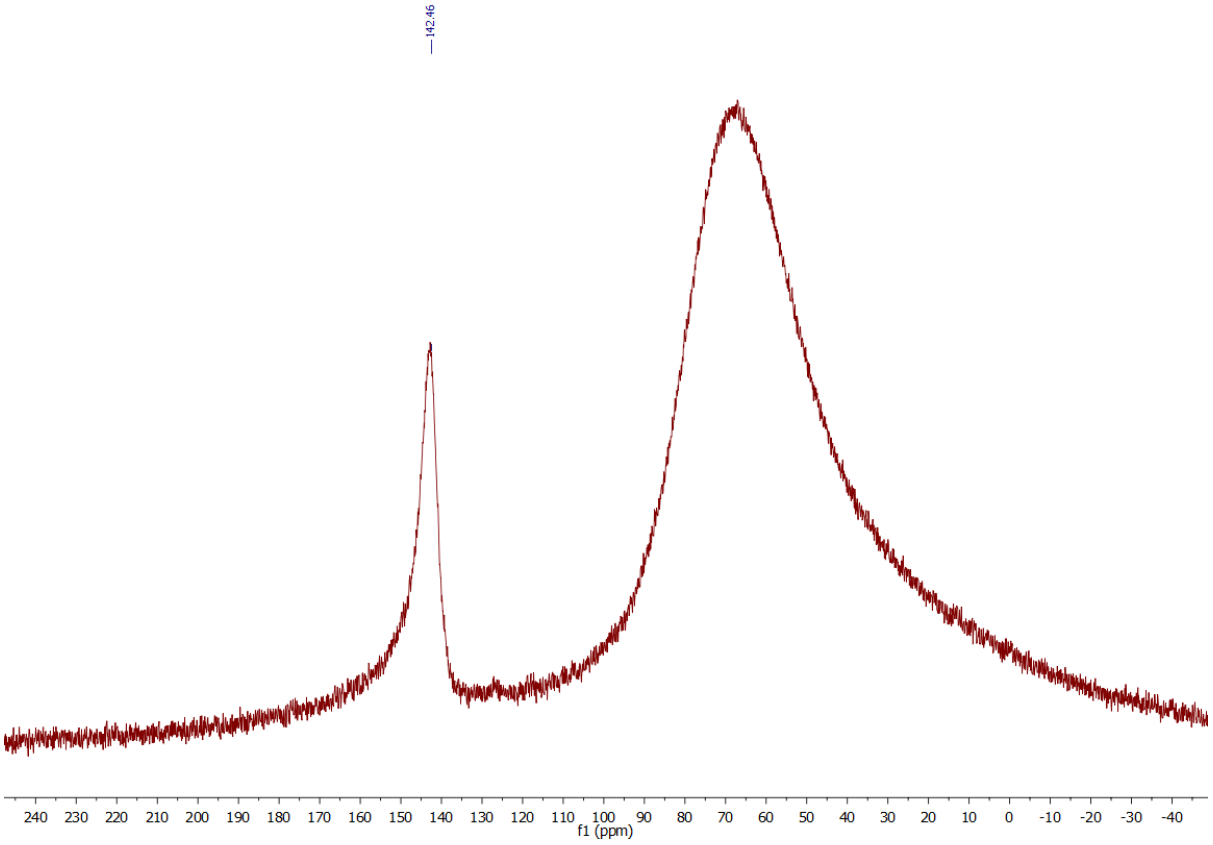

Figure 30. ^{27}Al NMR spectrum of ^{7}Li NMR spectrum of crude reaction mixture in attempt to make **41** (d_8-THF) (Instrument signal at δ 70 ppm)

Not only the reaction with Et_2AlCl was attempted, but also with R_2AlCl (R = Ph, ^tBu). In these cases, the reactants had to be synthesized, since they are not commercially available. For that, the corresponding lithiates RLi (R = Ph, ^tBu) were reacted with $AlCl_3$ in a 2:1 ratio for 1.5 hours at –78 °C in THF (see scheme XX).

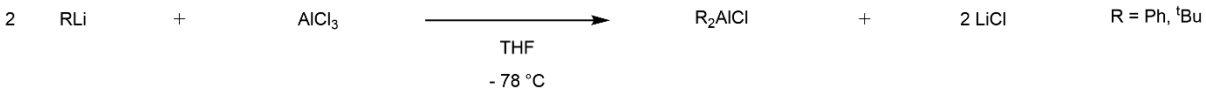

Scheme 6. General procedure for the synthesis of R_2AlCl (R = Ph, ^tBu)

The resulting products were used immediately to the solution formed by the reaction of 2-bromo-6-methylpyridine with ^nBuLi (1:1 equivalents) at –78 °C. After stirring for 16 hours and allowing the solution to warm up to room temperature, the solvent was substituted by toluene. Afterwards, the suspension was filtered through Celite to remove the LiCl formed in both reactions (formation of R_2AlCl and general reaction). Recrystallization from toluene was attempted in both cases, but no crystalline material could be obtained. However, ^1H NMR spectroscopy analysis was performed.

As expected, multiple peaks are observed in the ^1H NMR spectrum for the reaction with Ph_2AlCl (**42**) (see Figure 31).

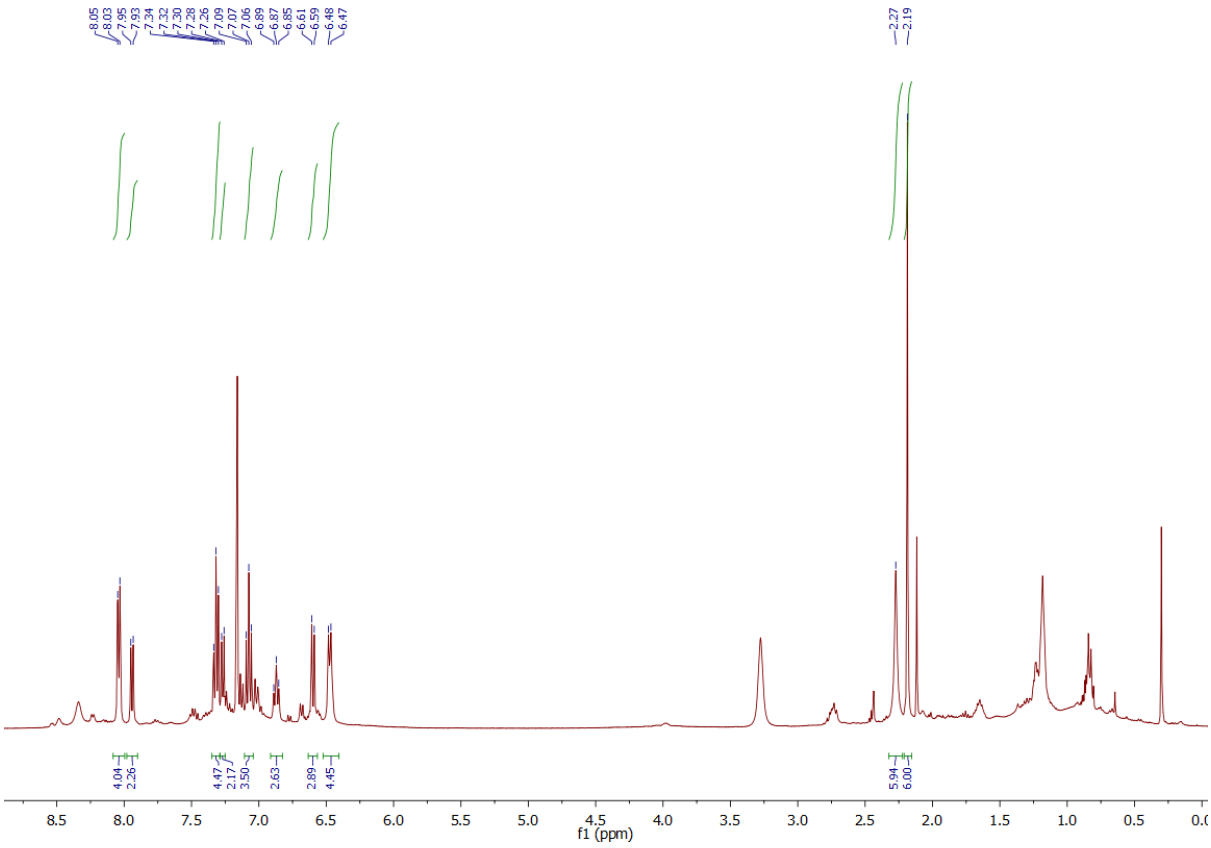

Figure 31. ^{1}H NMR spectrum of crude reaction mixture in attempt to make **42** (d_6-benzene)

When looking closer to the aromatic region different doublets and triplets are observed (see Figure 32). Given all the different types of aromatic protons in the expected molecule (pyridine and phenyl rings), it is not surprising to see that many peaks. For their assignment, a ^{1}H-^{1}H COSY NMR spectrum was necessary, to see how the different sets of signals couple to each other (see Figure 33).

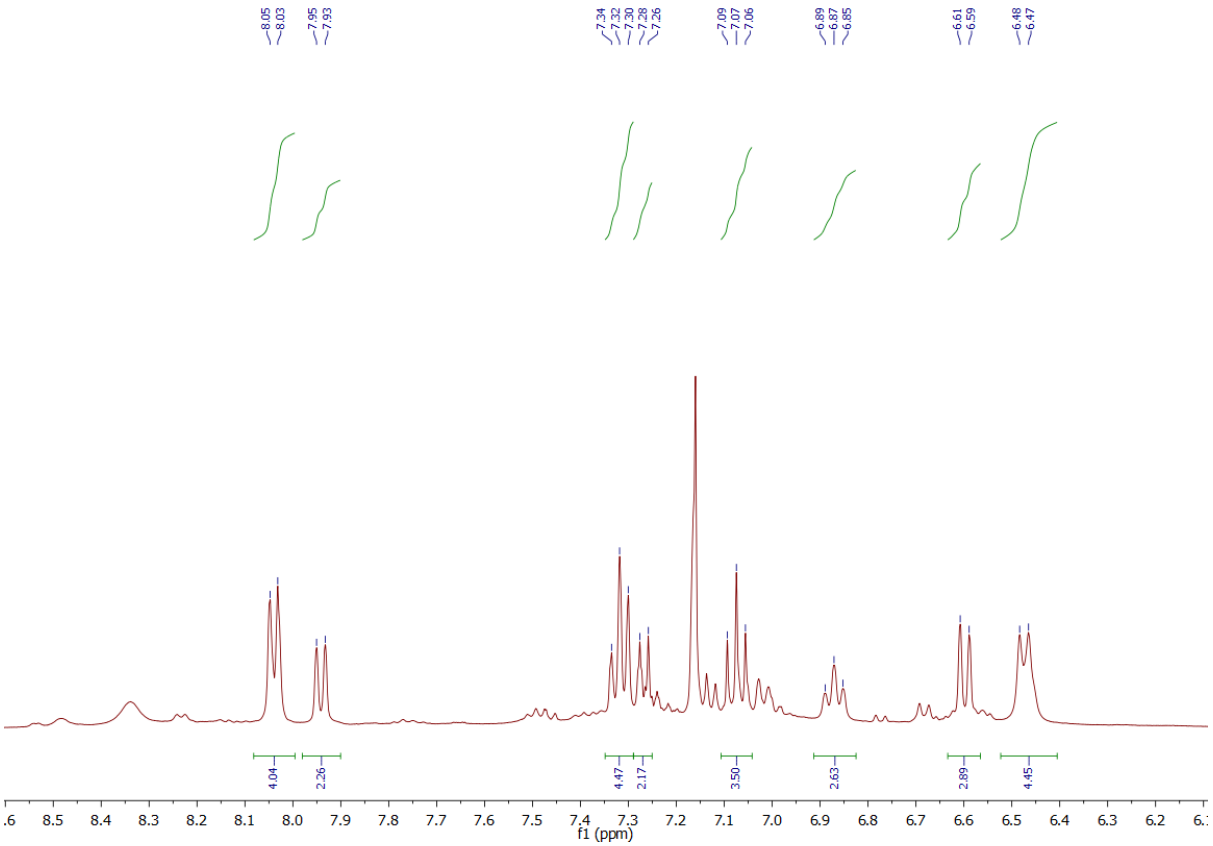

Figure 32. Aromatic region of the ^{1}H NMR spectrum of crude reaction mixture in attempt to make **42** (d_6-benzene)

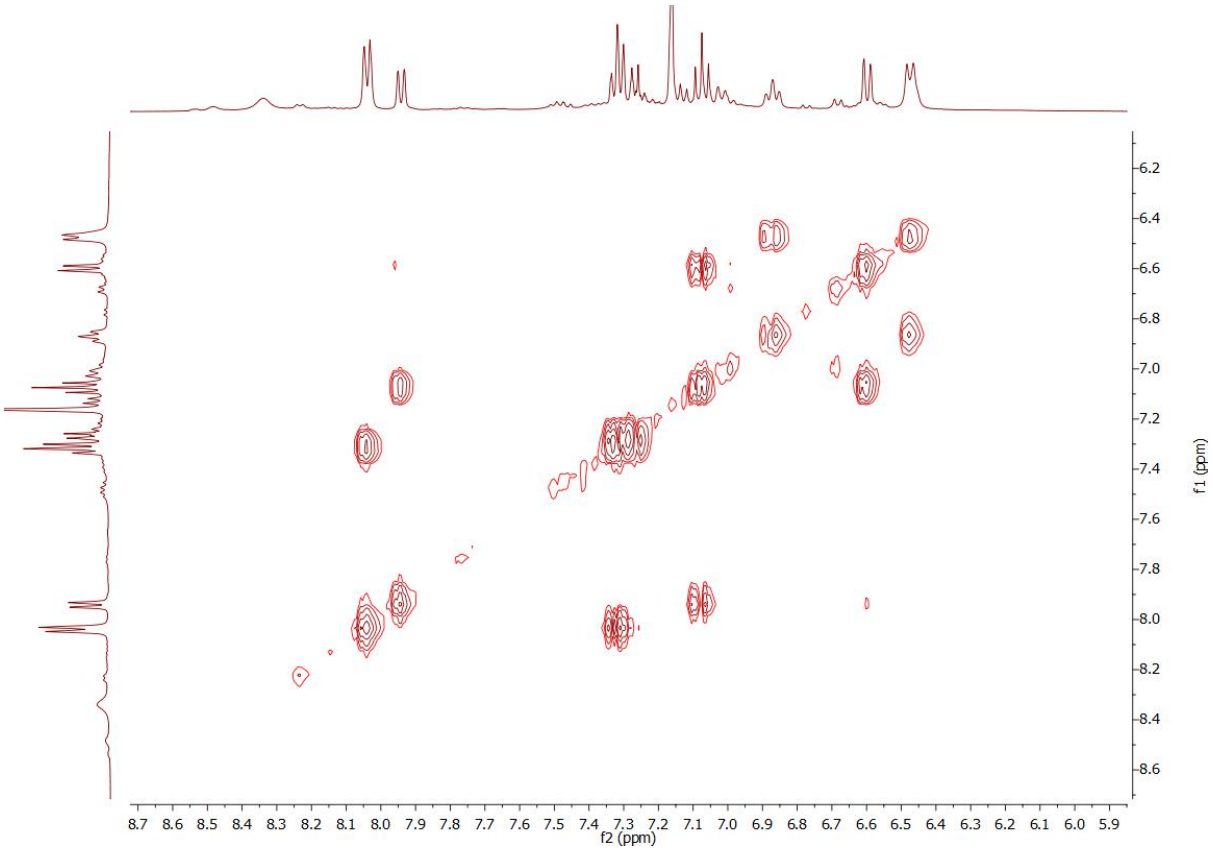

Figure 33. ^{1}H-^{1}H COSY NMR spectrum of crude reaction mixture in attempt to make **42** (d_6-benzene)

After analysis of the ^{1}H-^{1}H COSY spectrum, signals at δ 7.94, 7.07 and 6.60 ppm (doublet, triplet and doublet, respectively), can be assigned to a single pyridyl moiety. Meanwhile, peaks that can be attributed to a phenyl group can be found in the spectrum as well. There is a clear cross peak between the doublet at δ 8.04 ppm and the triplet at δ 7.32 ppm. Although weak, an additional correlation is found between the latter and the signal at δ 7.27 ppm. As seen in Figure 33, the triplet at δ 6.87 ppm and the doublet at δ 6.47 ppm are also correlated, but it was not possible to assign them. Moving to the aliphatic area, the singlet at δ 2.19 ppm is probably due to the methyl groups in the pyridyl rings, while the broad singlet at δ 2.27 ppm could be assigned to other methyl groups, but the results for the latter are inconclusive. For this assignment not only was the ^{1}H-^{1}H COSY spectrum used, but also the ^{1}H-^{13}C HMBC NMR spectrum (see Figure 34).

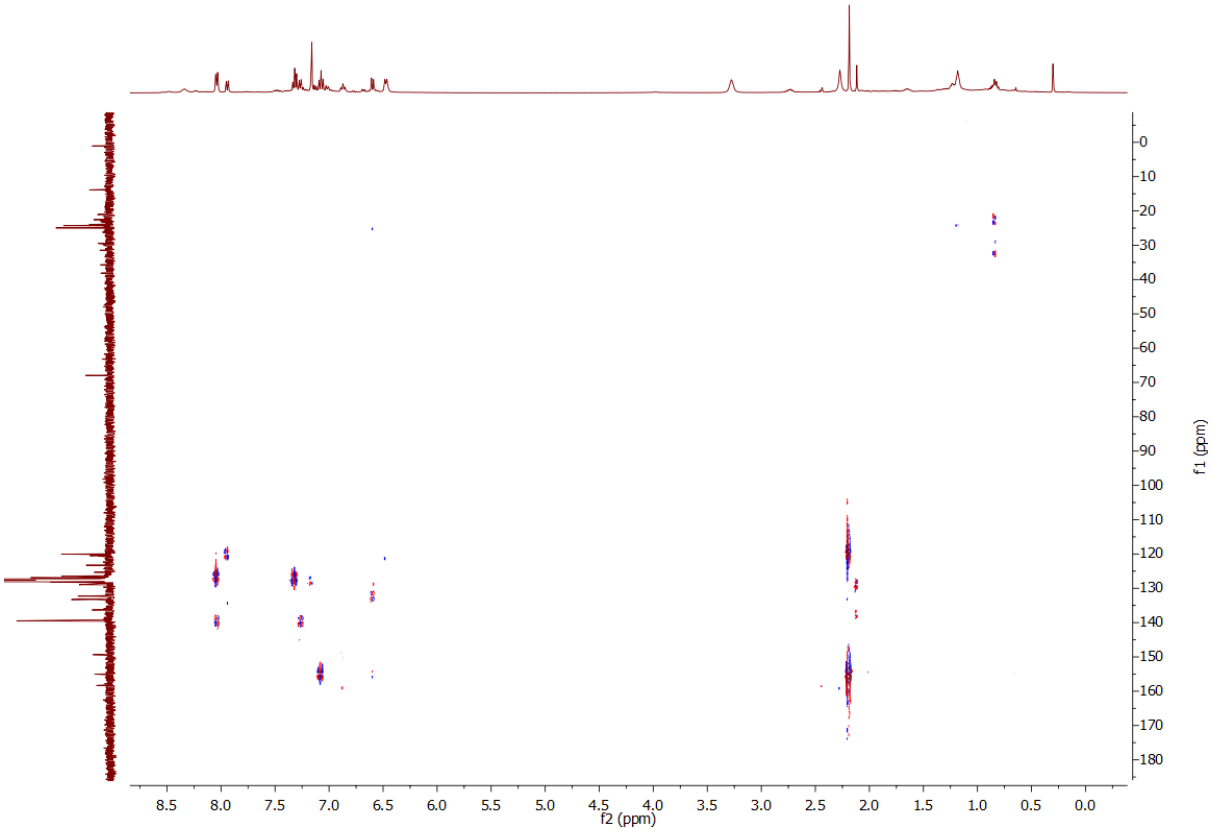

Figure 34. ^{1}H-^{13}C HMBC NMR spectrum of crude reaction mixture in attempt to make **42** (d_6-benzene)

As for **42**, [$^{t}Bu_2Al(6\text{-Me-2-py})_2Li{\cdot}2THF$] (**43**) was analysed by ^{1}H NMR spectroscopy analysis (see Figure 35). In this case however, the aromatic region clearly points towards the existence of multiple aromatic environments, while the expected product should only show two doublets and a triplet from

the pyridyl rings. Therefore, it is safe to say that the product obtained is a mixture of numerous species.

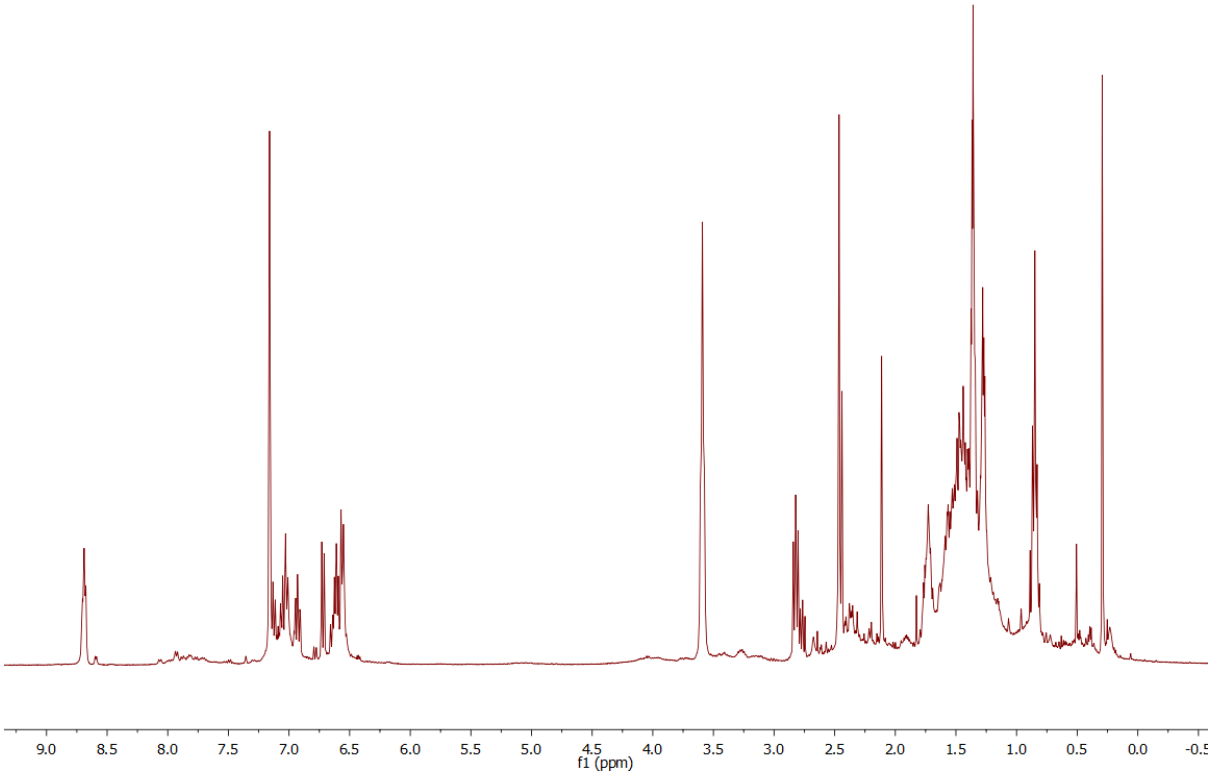

Figure 35. ^{1}H NMR spectrum of crude reaction mixture in attempt to make **43** (d_6-benzene)

As previously done for the tris(pyridyl) compounds, the influence in the coordination behaviour of the ligand was investigated by changing the methyl groups to different positions in the pyridyl ring . Changing 2-bromo-6-methylpyridine for 2-bromo-5-methylpyridine, and repeating the same procedure as for $[Me_2Al(6\text{-}Me\text{-}2\text{-}py)_2Li \cdot 2THF]$ (**40)** (reacting the bromopyridine with ^{n}BuLi at –78 °C and later with Me_2AlCl) gave $[Me_2Al(5\text{-}Me\text{-}2\text{-}py)_2Li \cdot 2THF]$ (**44**) (see Figure 36) . This new ligand is also solvated by two THF molecules that are coordinated to the Li^+ cation, which in turn is coordinated to both N-atoms from the two pyridyl groups. When comparing this molecule with the previous 6-methyl analogue, it can be seen that the steric constrain is decreased, as the methyl groups previously located in the 6-position, which are the cause for the steric hindrance around the Li^+ cation, are now in the 5-position. This can be observed when comparing the lengths and angles of the two species. The C_{py}–Al range for **44** is 2.026(3)-2.027(3) Å, in comparison with the one from **40**, which is 2.028(2)-2.030(2) Å. This suggests that the position of the Me group does not affect the C-Al distances.

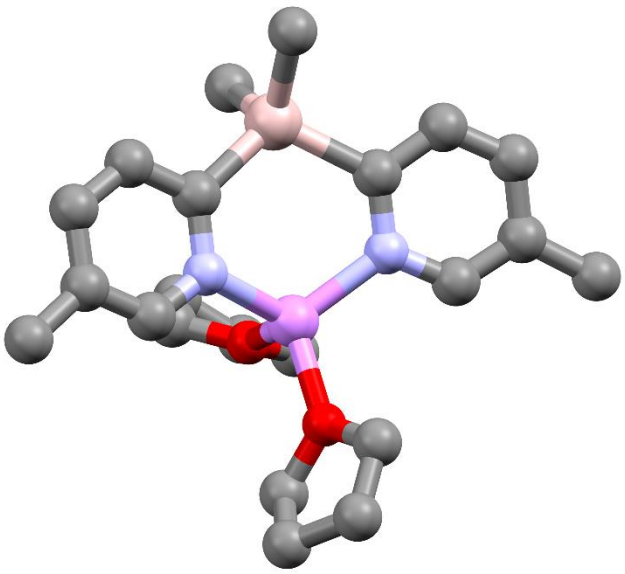

Figure 36. Solid-state structure of **44**. H-atoms omitted for clarity. Selected bond lengths (Å) and angles (°): C_{Me}–Al range 1.992(4)-2.003(3), C_{py}–Al range 2.026(3)-2.027(3), N–Li range 2.025(5)-2.025(5), Li–O range 1.958(6)-1.071(6), C_{py}–Al–C_{py} 111.75(13), C_{Me}–Al–C_{Me} 111.77(19), N–Li–N 115.4(2), O–Li–O 102.5(2). Colour code: C (grey), Al (pink), N (blue), Li (magenta), O (red).

The change becomes more noticeable when looking at the N–Li distance range. While for **40** the distances are between 2.052(3)-2.068(3) Å, for the 5-methyl complex **44** both N-Li distances are 2.025(5) Å. The change from the 6- to the 5-position opens the possibility for the rings to be closer to the lithium atom. In fact, that is also observed when looking at the angle between the two C_{py} carbons and the aluminium atom from the two compounds. There is a decrease of almost 2° from the angle in **40**, which is 113.70(8)°, to the one from **44**, which is 111.75°. Also important for this consideration is the N–Li–N angle change between the two of them. In this case, the angle decrease equals almost 3° (from 118.36(15) to 115.4(2)°). The coordination to the two THF molecules is also changed, regarding distances but mostly angles. While the Li–O distance range for the 6-methyl compound **40** is 1.971(3)-1.978(3) Å, the one found for the 5-methyl analogue **44** is 1.958(6)-1.971(6) Å, that is, the THF molecules are slightly closer to the Li^+ cation. However, a major difference between the two compounds is observed when the O-Li-O angle is considered, as the value is 102.5(2)° in **44**, while for ligand **40** the O-Li-O angle is 115.86(15)°. This contraction of the angle value can be due to the fact that the two THF molecules are closer to the Li^+ cation, therefore the angle between them cannot be as open as seen for the 6-methyl analogue **40**, in which the THF molecules are more spaced. In fact, when looking at the Al-Li distances it can be observed that the Li+ cation is closer to the Al bridgehead atom for compound **44** [3.452(5) Å] than it is for compound **40** [3.481(3) Å], indicating that the Li^+ cation is more encapsulated for the 5-methyl analogue **44**. This is probably due to the less steric environment around the Li atom.

It is interesting, not only comparing the [$Me_2Al(5\text{-}Me\text{-}2\text{-}py)_2Li \cdot 2THF$] (**44**) structure to that previously found for the [$Me_2Al(6\text{-}Me\text{-}2\text{-}py)_2Li \cdot 2THF$] (**40**) ligand, but also comparing it with the tris(pyridyl) analogue [$MeAl(5\text{-}Me\text{-}2\text{-}py)_3Li{\cdot}THF$] (**15**). The C_{Me}–Al distance for **15** is 1.976(3) Å, whilst, as previously mentioned, the ones found for the bis(pyridyl) 5-methyl ligand **44**, were slightly longer, in a range of 1.992(4)-2.003(3) Å. The same tendency is observed for the C_{py}-Al distance range, whose values are bigger for the bis(pyridyl) compound [2.026(3)-2.027(3) Å] than for the tris analogue [2.008(3)-2.020(3) Å]. However, the N–Li distances for the tris(pyridyl) ligand **15** are larger than the ones for the bis(pyridyl) compound **44** [2.064(5)-2.089(5) Å to 2.025(5) Å]. Moreover, while the Li–O distances are similar for both compounds, the angle between the C_{py} atoms and the Al bridgehead atom is greater for the [$Me_2Al(5\text{-}Me\text{-}2\text{-}py)_2Li{\cdot}2THF$] molecule **44** [11.75(13)°] than those found for the tridentate aluminate **15** [102.82(12) – 106.18(12)°].

The 1H NMR spectrum shows three different signals in the aromatic area at 8.22, 8.11, 7.07 ppm which corresponds to the C(6)-H, C(3)-H and C(4)-H. Meanwhile, the C(5)-CH3 singlet peak is located in 1.96 ppm and the Al-Me singlet is at 0.10 ppm (see Figure 37). Multiplets at 3.46 and 1.28 ppm are due to the THF peaks.

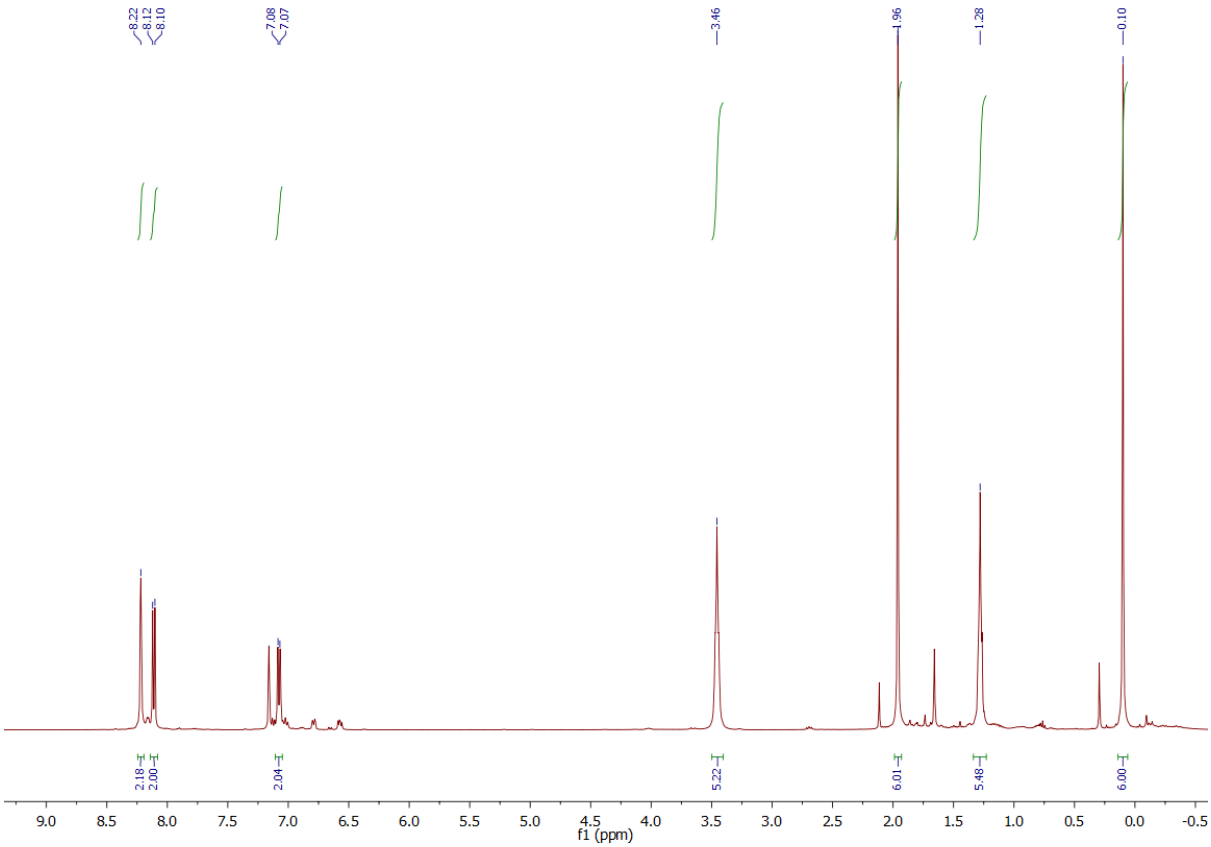

Figure 37. ^1H NMR spectrum of **44** (d_6-benzene)

The ^{13}C NMR spectrum shows 7 main peaks at 148.3, 133.9, 133.7, 128.4, 68.5, 25.4 and 18.4 ppm (see Figure 38). Signals at 68.5 and 25.4 ppm are caused by the THF solvent, while the 128.4 ppm singlet is due to toluene. Due to correlations observed in the ^{1}H-^{13}C HSQC NMR spectrum (see Figure 39) the C(6), C(4) and C(3) pyridyl carbons can be assigned to the 148.3, 133.9 and 133.7 ppm singlets. Moreover, the C(5)-CH_3 is observed at 18.4 ppm. The C(2) pyridyl carbon signal cannot be observed, presumably because of the proximity to the Al bridgehead atom.

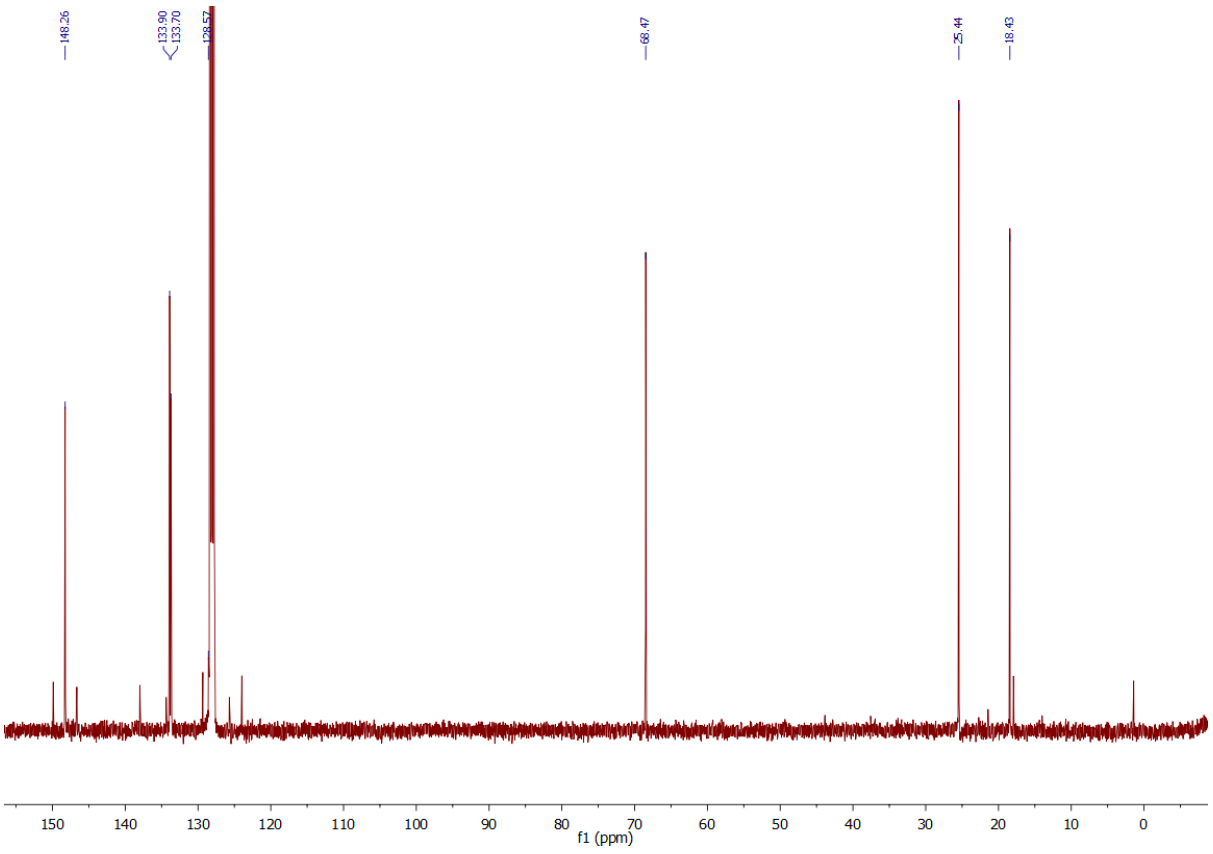

Figure 38. ^{13}C NMR spectrum of **44** (d_6-benzene)

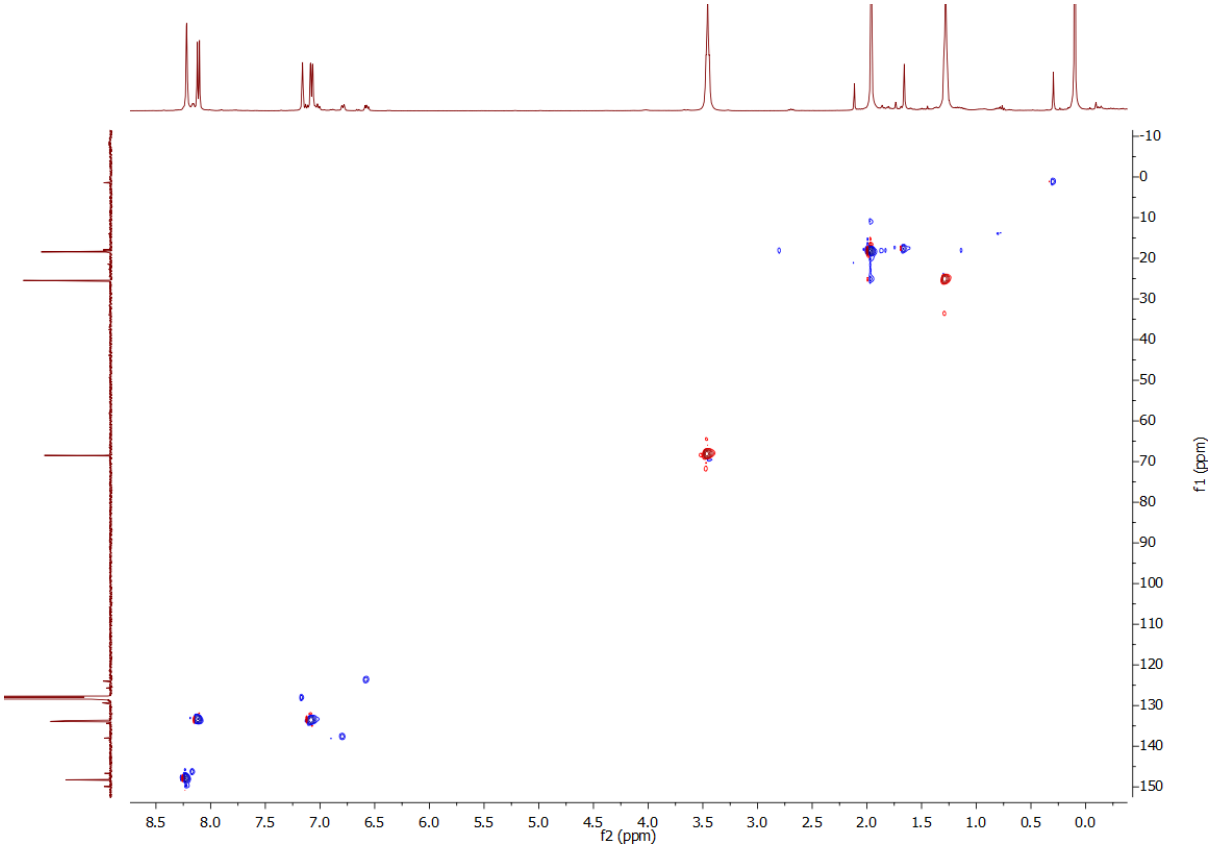

Figure 39. ^{1}H-^{13}C HSQC NMR spectrum of **44** (Colour code: red [CH, CH_3], blue [CH_2]) (d_6-benzene)

Not only was the change to the 5-methyl position tried, but also change to the 3-position in the pyridyl rings was attempted to form [$Me_2Al(3\text{-}Me\text{-}2\text{-}py)_2Li{\cdot}2THF$] (**45**). As in the previous compound, the R group attached to the Al bridgehead atom was a methyl group. Following the same procedure as for all the compounds (see Scheme 7), the 2-bromo-6-methylpyridine was reacted with $^{n}BuLi$ (1:1 equivalents) at –78 °C, followed by reaction with the commercially available precursor Me_2AlCl (2:1 ratio).

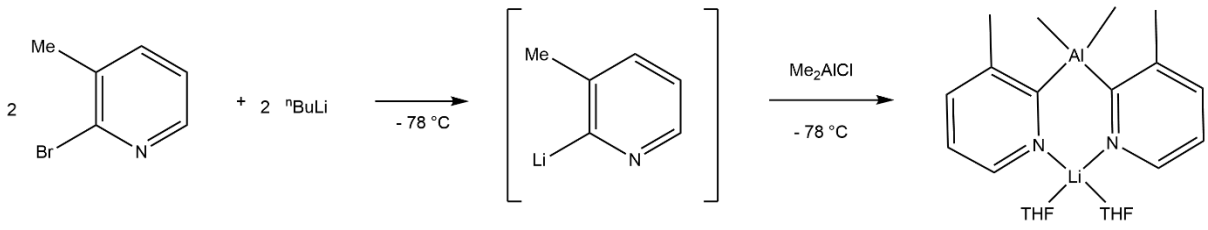

Scheme 7. Procedure followed for the synthesis of [$Me_2Al(3\text{-}Me\text{-}2\text{-}py)_2Li{\cdot}2THF$] ligand **45**. Figure of the expected product drawn based on the X-Ray structures obtained for the 6-methyl and 5-methyl analogues.

^{1}H NMR spectroscopy of compound **45** (see Figure 40) shows signals that could be assigned to the desired product, as those found between δ 7.0 and 7.5 ppm, and the singlets around δ 2.3 and 1.1 ppm. However, this last peak, which should correspond to the Al–Me protons, does not have the right integration. Moreover, the presence of other signals, such as those seen in the downfield region between δ 8.25 and 8.5 ppm, are indicators of the presence of another aromatic environment. Due to the expected sensitive nature of the compound, together with the fact that the product obtained was an oil, purification of the product was not attempted.

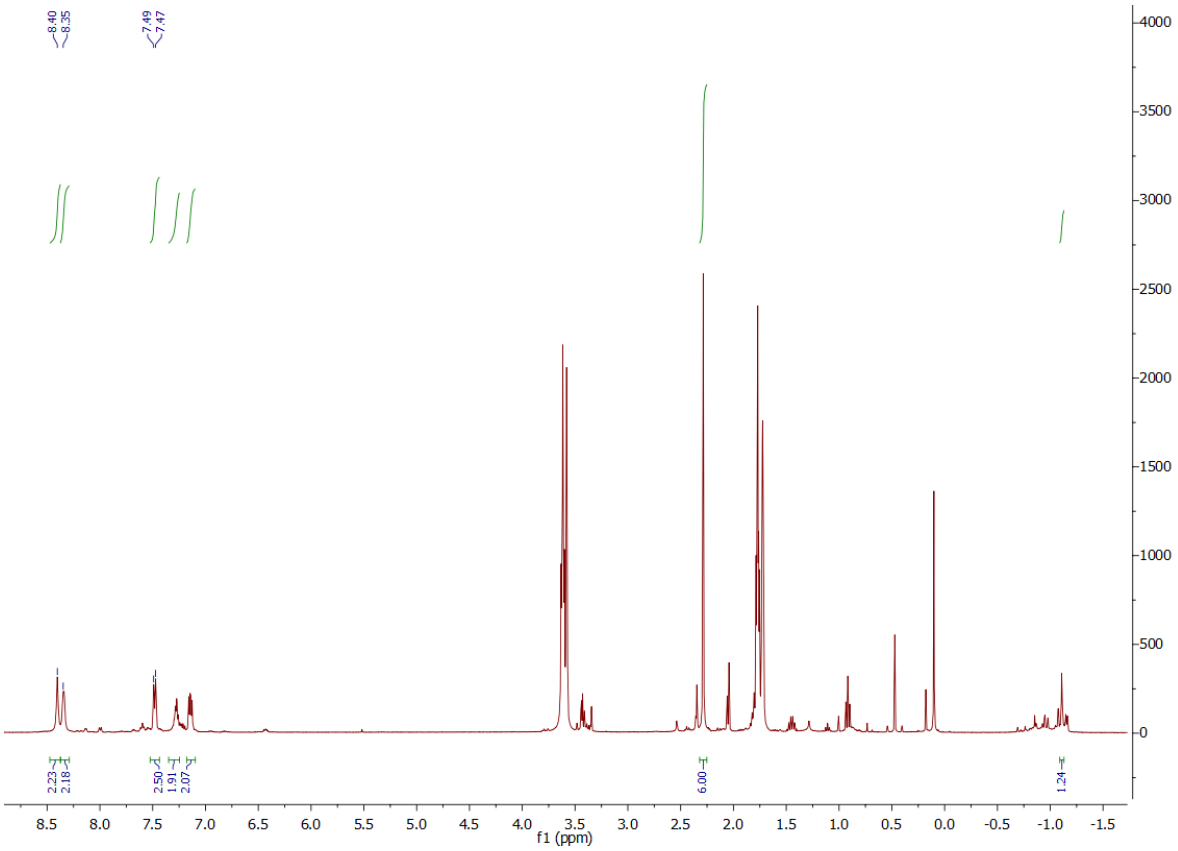

Figure 40. ^{1}H NMR spectrum of crude reaction mixture in attempt to make **45** (d_8-THF)

A reason for these other aromatic environments could be the presence of water. All processes of the reaction have to be done under inert gas conditions and without the presence of water. This meant Schlenk line techniques are required. However, the exposure to oxygen when adding some reactants can be possible, as well as the presence of water in any stage of the reaction. After realising that at some stage water could be being introduced inside the reaction solution, the possible sources of water

were investigated. It was decided that the most plausible situation was that the water came from the solvent. Although the THF used had been dried, it was collected and dried over sodium-wire to make sure that the minimum amount of water was present in the solvent used. After executing this change, reactions were repeated to check if the solvent was the source of water. Differences between ^{1}H NMR spectra before and after drying the solvent can be observed for figures 41-43.

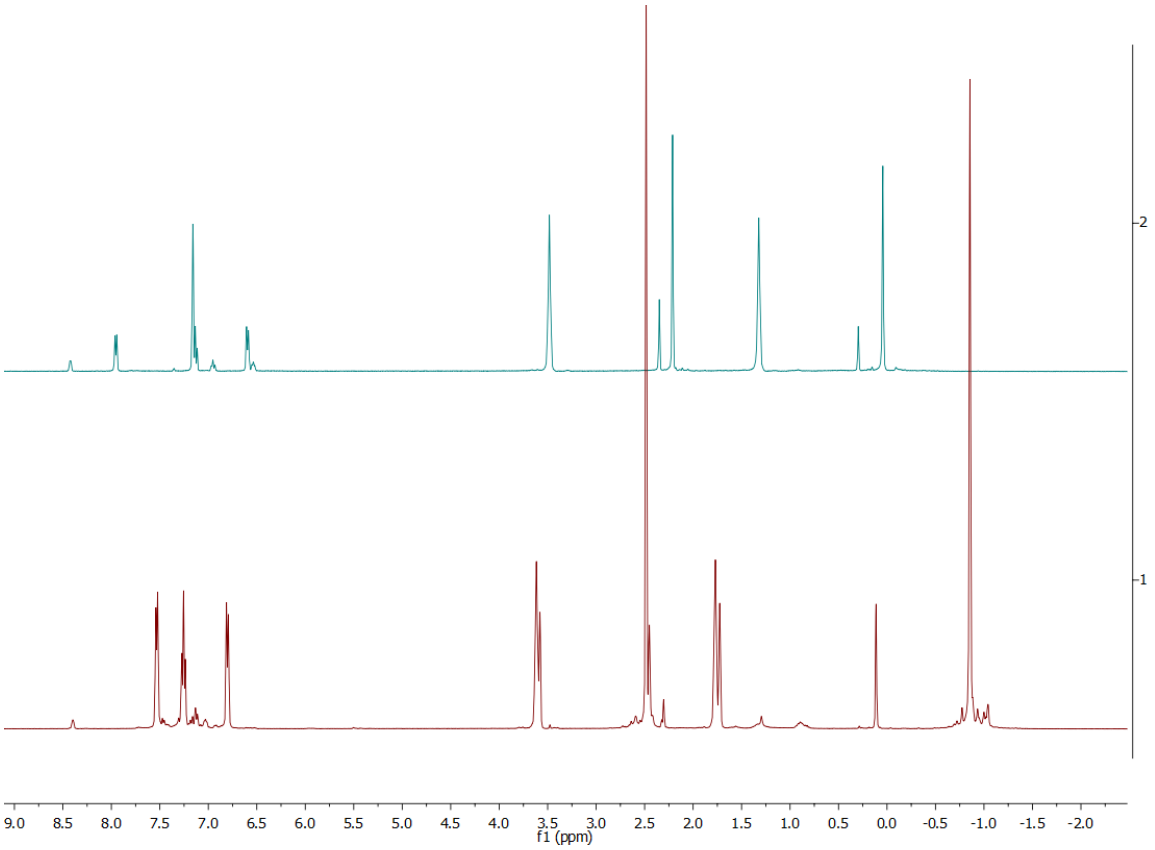

Figure 41. Comparison between the ^{1}H NMR spectra found for **40** before using the THF dried over Na-wire (2) (d_6-benzene) and after (1) (both in d_8-THF)

Comparison of the ^{1}H NMR spectra of **40** reveals that not much change is observed regarding the amount of peaks, but the ratio of the peaks of the desired product and the impurities is much higher after drying the solvent.

As for the previous comparison, the main difference between both spectra of **44** is the ratio between the different compounds.

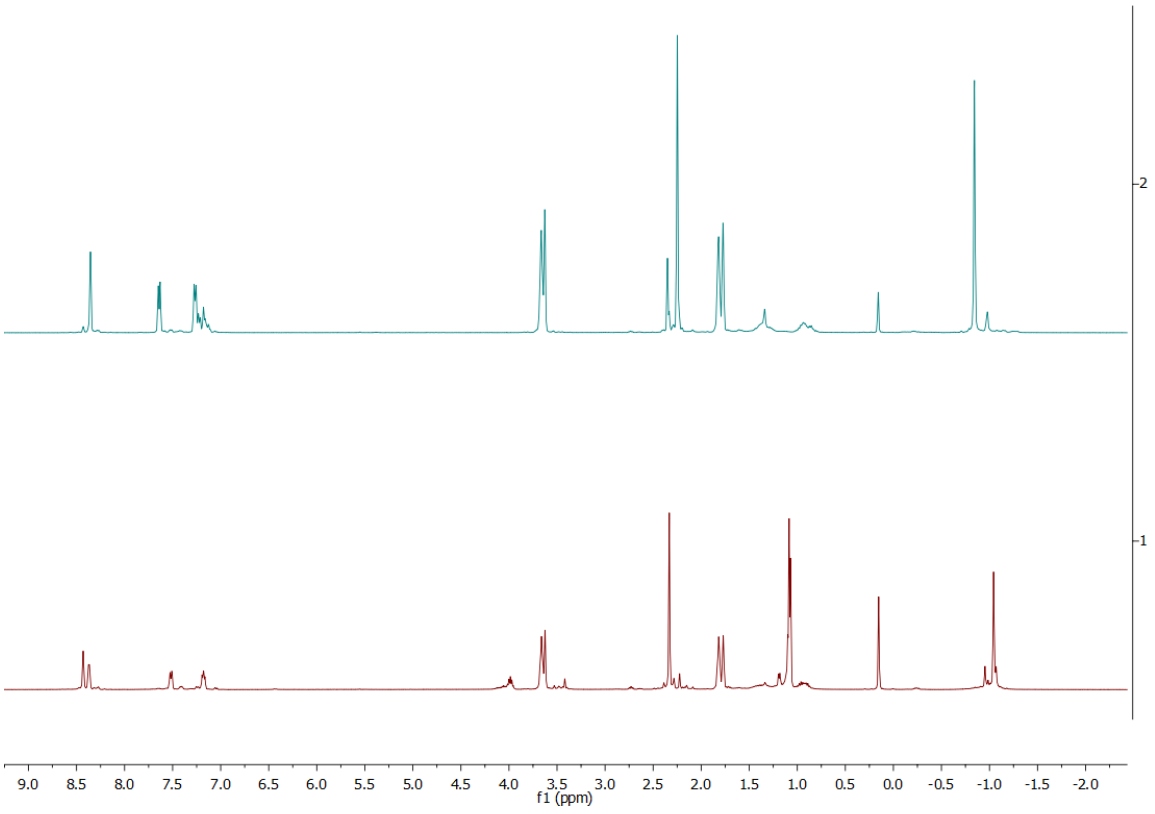

Figure 42. Comparison between the ^{1}H NMR spectra of **44** before drying the THF over Na-wire (1) and after (2) (both in d_8-THF)

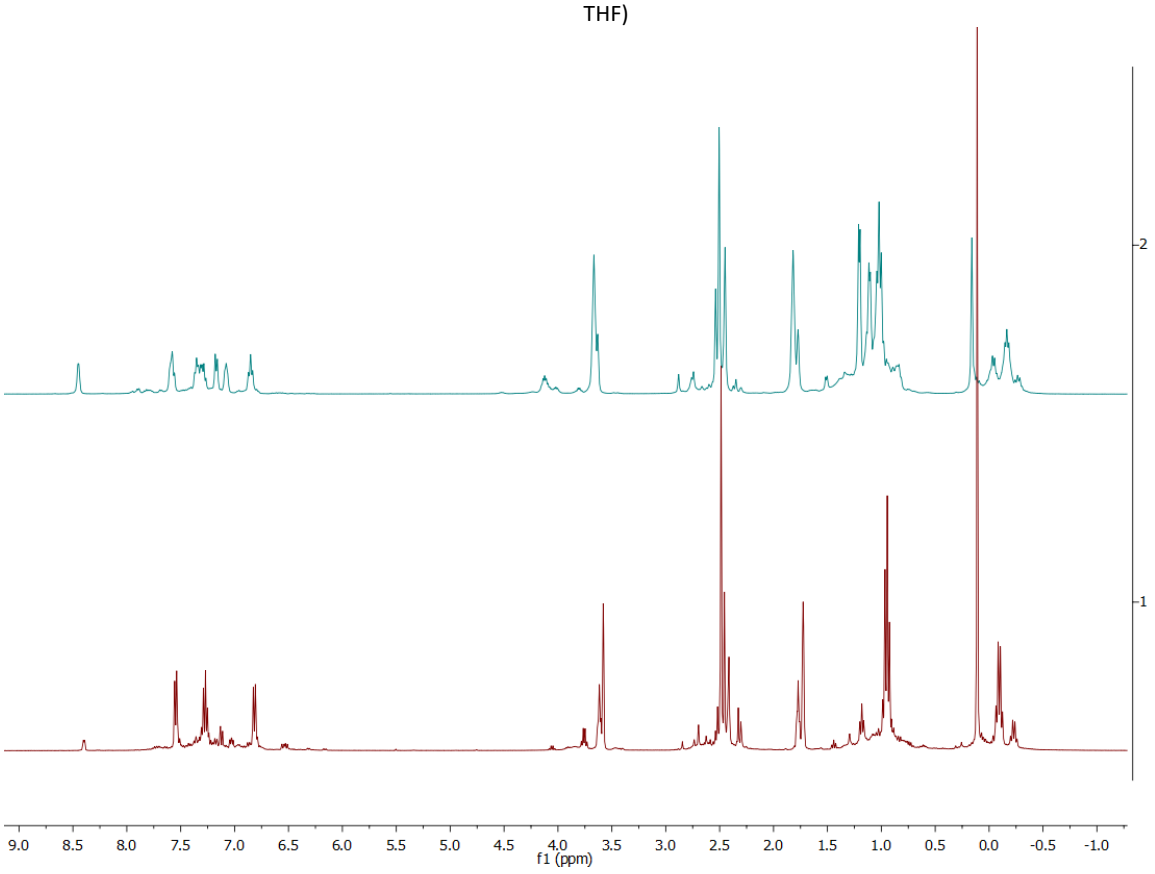

Figure 43. Comparison between the ^{1}H NMR spectra of **41** before drying the THF over Na-wire (2) and after (1) (both in d_8-THF)

Although changes are observed for the three spectra (see Figures 41 – 43), the major difference is seen for the comparison between the ^{1}H NMR spectra of compound **41**. While some impurities are still present, the aromatic region is much more defined after drying the THF, with the predominant peaks the two doublets (C(3)–H and C(5)–H pyridyl protons) and the triplet (C(4)–H pyridyl protons) (see Figure 43). Significant changes are also seen in the aliphatic region, in which, before drying the solvent, multiple peaks were found between δ 0.5 and 1.5 ppm and between δ –0.5 and 0.0 ppm. These facts indicate that there were multiple species present.

As indicated before, the first reason for the existence of impurities was the presence of water in the reaction mixture. This was supported by the crystal structure obtained when trying to grow crystals of ligand **45** (see Figure 44)

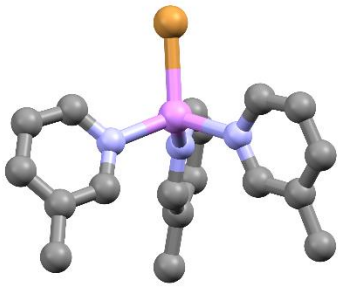

Figure 44. Solid-state structure of [BrLi(6-Me-py)$_3$]. H-atoms omitted for clarity. Selected bond lengths (Å) and angles (°): Br–Li 2.505(18), Li–N range 2.066(8)-2.066(8), N–Li–N 110.3(5), Br–Li–N 108.7(5). Colour code: C (grey), N (blue), Li (magenta), Br (orange).

In the crystal structure of the compound [BrLi(6-Me-py)$_3$], it can be seen that no aluminium atom is present. Instead, there is a Li^+ cation coordinated to three pyridyl ligands and a Br^- anion.

After synthesizing different bis(pyridyl) ligands, the next step was to attempt to obtain some metal complexes, using alkaline earth metals, transition metals and lanthanides. Most of the reactions were done following the procedures found for the tris(pyridyl) analogues.

Given that the [{Me$_2$Al(2-py)$_3$}$_2$Fe] (**3**) sandwich complex has been proven to be a highly selective epoxidation catalyst for the epoxidation of styrene,[19] the bis(pyridyl) ligand reaction that aroused the

most interest was that between [$Me_2Al(6\text{-}Me\text{-}2\text{-}py)_2Li{\cdot}2THF$] and FeX_2 (X = halide) in a 2:1 ratio. In the process of making this compound, different iron(II) halides were used. The first attempt of this reaction was done using $FeCl_2$; after reacting [$Me_2Al(6\text{-}Me\text{-}2\text{-}py)_2Li{\cdot}2THF$] with the iron salt for 24 hours in toluene, a change of colour from yellow to red was observed, which indicates that the reaction may have worked. After filtration through Celite and removal of the majority of the solvent, it was stored at –30 °C for a couple of days. This led to a change in the colour of the solution to light yellow together with an orange precipitate. A similar result was found when repeating the reaction multiple times with FeI_2. In these cases, a gradual change from the initial dark red colour to a colourless/light yellow colour, accompanied by an orange precipitate is observed. Although ^1H NMR spectroscopy was performed for some of the compounds, the paramagnetic nature of the metal made it difficult to obtain any information from them.

Reasoning for the change of the iron(II) halide is due to the poor solubility of the $FeCl_2$ in toluene. Although the addition of THF to the mixture helps dissolving the metal salt, using the iodide instead of the chloride helps increase solubility, given the increasing tendency down the group 17 to be more soluble. Proof of this was already reported for the reaction procedure of [{^{n}BuAl(2-py)$_3$}$_2$Fe] (**20**),[21] for which a 1:1 ratio of the aluminate to the iron(II) chloride was needed in order to obtain the sandwich compound, while other similar compounds with different metals were obtained using only a 2:1 ratio.

Although most of the transmetallation reactions were tried with the [$Me_2Al(6\text{-}Me\text{-}2\text{-}py)_2Li{\cdot}2THF$] (**40**) aluminate, a shortage of the commercially available Me_2AlCl led to the in situ reaction of the 6-Me-2-pyridyl lithiate with Et_2AlCl (2:1 equivalents), to immediately react it with $FeCl_2$ (2: 1 equivalents). The reaction solution had a very dark purple colour which did not let any light through. Although some crystalline material was obtained, a solid state structure could not be obtained from it. As previously mentioned, giving the paramagnetic nature of the Fe(II), no NMR spectroscopy could be performed, which, together with the extremely air sensitive nature of the compound made it difficult to obtain any data from the compound.

Following previous reactions done for the tris(pyridyl) ligands, further heterometallic complexes with Ca(II) and Mn(II) as metals were targeted.[21] Using a 2:1 ratio of **40** to CaI_2 in toluene gave a colourless solution which did not produce any suspension, as seen in other tris(pyridyl) experiments, indicating that the reaction had not taken place. The formation of the suspension would indicate that LiI, a side product of the reaction, has been produced, as this is not soluble in toluene (see Scheme 8).

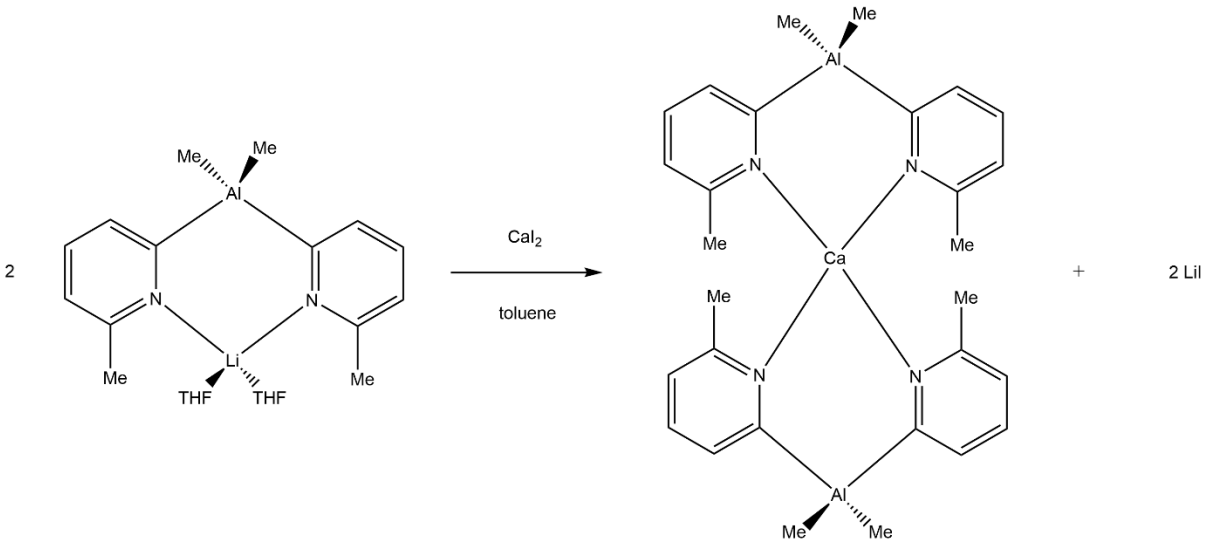

Scheme 8. Expected sandwich compound from the reaction of **40** with CaI_2

Reaction of the same compound with $MnCl_2$ in a 2 to 1 ratio initially gave a yellow solution, but it evolved into a dark green solution together with a residue. Given the previous results observed for the tris(pyridyl) calcium sandwich complex,[21] in which no change of colour was observed, led to the suspicion that the compound [{$Me_2Al(6\text{-}Me\text{-}2\text{-}py)_2$}$_2$Ca] had decomposed.

As previously mentioned, not only transition or alkaline earth metal salts were reacted with the aluminate precursor, but also some lanthanide salts. Again, the different lanthanides were chosen following the previous performed tris(pyridyl) aluminate transmetallation reactions.[24] Thus, [$Me_2Al(6\text{-}Me\text{-}2\text{-}py)_2Li\cdot 2THF$] (**40**) was reacted with the corresponding Sm(II), Eu(II) and Yb(II) iodides. Given the interesting structures obtained from the Sm(II) tris(pyridyl) sandwich complexes reaction with O_2,[20,22] the Sm(II) bis(6-Me-2-pyridyl) sandwich complex was an evident target. However, the initial dark green solution from the reaction of **40** with SmI_2 (2:1 equivalents) in toluene, converted into a colourless solution after filtration through Celite. The dark green solid that gave colour to the solution was removed by the Celite, indicating that probably the SmI_2 is not soluble in toluene, which could be the reason for the failure of the experiment. Both Eu and Yb reactions did not show any colour change or precipitation during the course of the reactions, as it happened for previous experiments,[24] which points towards the idea that there was no reaction taking place. The tris(pyridyl) analogues reportedly could be synthesized because of the steric shielding provided by the methyl groups in the 6-position of the pyridyl rings, as the reaction of the unsubstituted [$MeAl(2\text{-}py)_3Li$] (**1**) ligand with the respective lanthanide halides did not yield any compound. These methyl groups protect the lanthanide cation stabilizing the unusual oxidation state. Therefore, a possible reason for the failure of the lanthanide

reactions with **40** could be due to the fact that the steric shielding is not large enough for the cations to be stabilized.

Further experiments involved the exchange of the lithium cation with other metals such as Na (**46**) or K (**47**). In this procedure the in situ ligand **40** is reacted with Na or K tert-butoxide in a 1:1 ratio (see Scheme 9).

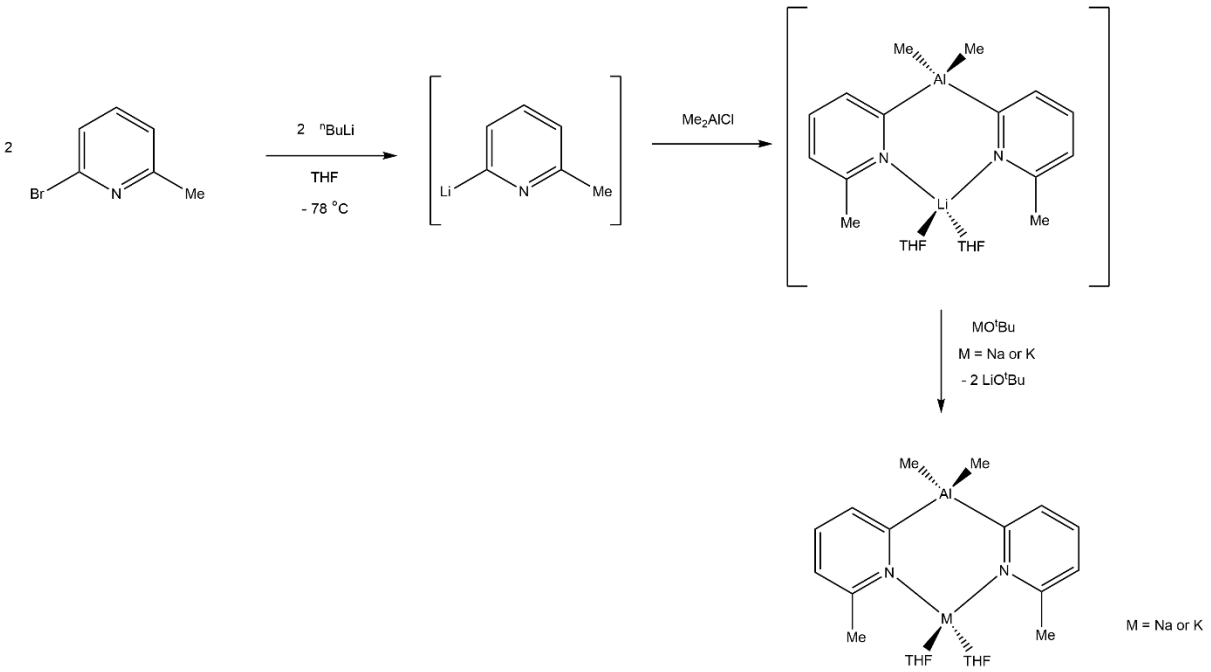

Scheme 9. General procedure for the obtention of the [$Me_2Al(6\text{-}Me\text{-}2\text{-}py)_3M{\cdot}2THF$] (M = Na or K)

For the reaction with NaO^tBu, the normal procedure for obtaining [$Me_2Al(6\text{-}Me\text{-}2\text{-}py)_2Li{\cdot}2THF$] (**40**) was done, that is, reacting the 2-bromo-6-methylpyridine with ^{n}BuLi at –78 °C (1:1 ratio) and then adding Me_2AlCl (2:1 equivalents) at –78 °C and stirring overnight. After warming up to room temperature, the solvent is removed and the resulting oil/solid is dissolved in toluene. The brown suspension is filtered through Celite to remove the LiCl present. After dissolving NaO^tBu in toluene with the help of gentle heating, this solution was added to the one containing the ligand. The resulting mixture was gently heated and the resulting dark red solution was stirred at room temperature for 1.5 hours. The solvent was removed in vacuo until precipitate was observed, and this was heated back into solution. Storage at room temperature for a couple of days resulted in the appearance of some precipitate. In order to redissolve the ligand some THF was added, but no significant change was observed, although commonly THF is a better solvent than toluene for these type of compounds. The

solvent was removed and the solid was dried under vacuum giving an orange oil. The ^{1}H NMR spectrum of the orange oil showed a multitude of peaks suggesting that different species were present (see Figure 45). The expected product would be expected to show some shifts when comparing it with **40**, as the only change is the metal coordinated to the two N-pyridyl atoms.

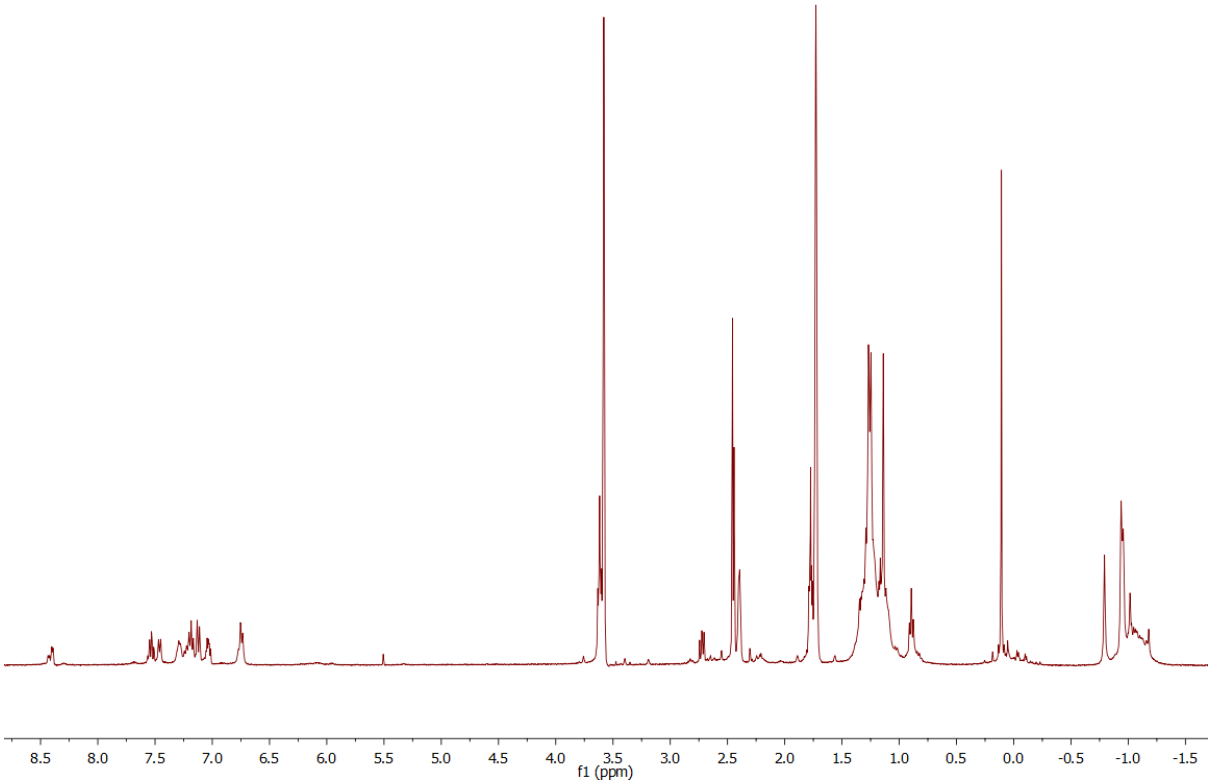

Figure 45. ^{1}H NMR spectrum of crude mixture from attempted synthesis of **46** (d_8-THF)

Focusing on the aromatic region, the expected product **46** would only show three signals, two doublets from the C(3)–H and C(5)–H pyridyl protons and a triplet from the C(4)–H pyridyl protons, while the ^{1}H NMR spectrum from the oil shows at least 9 different aromatic signals (see Figure 46). The existence of doublets around δ 8.4 ppm points towards the idea that the compound has been hydrolysed, probably by the addition of large amounts of THF in the process of trying to redissolve the precipitate. Although the THF used had been dried over Na-wire, the presence of water in it is possible, which could be the reason for the possible hydrolysis.

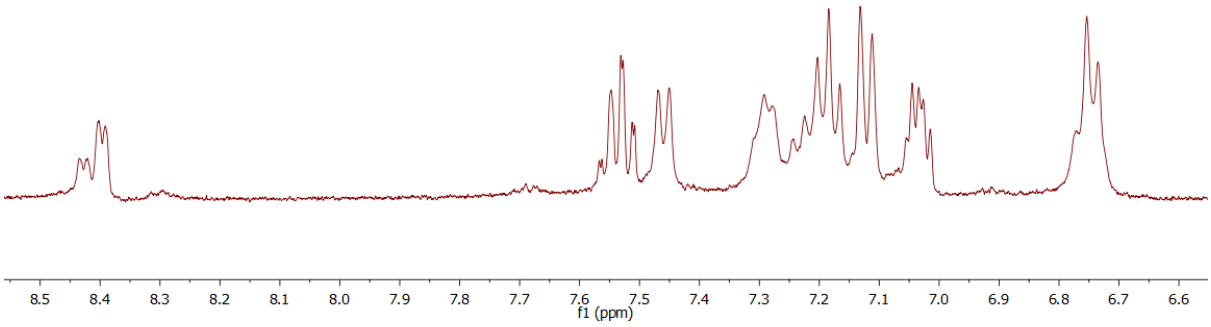

Figure 46. Aromatic region of the ^{1}H NMR spectrum of crude mixture from attempted synthesis of **46** (d_8-THF)

Moreover, the ^{7}Li NMR spectrum of the orange oil obtained shows two sharp peaks together with another broad peak, which suggests that at least two different Li-coordinating species are present (see Figure 47). This evidence, together with the ^{1}H NMR spectrum showed previously point to the idea that the desired product has not been formed, or if formed, the ratio of product to impurities is not very high.

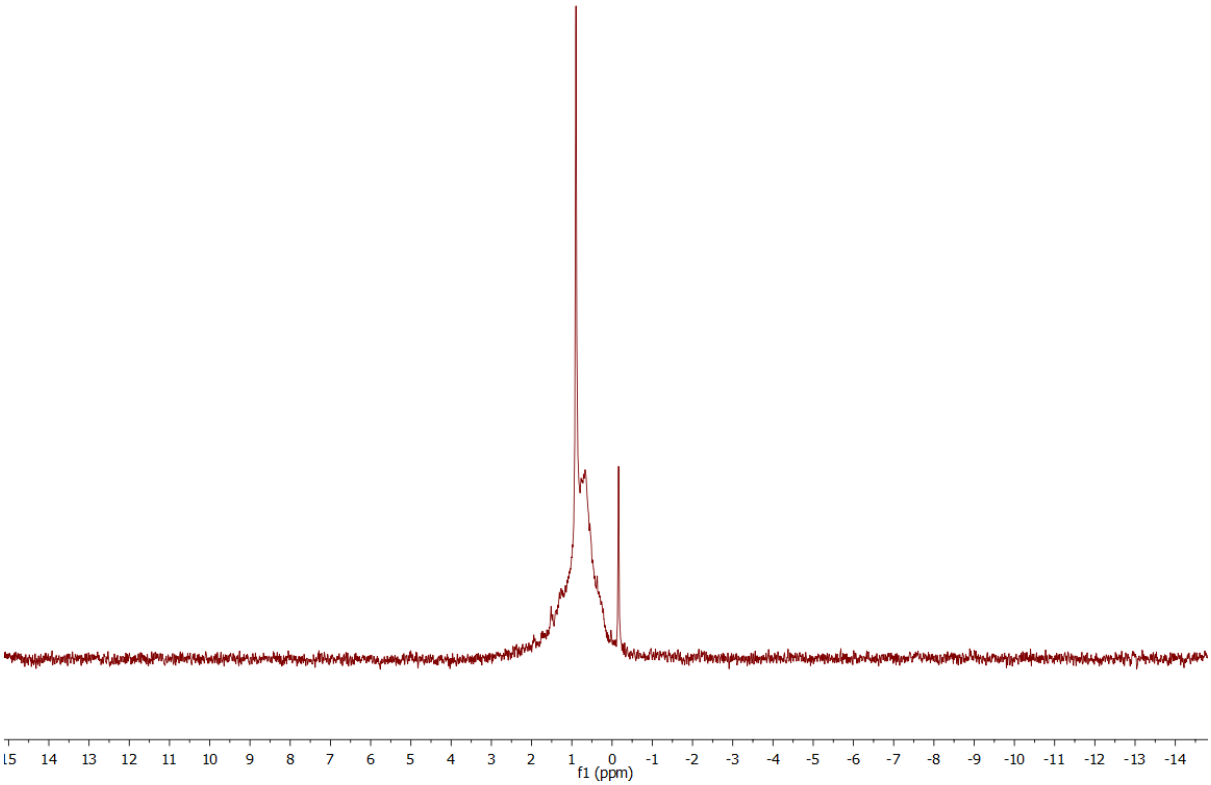

Figure 47. ^{7}Li NMR spectrum of crude mixture from attempted synthesis of **46** (d_8-THF)

The procedure for synthesis the KO^{t}Bu analogue (**47**) was the same as in the previous experiment. The in situ reaction of the [Me_2Al(6-Me-2-py)$_2$Li·2THF] ligand was done following the same procedure explained for the NaO^{t}Bu reaction. After filtration through Celite, a solution of KO^{t}Bu in toluene was added to the ligand solution with an immediate appearance of a precipitate. After gentle heating a brown suspension was formed and stirring for 3 hours at room temperature followed by the addition of THF and gentle heating due to the presence of some precipitate, gave a dark red solution. Storage of the solution at room temperature for a couple of days resulted in a dark brown solution that was stored at –30 °C. Due to the dark nature of the solution, no possible crystalline material could be observed.

2.2. Bismuth

Not only were tris(pyridyl) aluminates synthesized, but also tris(pyridyl) bismuthines. Following the already known procedure for the synthesis of [Bi(4-py)$_3$] (**48**), the synthesis of different metal coordination complexes was attempted.

In order to obtain the tris(4-pyridyl) ligand a solution of 4-bromopyridine was added dropwise at –115 °C to a THF solution of ^{n}BuLi. After stirring for 25 minutes a solution of $BiCl_3$ in toluene was added and stirred for another 4 hours at –115 °C and then for 40 hours at –78 °C. The cloudy pale yellow solution was warmed to room temperature and quenched with water. After phase separation, the aqueous phase was extracted with DCM and the combined organic layers were dried over anhydrous $MgSO_4$. The solvent of the filtrated solution was removed in vacuo and the white solid obtained was dissolved in a small amount of DCM. Slow evaporation of the solvent at room temperature gave light brown crystals, which were washed with Et_2O to remove the impurities.

^{1}H NMR spectroscopy of the product in d_8-THF shows two doublets at *δ* 8.67 and 7.66 ppm, both integrating for 6 protons, which can be assigned to the C(2)–H and C(3)–H pyridyl protons respectively (see Figure 48). Presumably, the additional doublets at *δ* 8.59 and 7.70 ppm are caused by the formation of 4,4'-bipyridine. The ^{1}H-^{1}H COSY NMR spectrum (see Figure 49) shows that there are in fact two sets of doublets. It can be observed that the *δ* 8.67 ad 7.66 ppm doublets show a correlation in the 2D spectrum, while the other *δ* 8.59 and 7.70 ppm doublets show the same. As there is no correlation between the two sets it is revealed that there are two different species present. However, the main species is the desired [Bi(4-py)$_3$] (**48**) ligand.

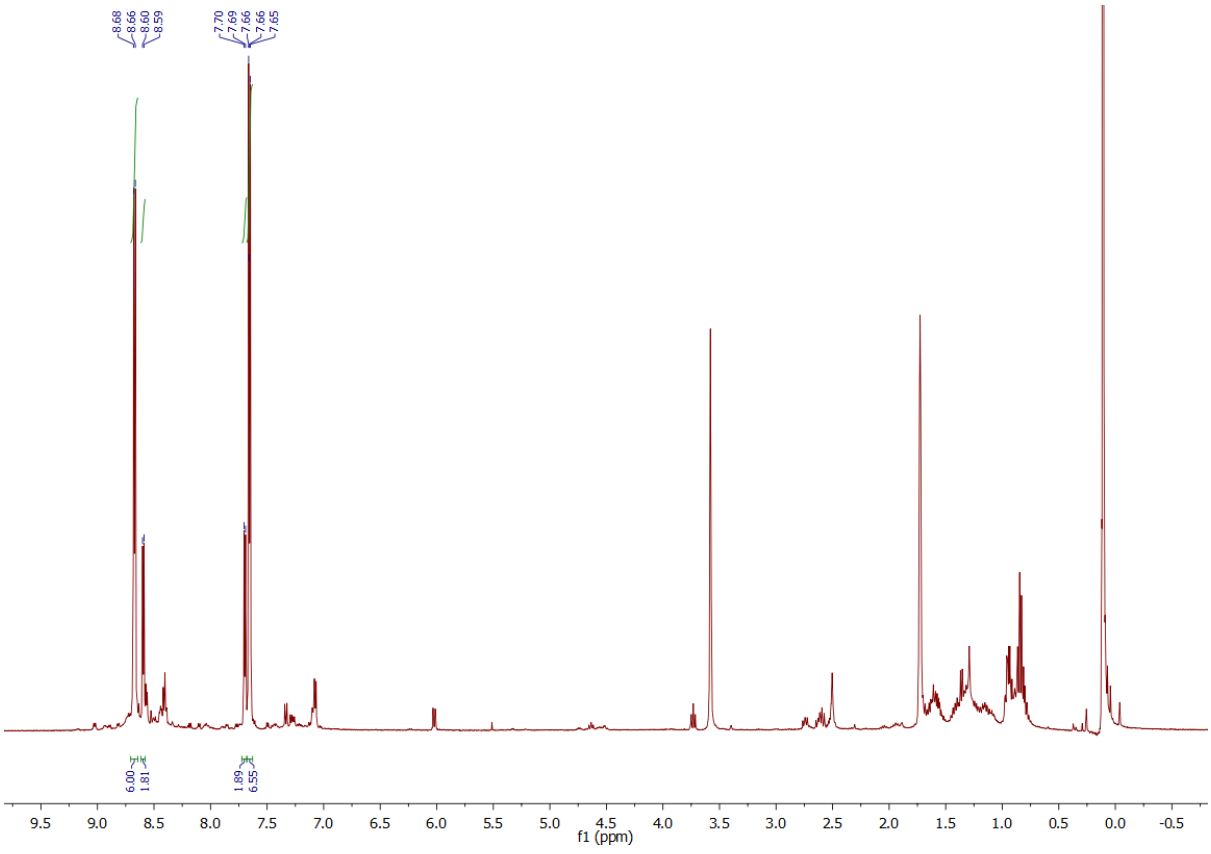

Figure 48. ^{1}H NMR spectrum of **48** (d_8-THF)

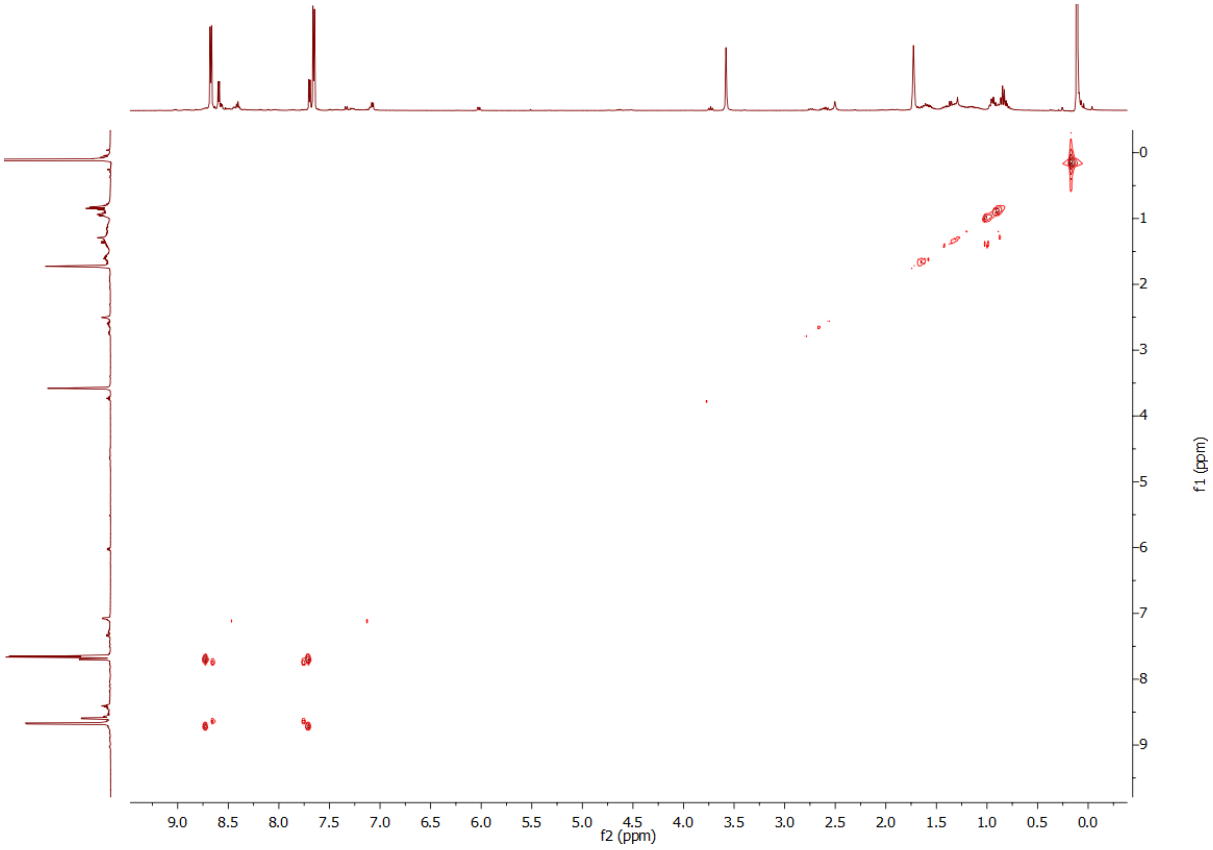

Figure 49. ^{1}H-^{1}H COSY NMR spectrum of **48** (d_8-THF)

The ^{13}C NMR spectrum shows 5 main peaks at *δ* 151.67, 151.43, 145.79, 133.09 and 121.68 ppm (see Figure 50). With the help of the ^{1}H-^{13}C HSQC and ^{1}H-^{13}C HMBC NMR spectra they can be assigned to the respective carbon atoms. The *δ* 151.43 and 121.68 ppm peaks correspond to the C(2) and C(3) carbons from **48**, while the *δ* 151.67 and 133.09 singlets would be the 4,4'-bipyridine compound. The singlet at *δ* 145.79 ppm does not show any correlation with the ^{1}H NMR spectrum peaks in either the ^{1}H-^{13}C HSQC in the ^{1}H-^{13}C HMBC spectra. The C(4) carbon signal cannot be observed in the ^{13}C NMR spectrum, probably because it is directly coordinated to the Bi bridgehead atom (see Figures 51-52)

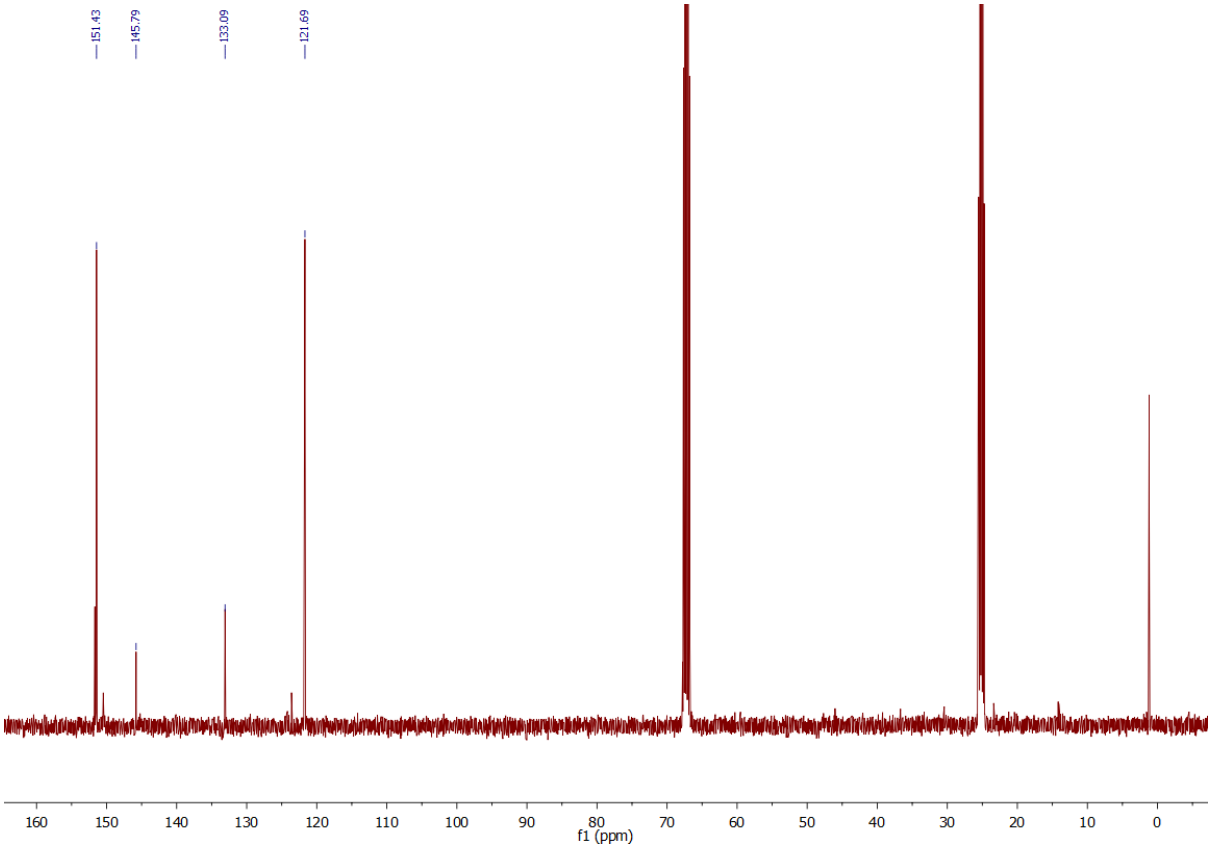

Figure 50. ^{13}C NMR spectrum of **48** (d_8-THF)

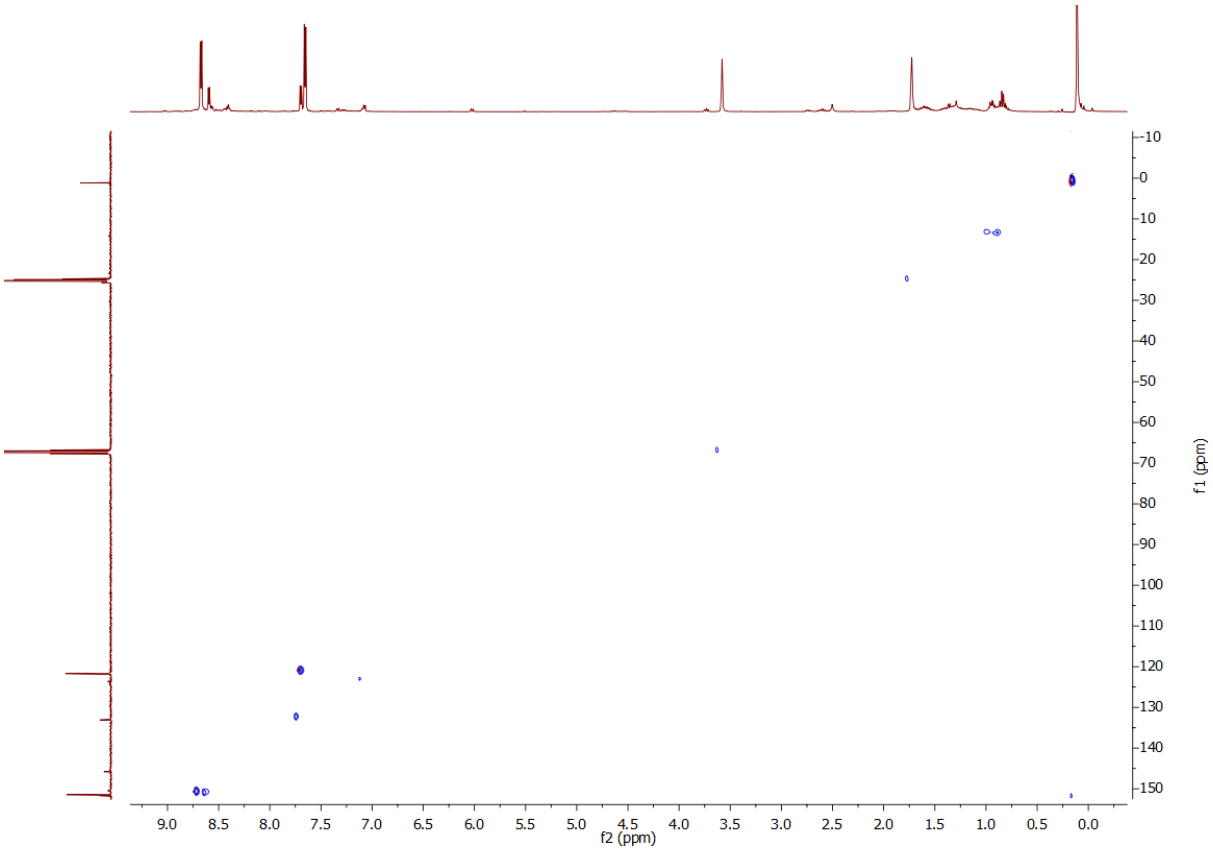

Figure 51. ^{1}H-^{13}C HSQC NMR spectrum of **48** (d_8-THF)

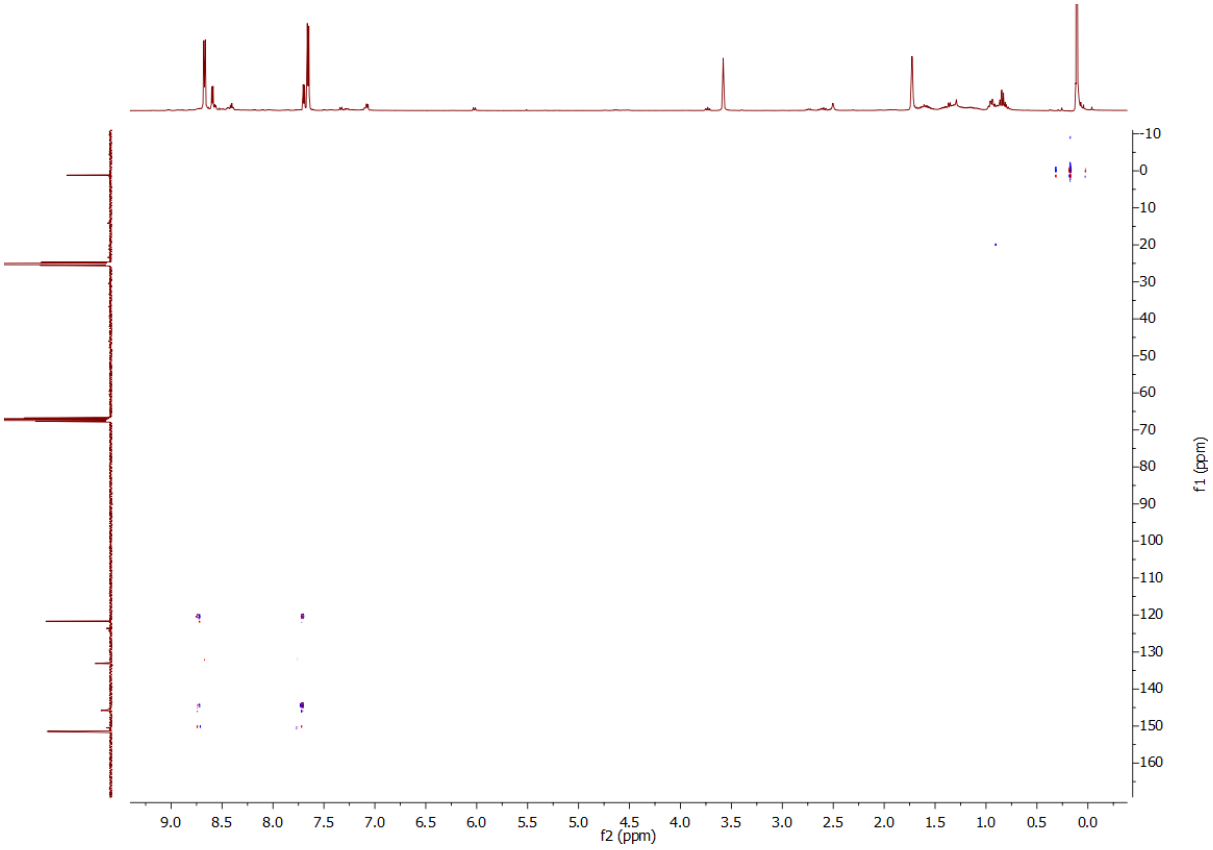

Figure 52. ^{1}H-^{13}C HMBC NMR spectrum of **48** (d_8-THF)

Although previous transmetallation reactions with ligand **48** have been reported,[30] further experiments were performed. The reactions were carried out with the transition metals Ni and Co.

The metal salts chosen were $Ni(BF_4)_2$, $NiBr_2$, $Co(BF_4)_2$ and $CoBr_2$. The procedure followed for all the experiments was that reported previously for the other transmetallation reactions, that is, layering a solution of the metal salt in ACN in top of the [Bi(4-py)$_3$] ligand in DCM (1:1 stoichiometric ratio) and then leaving them to crystallize at room temperature. It is important to note that [Bi(4-py)$_3$] is not very soluble in dichloromethane, which could be the reason of the experiments not working, as no crystals could be obtained. All of the reactions resulted in no crystals and only precipitated solids.

These experiments led to the idea that a new tris(pyridyl) bismuthine compound with different types of pyridyl ligands could be formed. In order to have two different types of pyridyl ligands a methyl-substituted 2-pyridyl ligand in the 6 position was chosen as the second type of ligand, with the tris(4-pyridyl) bismuthate ligand the first one. The experiments were carried out in a NMR scale, therefore the solvents used were all deuterated. The general procedure for the reaction is reacting the [Bi(4-py)$_3$] ligand with [Bi(6-Me-2-py)$_3$] ligand in a 1:2 ratio (see Scheme 10).

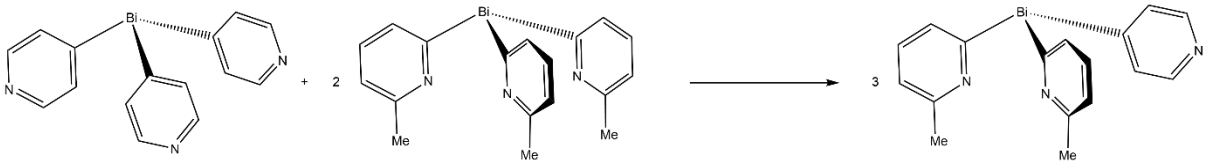

Scheme 10. General procedure for the formation of the bismuthine complex with combined pyridyl ligands.

The first attempt of the reaction was attempted using d_6-benzene as solvent. The ^{1}H NMR spectrum after the first 10 minutes of the reaction showed mainly peaks corresponding to the [Bi(6-Me-2-py)$_3$] ligand, although peaks for the [Bi(4-py)$_3$] ligand could also be seen, but in a lower ratio (see Figure 53). Another ^{1}H NMR spectrum taken one hour after the start of the reaction showed no change in the ratio or the shifts of the peaks, and the spectrum remained identical after leaving it overnight. After 40 hours of no changes, neither in the colour of the solution, nor in the ^{1}H NMR spectra, it was decided to heat the solution overnight at 50 °C (see Figure 54). The ^{1}H NMR spectra showed no shifting in the signals and the colour remained the same, thus it was concluded that the reaction was not successful.

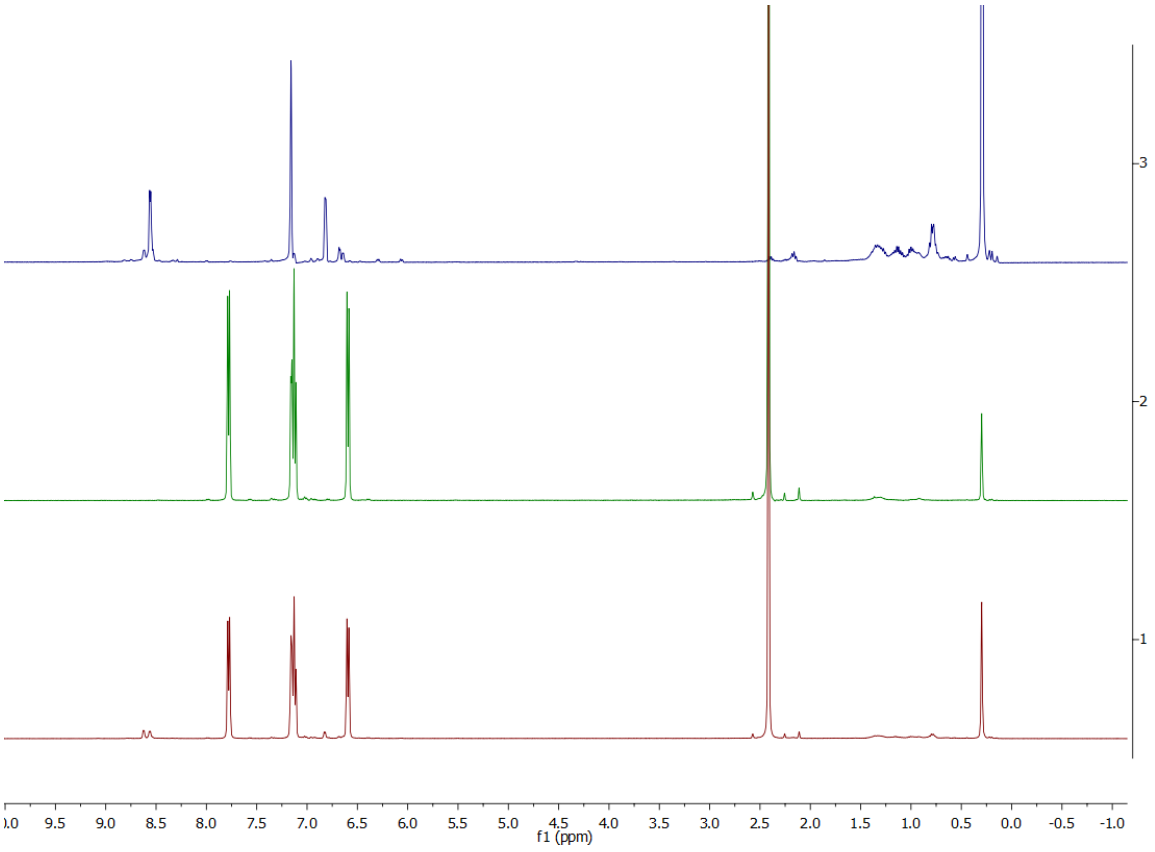

Figure 53. ^{1}H NMR spectra comparison between the combined ligand (1), [Bi(6-Me-2-py)$_3$] (2) and [Bi(4-py)$_3$] (3) (d_6-benzene)

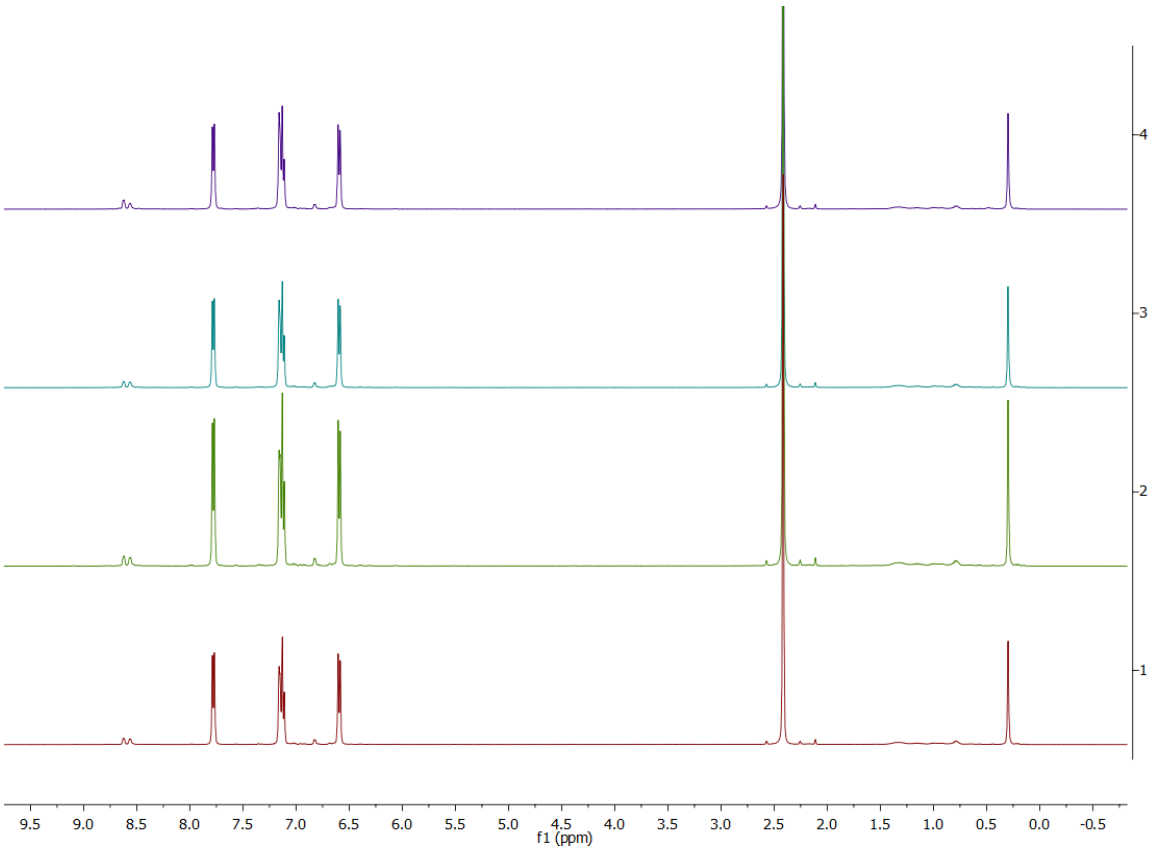

Figure 54. ^{1}H NMR spectra comparison between the different stages of the reaction to form the combined Bi ligand: After 10 min (1), after 1 hour (2), after 40 hours (3), and after heating it to 50 °C overnight (4) (d_6-benzene)

Reasoning for the lack of reaction could be the partial solubility of **48** in d_6-benzene. Therefore, it was decided to change the solvent to confirm that this was the cause for the failure of the reaction. The next solvent atempted was CD_3CN, but although ligand **48**, which was previously less soluble in d_6-benzene than the [Bi(6-Me-2-py)$_3$] ligand, was almost completely soluble, in this occasion the [Bi(6-Me-2-py)3] ligand was far less soluble in CD_3CN than in d_6-benzene. Given the insolubility of this compound in deuterated acetonitrile no reaction was carried out and a new solvent was chosen for the repetition of the experiment. In this case d_8-THF was the solvent in which both compounds were soluble. Although the ligands were not completely soluble in this solvent, it was a good compromise between both of the ligands. Monitoring of the reaction via ^{1}H NMR spectroscopy, as in the previous attempt, showed no changes throughout the reaction. The mixture showed no changes after leaving at room temperature overnight, but after heating it for several hours at 50 °C a colour change from red to brown, which could be a result of decomposition. However, the ^{1}H NMR spectra showed no change in the peaks throughout all the reaction time (see Figure 56).

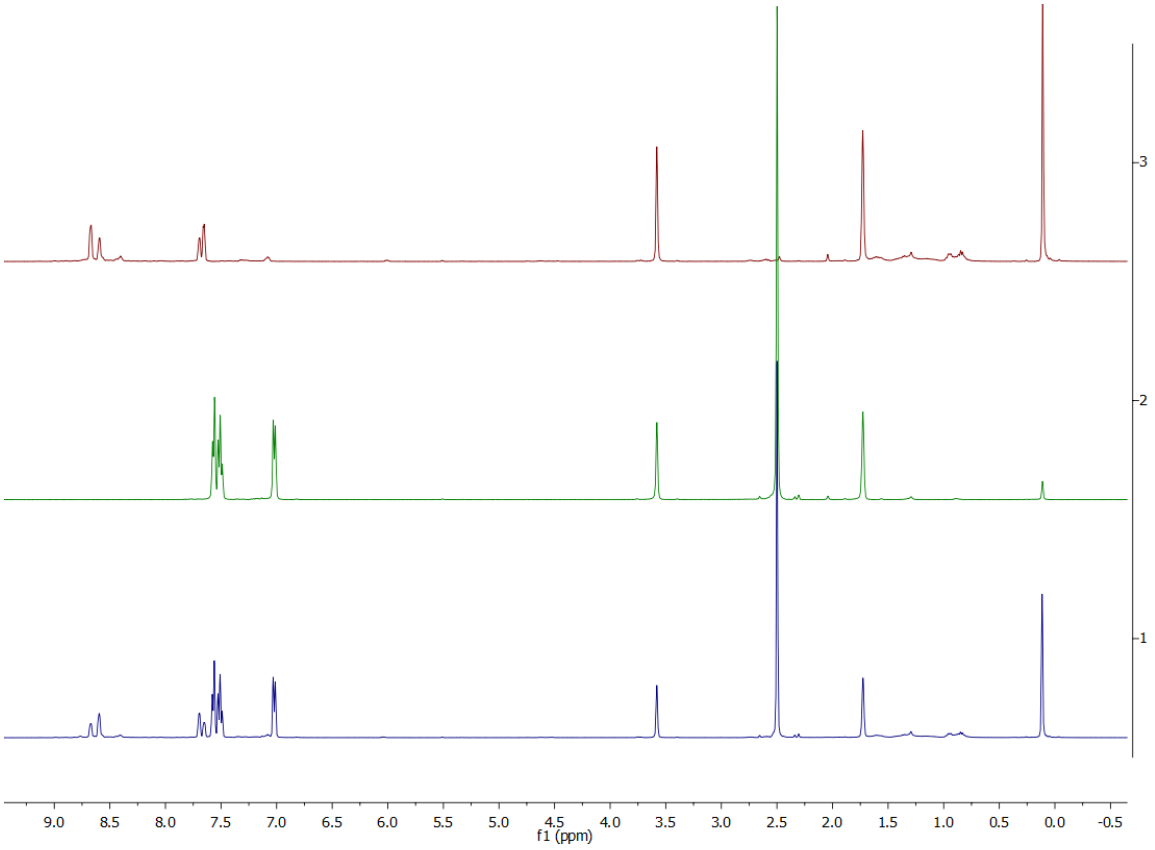

Figure 55. ^{1}H NMR spectra comparison between the combined Bi ligand (1), [Bi(6-me-2-py)$_3$] (2) and [Bi(4-py)$_3$] (3) (d_8-THF)

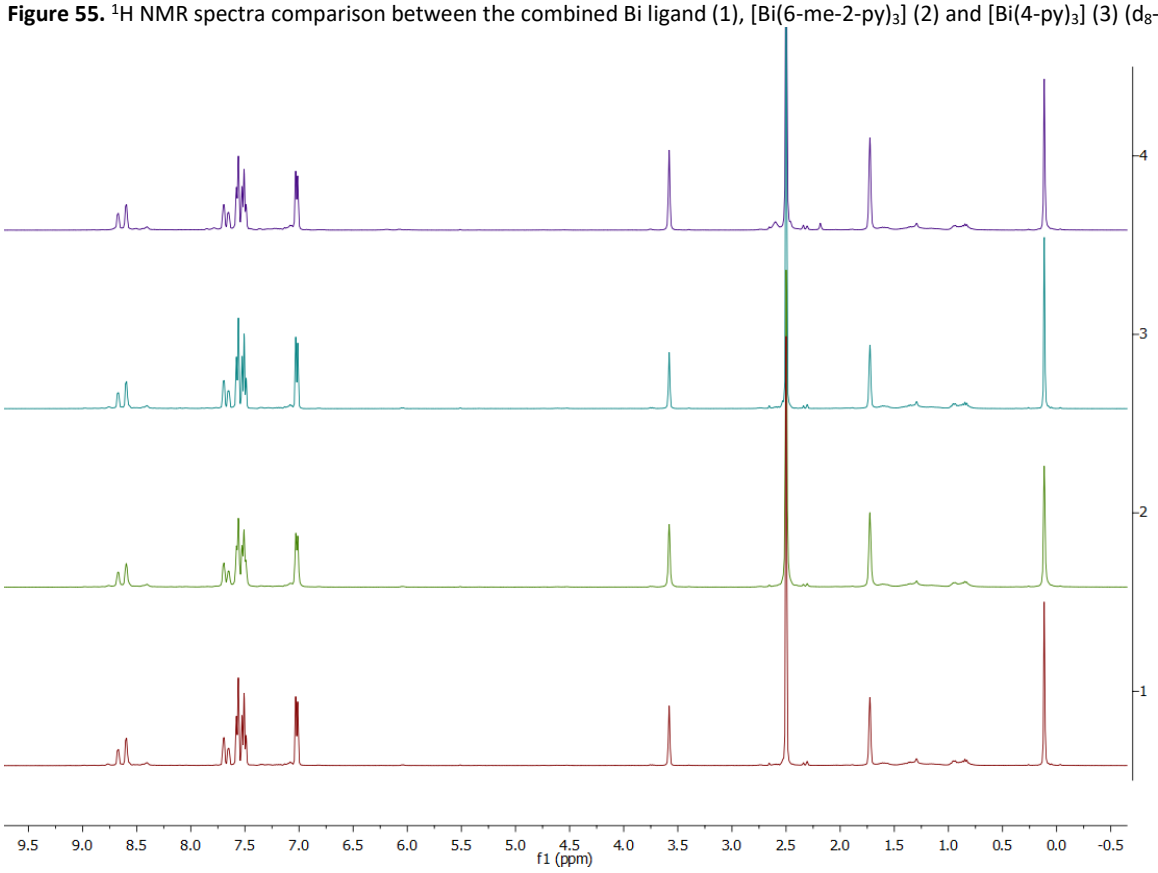

Figure 56. ^{1}H NMR spectra comparison between the different stages of the reaction to form the combined Bi ligand: after 1 hour (1), overnight (2), after heating it to 50 °C for 1 hour (3) and after heating it to 50 °C overnight (4) (d_8-THF)

A possible cause for the failure for both of the reactions could be the partial insolubility of the ligands in the different solvents used, as the amount of ligand weighed for both ligands was minimal due to the fact that it was done in on a NMR scale. Although repeating the reaction without solvent using a ball mill was another option, it could not be put into practice.

3. Conclusions

The results of this investigation show that it is possible to synthesize the bis(2-pyridyl) aluminates [$Me_2Al(6\text{-Me-2-py})_2Li{\cdot}2THF$] (**40**) and [$Me_2Al(5\text{-Me-2-py})_2Li{\cdot}2THF$] (**44**) following similar procedures to those used for the tris(2-pyridyl) analogues.[31] As expected, the presence of two Al-Me groups instead of one results in changes around the bridgehead atom due to the bulkier nature of the methyl groups when comparing them to the pyridyl rings, which results in the extension of the Al-Me distances for both compounds. Moreover, the coordination of two pyridyl rings instead of three has an effect on the Li^+ cation, which now coordinates two THF molecules instead of one. Coordination of these aluminates to metal atoms was not possible, presumably due to the lack of solubility of the metal salts in the chosen solvents, or the lack of steric shielding by the pyridyl rings.

Additionally, the inability to synthesize or isolate compounds **41**-**45** is believed to be due to the presence of water, which causes hydrolysis of the initial reagents.

[$Bi(4\text{-py})_3$] (**48**) transmetallation reactions also proved to be unsuccessful, being the main problem the lack of solubility of the ligand in the chosen solvents.

4. Future work

As some bis(2-pyridyl) aluminates have been synthesized during the course of this project ([Me_2Al(6-Me-2-py)$_2$Li·2THF] (**40**) and [Me_2Al(5-Me-2-py)$_2$Li·2THF] (**44**)), an obvious path of future work would be the investigation of similar compounds with different R-bridgehead groups or different substituents and positions in the pyridyl rings, as those already attempted during this project. Moreover, the synthesis of heteroleptic metal complexes with this type of ligands can open the scope of their applications, being particularly interesting the heterometallic iron-aluminate complexes. The comparison between all of them and their tris(2-pyridyl) analogues can provide useful information on the coordination behaviour of this type of ligands.

On the other hand, Bi(4-py)$_3$ transmetallation reactions can be attempted again using appropriate solvents, or trying different crystallization techniques.

5. Experimental Part

5.1. General procedures

Syntheses were carried out on a Schlenk line under a nitrogen atmosphere using oven-dried glassware, unless otherwise specified. Starting materials were commercially obtained from suppliers and used as received. Lower temperatures in synthesis were achieved using dry ice/acetone (−78 °C) baths. 2-bromo-6-methylpyridine was dried over CaH_2 and distilled under nitrogen. Et_2O, toluene and THF were dried over Na/benzophenone and distilled under nitrogen. Deuterated solvents were distilled and/or dried over molecular sieves before use. A nitrogen-filled glove box (Saffron type α) was used to manipulate solids, including room temperature reactions, product recovery and sample preparation for analysis. Room temperature ^{1}H, ^{7}Li, $^{13}C\{^{1}H\}$ and ^{27}Al NMR spectra were recorded on a Bruker 400 MHz Avance III HD Smart Probe spectrometer and referenced to the residual solvent peaks, unless otherwise specified. For ^{27}Al and ^{7}Li NMR, external references were used ($AlCl_3 \cdot 6H_2O$ and 1 M LiCl in D_2O, respectively). Unambiguous assignments of NMR resonances were made on the basis of 2D NMR experiments ($^{1}H–^{1}H$ COSY, $^{1}H–^{13}C$ HSQC, and $^{1}H–^{13}C$ HMBC). X-ray crystallographic data were collected using either a Nonius KappaCCD (sealed-tube MoKa) or a Bruker D8-QUEST PHOTON-100 (Incoatec IμS Cu microsource) diffractometer. The temperature was held at 180(2) K using an Oxford Cryosystems N_2 cryostat. Structures were solved using SHELXT[32] and refined using SHELXL.[33]

5.2. Synthesis of $[Me_2Al(6\text{-Me-2-py})_2Li \cdot 2THF]$ (40)

2-bromo-6-methylpyridine (0.5 ml, 4.4 mmol) was dissolved in THF (10 ml). $^{n}BuLi$ (1.6 M in hexanes, 2.75 ml, 4.4 mmol) was added dropwise to the solution at –78 °C, and the resulting dark red solution was stirred (2h, –78 °C). Me_2AlCl (1.0 M in hexanes, 2.2 ml, 2.2 mmol) was added to the solution and stirred for 16 h. After warming up to room temperature overnight, solvent was removed *in vacuo* and the resulting orange oil was dissolved in toluene (15 ml) to give a cloudy orange solution that was filtered through Celite. Solvent was removed to yield a dark orange solid (529 mg, 1.35 mmol, 61%). Crystal structure was obtained following the same procedure.

^{1}H NMR (298 K, 400.0 MHz, d_6-benzene) δ (ppm) = 7.95 (d, *J* = 7.16 Hz, 2H, C(3)-H py), 7.14 (t, *J* = 8.21, 8.21 Hz, 2H, C(4)-H py), 6.60 (d, *J* = 7.67 Hz, 2H, C(5)-H py), 3.41 (m, 4H, -CH_2-O, thf), 2.22 (s, 6H, C(6)-CH_3), 1.25 (m, 4H, -CH_2-, thf), 0.03 (s, 6H, Al-Me)

^{13}C NMR (298 K, 100.6 MHz, d_6-benzene) δ (ppm) = 154.92 (C(6)), 133.43 (C(4)), 130.86 (C(3)), 119.74 (C(5)), 68.70 (-CH_2-O, thf), 25.39 (-CH2-, thf), 24.61 (C(6)-Me)

^{7}Li NMR (298 K, 155.5 MHz, d_8-THF) δ (ppm) = 1.21 (s)

^{27}Al NMR (298 K, 104.2 MHz, d_8-THF) δ (ppm) = 142.02 (s)

5.3. Synthesis of [Et_2Al(6-Me-2-py)$_2$Li·2THF] (41)

2-bromo-6-methylpyridine (0.5 ml, 4.4 mmol) was dissolved in THF (10 ml). ^{n}BuLi (1.6 M in hexanes, 2.75 ml, 4.4 mmol) was added dropwise to the solution at –78 °C, and the resulting dark red solution was stirred (2h, –78 °C). Et_2AlCl (1.8 M in toluene, 1.25 ml, 2.2 mmol) was added to the solution and stirred for 16 h. After warming up to room temperature overnight, solvent was removed *in vacuo* and the resulting orange oil was dissolved in toluene (10 ml) to give a cloudy light orange solution that was filtered through Celite. Solvent was removed to yield a light brown residue.

^{1}H NMR (298 K, 400.0 MHz, d_6-benzene) δ (ppm) = 7.98 (d, *J* = 7.4 Hz, 2H, C(3)-H py), 7.15 (t, *J* = 7.5 Hz, 2H, C(4)-H py), 6.60 (d, *J* = 7.8 Hz, 2H, C(5)-H py), 3.37 (m, -CH_2-O, thf), 2.21 (s, 6H, C(6)-CH_3), 1.22 (m, -CH_2-, thf), 1.72 (t, *J* = 8.09 Hz, 6H, Al-CH_2-C*H*$_3$), 0.69 (q, *J* = 8.11 Hz, 4H, Al-CH_2)

^{13}C NMR (298 K, 100.6 MHz, d_6-benzene) δ (ppm) = 155.0 (C(6)-py), 133.3 (C(4)-py), 131.2 (C(3)-py), 119.8 (C(5)-py), 68.8 (THF), 25.4 (THF), 24.7 (C(6)-CH_3), 11.6 (Al-CH_2-CH_3). [C(2)-py and Al-CH_2 carbons could not be observed]

^{7}Li NMR (298 K, 155.5 MHz, d_8-THF) δ (ppm) = 1.29 (s)

^{27}Al NMR (298 K, 104.2 MHz, d_8-THF) δ (ppm) = 142.8 (s)

5.4. Synthesis of [Ph_2Al(6-Me-2-py)$_2$Li·2THF] (42)

To a solution of $AlCl_3$ (530 mg, 3.97 mmol) in THF (15 ml), another solution of PhLi (669 mg, 7.96 mmol) in THF (10 ml) was added at –78 °C. Stirring for 1.5 h at room temperature gave a colourless solution. Solvent was removed and the white residue was redissolved in toluene (10 ml) before filtration through Celite.

2-bromo-6-methylpyridine (0.55 ml, 4.8 mmol) was dissolved in THF (10 ml). ^{n}BuLi (1.6 M in hexanes, 3.0 ml, 4.8 mmol) was added dropwise to the solution at – 78 °C, and the resulting dark red solution was stirred (2h, –78 °C). The previous solution [Ph2AlCl] was added at –78 °C. After warming up overnight, the solvent was removed and toluene (10 ml) was added to produce a light brown suspension. After filtration through Celite the solvent was removed yielding an orange residue. Although crystallization at room temperature and –30 °C was tried, no crystalline product could be obtained.

5.5. Synthesis of [$^{t}Bu_2Al(6\text{-Me-2-py})_2Li{\cdot}2THF$] (43)

^{t}BuLi (1.7 M in pentane, 3.4 ml, 5.78 mmol) was added to a solution of $AlCl_3$ (378 mg, 2.83 mmol) in THF (20 ml) at –78 °C. Stirring for 3 h at room temperature gave a colourless solution. After removal of the solvent, the resulting white residue was redissolved in toluene (10 ml), giving a white suspension that was filtered through Celite.

2-bromo-6-methylpyridine (0.64 ml, 5.6 mmol) was dissolved in THF (10 ml). ^{n}BuLi (1.6 M in hexanes, 3.5 ml, 5.6 mmol) was added dropwise to the solution at –78 °C, and the resulting dark red solution was stirred (2h, –78 °C). The previous solution [$^{t}Bu_2AlCl$] was added at –78 °C. After warming up overnight, the solvent was removed and toluene (10 ml) was added to produce a light brown suspension. After filtration through Celite the solvent was removed yielding an orange residue. Although crystallization at room temperature and –30 °C was tried, no crystalline product could be obtained.

5.6. Synthesis of [$Me_2Al(5\text{-Me-2-py})_2Li{\cdot}2THF$] (44)

2-bromo-5-methylpyridine (825 mg, 4.8 mmol) was dissolved in THF (10 ml). ^{n}BuLi (1.6 M in hexanes, 3.0 ml, 4.8 mmol) was added dropwise to the solution at –78 °C, and the resulting dark red solution was stirred (2h, –78 °C). Me_2AlCl (1.0 M in hexanes, 2.4 ml, 2.4 mmol) was added to the solution and stirred for 16 h. After warming up to room temperature overnight, solvent was removed *in vacuo* and the resulting brown solid was dissolved in toluene (15 ml) to give a cloudy orange solution that was filtered through Celite. Solvent was removed to yield a brown oil (311 mg, 0.79 mmol, 33%). Crystal structure was obtained following the same procedure, although isolation from the crystals was not possible due to their low melting point.

^{1}H NMR (298 K, 400.0 MHz, d_6-benzene) δ (ppm) = 8.22 (s, 2H, C(6)-H py), 8.11 (d, J = 7.5 Hz, 2H, C(3)-H py), 7.07 (d, J = 7.5 Hz, 2H, C(4)-H py), 3.46 (m, 5H, -CH2-O thf), 1.96 (s, 6H, C(5)-CH3), 1.28 (m, 5H, -CH2- thf), 0.10 (s, 6H, Al-CH3).

^{13}C NMR (298 K, 100.6 MHz, d_6-benzene) δ (ppm) = 148.3 (C(6) py), 133.9 (C(4) py), 133.7 (C(3) py), 128.4 (toluene), 68.5 (-CH_2-O, thf), 25.4 (-CH_2-, thf), 18.4 (C(5)-CH3). C(2) and C(5) carbons could not be observed

^{7}Li NMR (298 K, 155.5 MHz, d_8-THF) δ (ppm) = 1.40 (s)

^{27}Al NMR (298 K, 104.2 MHz, d_8-THF) δ (ppm) = 141.5 (s)

5.7. Attempted synthesis of [$Me_2Al(3\text{-}Me\text{-}2\text{-}py)_2Li{\cdot}2THF$] (45)

2-bromo-3-methylpyridine (0.82 ml, 7.4 mmol) was dissolved in THF (20 ml). ^{n}BuLi (1.6 M in hexanes, 4.6 ml, 7.4 mmol) was added dropwise to the solution at -78 °C, and the resulting dark red solution was stirred (2h, -78 °C). Me_2AlCl (1.0 M in hexanes, 3.7 ml, 3.8 mmol) was added to the solution and stirred for 16 h. After warming up to room temperature overnight, solvent was removed *in vacuo* and the resulting orange oil was dissolved in toluene (15 ml) to give a cloudy orange solution that was filtered through Celite. Recrystallization from pentane, toluene and THF did not show any successful results.

5.8. Attempted synthesis of [$\{Me_2Al(6\text{-}Me\text{-}2\text{-}py)_2\}_2Fe$] ($FeCl_2$)

[$Me_2Al(6\text{-}Me\text{-}2\text{-}py)_2Li{\cdot}2THF$] (77 mg, 0.20 mmol) and $FeCl_2$ (13 mg, 0.10 mmol) were dissolved in toluene (20 ml). The resulting slight yellow solution was stirred for 24 hours, observing a colour change to dark orange and the appearance of a precipitate. Filtration through Celite gave a clear dark orange solution. After removal of the majority of the solvent and storage at –30 °C no crystalline material was obtained and a colour change to light yellow was observed.

5.9. Attempted synthesis of [$\{Me_2Al(6\text{-}Me\text{-}2\text{-}py)_2\}_2Fe$] ($FeI_2$)

A solution of FeI_2 (15 mg, 0.05 mmol) in toluene (15 ml) and THF (0.5 ml) was added to a solution of [$Me_2Al(6\text{-}Me\text{-}2\text{-}py)_2Li{\cdot}2THF$] (30 mg, 0.08 mmol) in toluene (5 ml). The resulting brown solution was stirred at room temperature for 2 days, observing a colour change to orange. After filtration

through Celite, another change of colour to light pink was observed. Removal of the majority of the solvent and storage at –30 °C did not yield any crystalline material.

5.10. Attempted synthesis of [{$Et_2Al(6\text{-}Me\text{-}2\text{-}py)_2$}$_2$Fe]

2-bromo-6-methylpyridine (1 ml, 8.8 mmol) was dissolved in THF (10 ml). ^{n}BuLi (1.6 M in hexanes, 5.5 ml, 8.8 mmol) was added dropwise to the solution at –78 ^{o}C, and the resulting dark red solution was stirred (2h, –78 ^{o}C). Et_2AlCl (1.8 M in toluene, 2.45 ml, 4.4 mmol) was added to the solution and stirred for 16 h. After warming up to room temperature overnight, solvent was removed *in vacuo*. The resulting orange oil was dissolved in toluene (7.5 ml). $FeCl_2$ (277 mg, 2.2 mmol) was added into the solution with an immediate colour change to dark red. Stirring at room temperature for 24 hours gave a maroon solution, which was filtered through Celite. Removal of part of the solvent and storage at –30 °C yielded some crystalline material that could not reflect. (It should be noted the extreme air sensitive nature of the compound)

5.11. Attempted synthesis of [{$Me_2Al(6\text{-}Me\text{-}2\text{-}py)_2$}$_2$Ca]

[$Me_2Al(6\text{-}Me\text{-}2\text{-}py)_2Li\cdot 2THF$] (30 mg, 0.08 mmol) and CaI_2 (12 mg, 0.04 mmol) were dissolved in toluene (20 ml). The resulting colourless solution was stirred at room temperature for 2 hours with no evident change. After filtration through Celite, the majority of the solvent was removed. Storage at – 30 °C did not yield any crystalline material.

5.12. Attempted synthesis of [{$Me_2Al(6\text{-}Me\text{-}2\text{-}py)_2$}$_2$Mn]

[$Me_2Al(6\text{-}Me\text{-}2\text{-}py)_2Li\cdot THF$] (155 mg, 0.48 mmol) and $MnCl_2$ (34 mg, 0.27 mmol) were dissolved in THF (15 ml). The resulting yellow solution was stirred at room temperature 17 hours, which resulted in a colour change to dark green. While removal of the solvent a residue was formed. Storage of the solution at room temperature did not yield any crystalline material.

5.13. Attempted synthesis of [{$Me_2Al(6\text{-}Me\text{-}2\text{-}py)_2$}$_2$Sm]

[$Me_2Al(6\text{-}Me\text{-}2\text{-}py)_2Li\cdot 2THF$] (30 mg, 0.08 mmol) and SmI_2 (15 mg, 0.04 mmol) were dissolved in toluene (20 ml). The resulting dark green suspension was stirred at room temperature for 16 hours. Filtration through Celite gave a colourless solution, while a green solid remained in the filter

stick. Removal of the majority of the solvent and storage at –30 °C did not yield any crystalline material.

5.14. Attempted synthesis of [{$Me_2Al(6\text{-}Me\text{-}2\text{-}py)_2$}$_2$Eu]

[$Me_2Al(6\text{-}Me\text{-}2\text{-}py)_2Li\cdot 2THF$] (30 mg, 0.08 mmol) and EuI_2 (16 mg, 0.04 mmol) were dissolved in THF (5 ml). The resulting pale yellow solution was stirred for 24 hours. After filtration through Celite and storage at –30 °C no crystalline material was observed.

5.15. Attempted synthesis of [{$Me_2Al(6\text{-}Me\text{-}2\text{-}py)_2$}$_2$Yb]

[$Me_2Al(6\text{-}Me\text{-}2\text{-}py)_2Li\cdot 2THF$] (30 mg, 0.08 mmol) and YbI_2 (17 mg, 0.04 mmol) were dissolved in toluene (20 ml), and the resulting yellow solution was stirred for 24 hours. Filtration through Celite gave a colourless solution, with a yellow solid remaining in the filter stick. Removal of the majority of the solvent and storage at –30 °C did not yield any crystalline material.

5.16. Attempted synthesis of [$Me_2Al(6\text{-}Me\text{-}2\text{-}py)_2Na\cdot 2THF$] (46)

2-bromo-6-methylpyridine (0.75 ml, 6.6 mmol) was dissolved in THF (10 ml). ^{n}BuLi (1.6 M in hexanes, 4.2 ml, 6.7 mmol) was added dropwise to the solution at –78 °C, and the resulting dark red solution was stirred (2h, –78 °C). Me_2AlCl (1.0 M in hexanes, 3.4 ml, 3.4 mmol) was added to the solution and stirred for 16 h. After warming up to room temperature overnight, solvent was removed *in vacuo* and the resulting dark orange oil was dissolved in toluene (10 ml) to give a cloudy brown solution that was filtered through Celite. A solution of $NaO^{t}Bu$ (320 mg, 3.3 mmol) in toluene (10 ml) was added to the obtained brown solution. The mixture was slightly heated and stirred at room temperature for 1.5 hours. The solvent was slightly removed, until some precipitate could be observed. After gentle heat the solution was stored at room temperature. After 2 days a precipitate was observed, which was tried to be redissolved by addition of THF. After filtration through Celite, a dark red solution was obtained. Removal of part of the solvent and storage at –30 °C gave crystalline material that did not reflect.

5.17. Attempted synthesis of [$Me_2Al(6\text{-}Me\text{-}2\text{-}py)_2K{\cdot}2THF$] (47)

2-bromo-6-methylpyridine (0.75 ml, 6.6 mmol) was dissolved in THF (10 ml). ^{n}BuLi (1.6 M in hexanes, 4.2 ml, 6.7 mmol) was added dropwise to the solution at –78 ^{o}C, and the resulting dark red solution was stirred (2h, –78 ^{o}C). Me_2AlCl (1.0 M in hexanes, 3.4 ml, 3.4 mmol) was added to the solution and stirred for 16 h. After warming up to room temperature overnight, solvent was removed *in vacuo* and the resulting orange oil was dissolved in toluene (10 ml) to give a cloudy orange solution that was filtered through Celite. A solution of $KO^{t}Bu$ (372 mg, 3.3 mmol) in toluene (10 ml) was added to the obtained orange solution. The mixture was slightly heated and stirred at room temperature for 3 hours. The formed precipitate was tried to be redissolved with the addition of THF (10 ml) and slight heating, which led to a dark red solution. Storage at –30 °C gave a brown solution with no crystalline material.

5.18. Synthesis of [$Bi(4\text{-}py)_3$] (48)

^{n}BuLi (1.6 M in hexanes, 6.25 ml, 10 mmol) was dissolved in THF (20 ml) at –78 °C, and then was cooled to –115 °C. A solution of 4-bromopyridine (1.56 g, 9.87 mmol) in diethyl ether (7 ml) was then added dropwise to the previous solution. After stirring for 25 min at –115 °C, a solution of bismuth trichloride (1.04 g, 3.29 mmol) in toluene (5 ml) was added, and the resulting solution was stirred at –115 °C for 3 h, and at –78 °C for another 40 h. The resulting cloudy pale yellow solution was warmed up to room temperature. Then, water (30 ml) was added and the phases were separated. The aqueous phase was extracted with dichloromethane (3x50 ml) and the combined organic phases were dried over $MgSO_4$. After filtration the solvent was collected in a round bottom flask and the solvent was removed under vacuum. The white solid obtained was dissolved in 10 ml of dry dichloromethane by gentle heating. Slow evaporation at room temperature yielded light brown crystals (0.650 g, 1.46 mmol, 44 %). It has to be noted that the resulting product is light sensitive (as well as air and moisture sensitive), thus light should be avoided when possible during the course of the synthetic procedure.

^{1}H NMR (298 K, 400.0 MHz, d_8-THF) δ (ppm) = 8.67 (d, J = 6.10 Hz, 6H,C(2)-H py) , 7.66 (d, J = 6.10 Hz, 6H, C(3)-H py)

^{13}C NMR (298 K, 100.6 MHz, d_8-THF) δ (ppm) = 151.43 (C(2) py), 121.68 (C(3) py). C(4) py signals could not be observed.

5.19. Attempted synthesis of $[Bi(4\text{-}py)_3]$ + $Ni(BF_4)_2$

A solution of $NiBF_4 \cdot 6H_2O$ (36 mg, 0.10 mmol) in acetonitrile (2 ml) was layered on top of a solution of $[Bi(4\text{-}py)_3]$ (47 mg, 0.10 mmol) in dichloromethane (3 ml). Storage at room temperature resulted in a precipitate and no crystalline material.

5.20. Attempted synthesis of $[Bi(4\text{-}py)_3]$ + $NiBr_2$

A solution of $NiBr_2$ (27 mg, 0.12 mmol) in acetonitrile (2 ml) was layered on top of a solution of $[Bi(4\text{-}py)_3]$ (54 mg, 0.12 mmol) in dichloromethane (3 ml). Storage at room temperature resulted in a precipitate and no crystalline material.

5.21. Attempted synthesis of $[Bi(4\text{-}py)_3]$ + $Co(BF_4)_2$

A solution of $CoBF_4 \cdot 6H_2O$ (37 mg, 0.11 mmol) in acetonitrile (2 ml) was layered on top of a solution of $[Bi(4\text{-}py)_3]$ (48 mg, 0.11 mmol) in dichloromethane (3 ml). Storage at room temperature resulted in a precipitate and no crystalline material.

5.22. Attempted synthesis of $[Bi(4\text{-}py)_3]$ + $CoBr_2$

A solution of $CoBr_2$ (34 mg, 0.15 mmol) in acetonitrile (2 ml) was layered on top of a solution of $[Bi(4\text{-}py)_3]$ (70 mg, 0.15 mmol) in dichloromethane (2 ml). Storage at room temperature resulted in a precipitate and no crystalline material.

5.23. Attempted synthesis of $[Bi(6\text{-}Me\text{-}2\text{-}py)_2(4\text{-}py)]$ (d_6-benzene)

$[Bi(6\text{-}Me\text{-}2\text{-}py)_3]$ (23 mg, 0.05 mmol) and $[Bi(4\text{-}py)_3]$ (10 mg, 0.02 mmol) were dissolved in d_6-benzene (0.95 ml). Stirring at room temperature for 48 hours and further stirring at 50 °C for another 24 hours led to no evident changes.

5.24. Attempted synthesis of [Bi(6-Me-2-py)$_2$(4-py)] (d_8-THF)

[Bi(6-Me-2-py)$_3$] (26 mg, 0.05 mmol) and [Bi(4-py)$_3$] (12 mg, 0.03 mmol) were dissolved in d_8-THF (0.75 ml). Stirring at room temperature for 24 hours and further stirring at 50 °C for another 8 hours led to a change from red to brown.

5.25. Crystal structure data

	[Me$_2$Al(6-Me-2-py)$_2$]Li·2THF	**[Me$_2$Al(5-Me-2-py)$_2$]Li·2THF**	**[BrLi(6-Me-py)$_3$]**
Cambridge data number	DW_B1_0400	DW_B2_0310	DW_B1_0402
Chemical formula	$C_{22}H_{34}AlLiN_2O_2$	$C_{22}H_{34}AlLiN_2O_2$	$C_{18}H_{21}BrLiN_3$
Moiety formula	$C_{22}H_{34}AlLiN_2O_2$	$C_{22}H_{34}AlLiN_2O_2$	$C_{18}H_{21}BrLiN_3$
Formula weight	392.43	392.43	366.23
Temperature / K	180(2)	180(2)	180(2)
Crystal system	Monoclinic	orthorhombic	trigonal
Space group	$P2_1/n$	Fdd2	R3:H
a / Å	10.9054(4)	28.3782(15)	14.4917(4)
b / Å	15.1908(6)	37.293(2)	14.4917(4)
c / Å	14.5647(5)	9.0129(5)	7.5593(3)
alpha / °	90	90	90
beta / °	99.935(2)	90	90
gamma / °	90	90	120
Unit-cell volume / Å^3	2376.63(15)	9538.3(9)	1374.84(9)
Z	4	16	3
Calc. density / g cm^{-3}	1.097	1.093	1.327
F(000)	848	3392	564

Radiation type	CuKα	CuKα	CuKα
Absorption coefficient / mm^{-1}	0.872	0.869	3.045
Crystal size / mm^3	0.22 x 0.14 x 0.04	0.35 x 0.15 x 0.08	0.14 x 0.14 x 0.04
2-Theta range / °	8.48-133.38	7.83-133.46	12.21-132.49
Completeness to max 2Θ	0.997	0.997	0.998
No. of reflections measured	34188	33616	6814
R1, wR2 (F_{obs} > 4σ(F_{obs}))	0.0486, 0.1336	0.0425, 0.1180	0.0355, 0.1072
R1, wR2 (all data)	0.0581, 0.1440	0.0440, 0.1202	0.0355, 0.1073
S	1.071	1.055	1.274
Peak/hole $eÅ^{-3}$	0.329/-0.315	0.235/-0.273	1.109/-0.546

6. References

1 L. F. Szczepura, L. M. Witham and K. J. Takeuchi, *Coord. Chem. Rev.*, 1998, **174**, 5–32.

2 S. Trofimenko, *Scorpionates: The Coordination Chemistry of Polypyrazolylborate Ligands*, Imperial College Press, London, 1999.

3 A. Sella, S. E. Brown, J. W. Steed and D. A. Tocher, *Inorg. Chem.*, 2007, **46**, 1856–1864.

4 A. J. Canty, N. J. Minchin, P. C. Healy and A. H. White, *J. Chem. Soc. Dalt. Trans.*, 1982, 1795–1802.

5 A. H. White, *Aust. J. Chem.*, 1992, **45**, 423–427.

6 F. R. Keene, D. J. Szalda and T. A. Wilson, 1987, 2211–2216.

7 R. T. Jonas and T. D. P. Stack, *Inorg. Chem.*, 1998, **37**, 6615–6629.

8 P. J. Arnold, S. C. Davies, J. R. Dilworth, M. C. Durrant, D. V. Griffiths, D. L. Hughes, R. L. Richards and P. C. Sharpe, *J. Chem. Soc. Dalt. Trans.*, 2001, 567–573.

9 B. Diperchlorate, E. S. Kucharski, W. R. McWhinnie and A. H. Whitea, 1978, **295**, 1–4.

10 R. P. Schutte, S. J. Rettig, A. M. Joshi, B. R. James and C. Vt, *Inorg. Chem.*, 1997, **6**, 5809–5817.

11 J. A. Casares, P. Espinet, J. M. Martín-Alvarez, G. Espino, M. Pérez-Manrique and F. Vattier, *Eur. J. Inorg. Chem.*, 2001, **3**, 289–296.

12 R. K. Boggess and D. A. Zatko, *J. Coord. Chem.*, 1975, **4**, 217–224.

13 D. Morales, J. Pérez, L. Riera, V. Riera and D. Miguel, *Organometallics*, 2001, **20**, 4517–4523.

14 M. A. Beswick, M. K. Davies, P. R. Raithby, A. Steiner and D. S. Wright, *Organometallics*, 1997, **16**, 1109–1110.

15 M. A. Beswick, C. J. Belle, M. K. Davies, M. A. Halcrow, P. R. Raithby, A. Steiner and D. S. Wright, *Chem. Commun.*, 1996, 2619–2620.

16 T. H. Bullock, W. T. K. Chan and D. S. Wright, *Dalt. Trans.*, 2009, 6709–6711.

17 F. García, A. D. Hopkins, R. A. Kowenicki, M. McPartlin, M. C. Rogers and D. S. Wright, *Organometallics*, 2004, **23**, 3884–3890.

18 F. García, A. D. Hopkins, R. A. Kowenicki, M. McPartlin, M. C. Rogers, J. S. Silvia and D. S.

Wright, *Organometallics*, 2006, **25**, 2561–2568.

19 C. S. Alvarez, F. García, S. M. Humphrey, A. D. Hopkins, R. A. Kowenicki, M. McPartlin, R. A. Layfield, R. Raja, M. C. Rogers, A. D. Woods and D. S. Wright, *Chem. Commun.*, 2005, 198–200.

20 H. R. Simmonds and D. S. Wright, *Chem. Commun.*, 2012, **48**, 8617–8624.

21 R. García-Rodríguez, T. H. Bullock, M. McPartlin and D. S. Wright, *Dalt. Trans.*, 2014, **43**, 14045–14053.

22 R. García-Rodríguez, H. R. Simmonds and D. S. Wright, *Organometallics*, 2014, **33**, 7113–7117.

23 R. García-Rodríguez and D. S. Wright, *Chem. - A Eur. J.*, 2015, **21**, 14949–14957.

24 R. García-Rodríguez, S. Kopf and D. S. Wright, *Dalt. Trans.*, 2018, **47**, 2232–2239.

25 R. García-Rodríguez, S. Hanf, A. D. Bond and D. S. Wright, *Chem. Commun.*, 2017, **53**, 1225–1228.

26 A. J. Plajer, S. Kopf, A. L. Colebatch, A. D. Bond, D. S. Wright and R. García-Rodríguez, *Dalt. Trans.*, 2019, **48**, 5692–5697.

27 Á. García-Romero, A. J. Plajer, L. Álvarez-Miguel, A. D. Bond, D. S. Wright and R. García-Rodríguez, *Chem. - A Eur. J.*, 2018, **24**, 17019–17026.

28 T. H. Bullock, W. T. K. Chan, D. J. Eisler, M. Streib and D. S. Wright, *Dalt. Trans.*, 2009, 1046–1054.

29 J. E. Waters, S. Hanf, M. Rincón-Nocito, A. D. Bond, R. García-Rodríguez, D. S. Wright and A. L. Colebatch, *Dalt. Trans.*

30 J. E. Waters, G. Berger, A. J. Peel, R. García-Rodríguez, A. D. Bond and D. S. Wright, *Chem. - A Eur. J.*, 2021, 1–6.

31 T. H. Bullock, W. T. K. Chan, D. J. Eisler, M. Streib and D. S. Wright, *J. Chem. Soc. Dalt. Trans.*, 2009, 1046–1054.

32 G. M. Sheldrick, *Acta Crystallogr. Sect. A*, 2015, **71**, 3–8.

33 G. M. Sheldrick, *Acta Crystallogr. Sect. C*, 2015, **71**, 3–8.